TECHNISCHE UNIVERSITÄT MÜNCHEN

TUM School of Management

Markovian Stochastic Optimization in Energy Planning: Discrete Approximation and Applications in Optimal Power Flow Problem

Adriana Kiszka

b

Abstract

The transition of the power network towards cleaner and sustainable energy generation requires appropriate planning of the future power infrastructure, considering both the technical and economic aspects. With this thesis, I propose an optimization model to address the arising challenges and provide the necessary tools to effectively solve energy planning problems. The proposed optimization model simultaneously incorporates a multi-stage formulation, a finitely supported Markov structure of random processes, and the alternating current (AC) nature of power flow dynamics, filling a gap in the existing literature.

First, I propose a semi-metric for Markov processes involved in linear stochastic optimization problems. The distance aims to assess the accuracy of a discrete approximation and its influence on the optimal value of a multi-stage stochastic optimization. The distance relies on transportation metrics and depends on problem parameters, allowing for consideration of randomness in both the objective function and the constraints. Next, I provide a solution strategy for multi-stage stochastic optimal power flow (OPF) problems. This strategy is based on recent developments in convex semi-definite programming relaxations of OPF problems and the adaptation of the stochastic dual dynamic programming (SDDP) algorithm. I discuss the convergence conditions and properties of the algorithm. Lastly, I set up an extensive case study focusing on renewable expansion and storage integration planning within the IEEE RTS-GMLC network. The study illustrates the applicability and computational tractability of the presented framework.

d

Acknowledgements

I would like to express my sincere gratitude to the following individuals and organizations who have played a significant role in the completion of this dissertation:

First and foremost, I am deeply thankful to my supervisor, Prof. Dr. David Wozabal, for his invaluable guidance, insightful feedback, and unwavering support throughout the entire research journey. His expertise and encouragement have been instrumental in shaping the direction of this dissertation.

I am also grateful to all my colleagues from the Center for Energy Markets, Prof. Sebastian Schwenen, Dr. Goncalo Terca, Dr. Moritz Bohland, and Dr. Vadim Gorski for the fruitful discussions and support during both challenging and rewarding moments of this academic endeavor.

I would like to thank Karin Papavlassopoulos and Henriett Kakonyi, whose help and guidance through all administrative procedures remain invaluable.

I am grateful to the Technical University of Munich for providing the necessary resources, facilities, and a conducive research environment. The School of Management has been an excellent academic home.

Lastly, special thanks go to my family for their love, patience, and encouragement. Their support has been my strength, and I am profoundly grateful for their unwavering belief in my abilities.

f

Contents

List of Figures

List of Tables

m

List of Algorithms

Chapter 1

Introduction

1.1 Motivation

Climate change and the reduction of greenhouse gas emissions are pressing environmental concerns capturing the attention of countries worldwide. National governments and international organizations have implemented ambitious plans and policies to bolster climate action. Notably, the Paris Agreement stands out as a legally binding global climate consensus, adopted during the Paris Climate Conference in December 2015 (see United Nations Framework Convention on Climate Change 2015). The agreement outlines a target to restrict the global average temperature increase to 1.5 degrees Celsius above pre-industrial levels, aiming to mitigate the risks and impacts of climate change. To realize this objective, emissions must be reduced by 45% from the 2010 level by 2030, ultimately achieving carbon neutrality by 2050 according to Intergovernmental Panel on Climate Change (2018). Given that the energy sector accounts for over two-thirds of total global greenhouse gas emissions, it emerges as a pivotal area for substantial actions to combat climate change. A fundamental step involves transitioning the power network towards cleaner and more sustainable energy generation, predominantly through the adoption of renewable energy sources in future infrastructure planning (see International Renewable

Energy Agency 2017b).

Among renewable energy technologies, two categories can be distinguished: dispatchable (e.g., biomass, concentrated solar power with storage, geothermal power, and hydro) and non-dispatchable, also known as variable renewable energy (e.g., ocean power, solar photovoltaics, wind). Variable renewable energy sources (VRE) can be characterized by properties that differentiate them from conventional generators. Firstly, the output of VRE can not be controlled and exhibits variable seasonal and diurnal production patterns due to its weather-dependent nature, leading to inherent forecasting uncertainty. Additionally, renewable energy generation is location-constrained, and the areas with high output can be placed far from demand centers, imposing additional requirements on the necessary power network infrastructure.

The transformation of the existing power grid infrastructure towards renewable energy sources necessitates an evaluation of the operation and planning of the future power network from both technical and economic perspectives. According to International Renewable Energy Agency (2017a), four components are discernible in energy planning to ensure the reliability of the power system and meet ambitious targets driven by national commitments, international agreements, and rapid technological development.

The first component involves planning for *firm capacity*, signifying the portion of variable renewable energy that is assured to be produced even during periods of low renewable generation.

The second component encompasses planning for *flexibility*. A techno-economic definition by the International Energy Association states that power system flexibility is the ability of a power system to reliably and cost-effectively manage the variability and uncertainty of demand and supply across all relevant timescales (see International Energy Agency 2018). As VRE introduces intermittency and high uncertainty of supply, it imposes a necessesity of investments in flexibility measures.

Another crucial component is planning for *transmission capacity*, essential for transmitting power from VRE resources to centers of demand. Additionally, long-distance transmission lines may necessitate enhanced methods for controlling voltage.

The final element in integrating VRE into the power system is planning for *stability*, ensuring the capability to respond to contingency events and control voltage. Achieving this goal involves improving operational practices and implementing other technical solutions.

These components highlight the complexity of the expansion planning problem and the importance of handling it properly. To identify a cost-optimal strategy, one effective approach is to formulate and solve an optimization problem. Therefore, developing an optimization model becomes crucial to effectively account for economic, technical, environmental, and other constraints. Due to the increasing integration of renewable energy sources and the uncertainty of their output, it also becomes evident that traditional deterministic approaches to energy planning encounter significant limitations.

Stochastic optimization is an approach to solve an optimization problem involving uncertainty (see Birge and Louveaux 2011, for an introduction). Therefore, it emerges as a compelling solution in response to the inherent uncertainties associated with renewable energy generation, demand fluctuations, and unforeseen system disturbances. Applying stochastic optimization techniques in energy planning acknowledges the dynamic and uncertain nature of the energy environment. It also empowers decision-makers to develop robust strategies that can adapt to unforeseen events and market fluctuations.

Furthermore, the global commitment to reducing carbon emissions and the increasing emphasis on achieving ambitious renewable energy targets necessitate innovative planning approaches. Stochastic optimization could contribute as a tool for achieving sustainability goals while ensuring the reliability and cost-effectiveness of energy systems by appropriate problem formulation.

1.2   Contribution

Stochastic programming is an approach used to model and solve optimization problems involving uncertainty (Shapiro et al. 2009). Unlike deterministic optimization, which assumes complete knowledge of all parameters, stochastic programming accounts for the uncertainty of the parameters by considering their probability distributions, whether known or estimated. Given the significance of including the variability of renewable generation in energy planning, stochastic programming seems adequate to address this challenge and provide optimal decisions.

In the literature, energy planning models accounting for uncertainty are explored mainly by the application of a straightforward discrete approximation of the random process or by employing a relaxation of the optimization problem (e.g. Lara et al. 2018, Peter and Wagner 2021). The authors often neglect some important factors and allow for less accurate solutions in their approach in favor of computational efficiency, for example, by considering direct current (DC) instead of alternating current (AC) in the optimal power flow (OPF) (see Bent et al. 2011, for a comparison). In contrast to existing approaches, I have developed a theory that simultaneously incorporates three important components into the stochastic optimization model: a multi-stage formulation, a finitely supported Markovian structure of the random process, and the alternating current (AC) nature of the power system. Undoubtedly, this introduces a significant increase in the complexity of the problem, but this effort is compensated by attaining more precise results.

1.2.1   Assumptions

In the thesis, stochastic optimization models are developed and applied under the following assumptions:

Multi-stage formulation

First, I consider a multi-stage stochastic formulation of the optimization problem. In contrast, a two-stage optimization model is applied by most of the researchers in energy planning (e.g. Byon et al. 2020, López-Ramos et al. 2020).

Two-stage and multi-stage optimization models differ in the number of decision-making stages involved in the planning process. In a two-stage optimization, the decision-maker makes initial decisions in the first stage without knowing the specific realization of uncertain parameters, which are realized in the second stage. Subsequently, after the uncertainties are revealed, the decision-maker makes additional decisions in the second stage, considering both the actual values of the uncertain parameters and the decisions made in the previous stage. It is recommended to see Birge and Louveaux (2011) and Shapiro et al. (2009) for a comprehensive overview.

Multi-stage optimization models involve more than two decision-making points, each associated with a specific point in time or a particular phase of the decision process (Pflug and Pichler 2014). The decision-maker considers uncertainties and makes decisions sequentially at each stage, adapting to new information as it becomes available in the form of the actual values of uncertain parameters and decisions taken in the previous stages. However, the dynamic and evolving information poses a challenge of making optimal decisions with incomplete or changing data.

A multi-stage optimization model is a natural extension of a two-stage optimization, but due to the complexity and the dynamic nature of the decision-making process across multiple stages, the problem is often intractable (see Shapiro 2006, 2010). As the number of stages increases, one can observe an exponential increase in the size of the solution space introduced as the curse of dimensionality in Hanasusanto et al. (2016). Multi-stage optimization problems, with decisions across multiple stages, can suffer from this curse, making it harder to find feasible and optimal solutions. Furthermore, interpreting the outcome becomes more challenging as the decision-makers have to understand the implications of multi-stage solutions.

Managing and solving problems with numerous decision points, variables, and constraints can become challenging and demand sophisticated optimization algorithms and significant computational resources. On the other hand, multi-stage models allow for a more detailed and dynamic representation of the decision-making process. In energy planning, the assumption of the multi-stage formulation of the optimization problem facilitates accounting for the extended horizon of the power network operation, enabling a more precise evaluation of the impact of investment decisions as in Lara et al. (2020).

Finitely supported Markovian structure of the random process

Secondly, I assume that the random process involved in the multi-stage stochastic optimization problem is a finitely supported Markov process represented by a scenario lattice.

In many optimization problems, the random process is naturally continuously distributed, and it requires the numerical evaluation of high dimensional integrals, which is a challenge. Therefore, researchers use representative scenarios to approximate the stochastic process or assume finite support to solve the problem.

The majority of the authors use scenario trees as a discrete representation of the random process (e.g. Heitsch and Römisch 2009, Pflug and Pichler 2012). In a scenario tree, every node has only one predecessor and possibly more than one successor, leading to the exponential growth of nodes as the number of stages increases. Therefore, scenario trees are typically restricted to having only a few stages or contain nodes with only one successor, resulting in deterministic sub-problems at these nodes.

A possible solution to this dilemma is to assume that the random process satisfies the Markov property, meaning that the value of the process at time t depends only on the value at time $t-1$, and there is no need to remember the whole history of the process. This property can be expressed by the following relation for the conditional

probabilities:

$$P(\xi_t = \xi_t(\omega_t)|\xi_{t-1}(\omega_{t-1}), \ldots, \xi_0(\omega_0)) = P(\xi_t = \xi_t(\omega_t)|\xi_{t-1}(\omega_{t-1})) \quad t \in \{1, \ldots, T\}$$

where $\xi = (\xi_0, \xi_1, \ldots, \xi_T)$ with $\xi_t : \Omega_t \to \mathbb{R}^{n_t}$ is a Markov process. The restriction to Markov processes strikes a good balance between capturing the realistic dynamics of the system across multiple stages and the accurate representation of interdependencies.

A natural representation of a discrete Markov process is a scenario lattice that consists of the same building blocks as a scenario tree but relaxes the requirement that every node has only one predecessor, as depicted in Figure 1.1. The growth of the number of nodes as the number of stages increases is linear, contrasting with the exponential growth observed in a scenario tree. Thereby, scenario lattice offers computational advantages over a scenario tree.
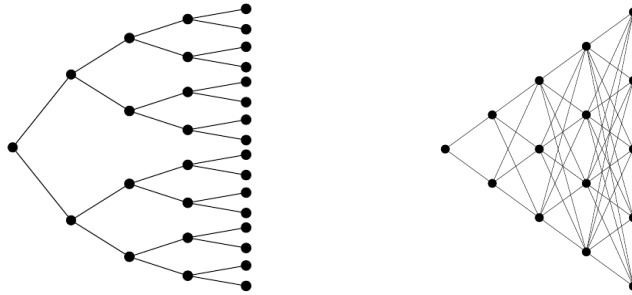
Figure 1.1: Comparison of a scenario tree with 31 nodes representing 16 scenarios on the left with a scenario lattice with 15 nodes representing 120 scenarios on the right.

The decision-making process in multi-stage stochastic optimization problems where the random process satisfies the Markov property is called the Markov Decision Process (MDP). It was officially introduced in Horward (1960) and later elaborated in Puterman (1994). It serves as a structured framework for modeling and solving sequential decision problems that involve actions taken over time, and MDPs effectively capture this dynamic nature. Markov Decision Processes are successfully

applied in many areas, including operations research, logistics, and supply chain management, where they are used to optimize resource allocation (e.g. Huang et al. 2023), scheduling (e.g. He et al. 2022), and inventory management (e.g. Shin and Lee 2015). MDPs offer a systematic approach to decision-making, which is particularly relevant in designing investment strategies (see Chang and Lee 2017), managing network resources (see Williams 2009), and planning energy generation and distribution (see Reyes et al. 2020).

In summary, Markov Decision Processes are important because they provide a versatile and principled framework for modeling, analyzing, and solving sequential decision problems in the presence of uncertainty, leading to optimal decision policies in a wide range of applications across different domains. Nevertheless, the literature on Markov Decision Processes in the context of energy planning remains limited, leaving a place for improvement. Therefore, I intend to contribute to fill this gap with my findings.

AC OPF

Finally, I assume that the formulation of the optimization problem applied to energy planning, where the operational planning of the power network is included in the model, consists of the optimal power flow (OPF) problem constructed under alternating current (AC).

Optimal power flow problems represent a framework for determining the most economical and reliable configuration of power system operating parameters. The primary objective is to achieve the optimal allocation of power generation, transmission, and distribution resources while adhering to system constraints and ensuring the secure and stable functioning of the grid. OPF, as a mathematical optimization problem, involves the simultaneous optimization of various operational variables within a power network, encompassing generator setpoints, transformer tap ratios, and bus voltages.

Two approaches to formulating the OPF problem can be distinguished: direct current (DC) and alternating current. The optimal power flow between units for alternating current is an NP-hard problem (see Bienstock and Verma 2019), and therefore, many researchers use direct current approximation as in Pandzic et al. (2015), Qiu et al. (2017). The DC optimal power flow model simplifies the complexities of AC power systems to provide a computationally efficient solution for large-scale power system optimization. In the DC model, voltage magnitudes are assumed constant, and only active power flows are considered. This simplification significantly reduces the computational burden, making it suitable for quick and preliminary power system operation and planning analyses.

Advantages of the DC approach include its speed and scalability, making it particularly useful for large-scale grid studies and real-time applications. However, its simplicity comes at the cost of accuracy. The DC model neglects reactive power flows, voltage variations, and transmission line impedance, leading to inaccuracies in certain situations, especially when dealing with heavily loaded or highly stressed power systems.

In contrast, the AC optimal power flow model provides a more accurate representation of power system behavior by considering both active and reactive power flows, as well as voltage magnitudes and phase angles. The AC model incorporates the complexities of transmission line impedances and voltage constraints, making it suitable for detailed studies requiring higher accuracy.

The advantages of the AC approach lie in its ability to capture voltage stability, reactive power interactions, and the impact of network constraints more accurately. This makes it essential for detailed planning, especially in scenarios involving high renewable energy penetration and increased complexity in power system configurations. Nevertheless, the AC model requires higher computational resources than the DC model.

In summary, the AC approach better reflects reality and provides a more accurate

solution for the power network operation. However, its implementation involves a combination of advanced optimization techniques, computational methods, and a profound understanding of the specific problem domain.

1.2.2   A Stability Result for Linear Markovian Stochastic Optimization Problems

In the first paper, I focus on the problem of approximation of random processes (possibly continuous) involved in the optimization problem. Having a discrete approximation of the random process allows us to formulate an approximating optimization problem by replacing the original process with generated scenarios and obtain a solution to the original problem, which was often intractable in reasonable computational time. The way of constructing scenarios is not obvious and differs from standard scenario generation approaches, as we want to guarantee that an optimal value of approximating optimization problem lies within reasonable accuracy to the optimal value of the original optimization problem.

Stochastic programming provides many different methods of constructing a discrete approximation of the random process. The most common and widely used approach is applying a sampling technique, e.g., Monte Carlo, to construct scenarios and approximate the expectation function by the average over generated scenarios in the objective function of an optimization problem. This simple idea was suggested by different authors (e.g. Kleywegt et al. 2001), and it is known as the *sample average approximation* in the recent literature. More information about the statistical properties of this method can be found in Shapiro (2006) and a discussion on the complexity of two and multi-stage versions in Shapiro and Nemirovski (2005), indicating that the method is practically inapplicable for solving multi-stage problems. Another approach relies on the explicit choice of representative scenarios, and it can be accomplished in various ways, which are mentioned in Section 2.1.

In this paper, I focus on the method that uses probability metrics to assess the

accuracy of an approximation. The probability metric usually refers to the distance between probability distributions, but it can be easily defined for stochastic processes. Concerning optimization problems, the distance is used to bound the difference between optimal values of stochastic optimization problems for different random processes, thereby allowing us to infer the accuracy of the approximation. Proving such relation for a certain probability metric is analogous to the basic concept of the Lipschitz property (see Definition 1.1) for a function f which returns the optimal value of defined stochastic optimization problem for the given stochastic process being the argument of this function. The difficulty relies on finding a proper metric d_X for stochastic processes that satisfies the required relation.

Definition 1.1. *Given two metric spaces (X, d_X) and (Y, d_Y) where d_X and d_Y are metrics on the set X and Y respectively, a function $f : X \to Y$ is called a Lipschitz function if there exists a real constant $L \geq 0$ such that for all $x_1, x_2 \in X$*

$$d_Y(f(x_1), f(x_2)) \leq L d_X(x_1, x_2) \tag{1.1}$$

Looking into literature, different definitions of the distance between stochastic processes can be found (e.g. Dupacová et al. 2003, Heitsch and Römisch 2011, Heitsch et al. 2006, Pflug and Pichler 2012). These metrics are usually based on the Wasserstein or Kantorovich distance introduced in Kantorovich (1942)(see also Villani 2003), which is defined as an optimization problem minimizing the total cost of passing from an original distribution to a desired one by moving probability mass. Similarly to other researchers, I used the Wasserstein distance as a starting point for the study.

In existing approaches, most authors focus mainly on scenario trees as a discrete representation of the random process (e.g. Heitsch and Römisch 2011, Pflug and Pichler 2012). As previously mentioned, this structure exhibits exponential growth of nodes as the number of stages increases, significantly impacting the computational tractability of a multi-stage optimization problem. Therefore, I restrict the

type of random processes to Markov processes and use scenario lattice as a discrete representation as in Löhndorf et al. (2013).

Another difficulty associated with existing metrics relies on finding the exact value of the Lipschitz constant, as it has to be the same value for all stochastic processes depending only on the optimization problem. In the presented approach, the constant is included in the distance itself, and detailed instructions for its calculations are provided, considering all specifics of the optimization problem in contrast to existing results. Unfortunately, it can be assured only when the optimization problem with a certain structure is considered, e.g., linear, quadratic, etc. Therefore, I focus on linear optimization problems, which are widely applied in many areas, including energy planning problems.

The advantage and novelty of the presented distance in the context of stability results is the inclusion of uncertainty in the objective function as well as in the constraints. The latter significantly increases the complexity of the optimization problem, as the feasible set can change for every realization of the stochastic process. In comparison to the existing approaches (e.g. Heitsch and Römisch 2011, Heitsch et al. 2006) where equality constraints involving random parameters are considered, I relax this assumption and allow for dependence on randomness in inequality constraints as well.

The important contribution of this paper is also the description of distance implementation for a scenario lattice. In section 2.5, I provide a pseudocode for the calculation of the distance and numerical results for the flower girl problem. Additionally, I consider a simplified version of the example (without uncertainty in constraints) and compare the performance of the proposed metric with the nested distance introduced by Pflug and Pichler (2012). The metric defined in Pflug and Pichler (2012) is suitable for general stochastic processes and multi-stage stochastic optimization problems with uncertainty in the objective function, and therefore it is the perfect reference point. The experiment reveals that the proposed distance

provides a tighter bound than the nested distance, improving existing results and demonstrating that this metric is innovative due to the covered research area.

Furthermore, I show that every Markov process can be approximated to arbitrary precision in terms of the defined distance, laying the solid foundations for advancing research in scenario generation methods that employ a distance of probability measures (e.g. Kaut 2021). The proposed distance offers a means to control the error in optimal values resulting from replacing a complex Markov process with a simpler scenario lattice, thereby significantly reducing problem complexity.

In summary, this paper introduces the distance between Markov processes and demonstrates that the optimal value of a stochastic linear optimization problem, with predetermined form, is a function of a random process satisfying the Lipschitz property with respect to the lattice distance. The innovation of the considered model lies in the multi-stage structure, Markovian randomness, and the incorporation of uncertainty in both the objective function and constraints. Consequently, this model fills a gap in the literature, contributing to the field of probability metrics and exploiting the properties of Markov processes. Furthermore, the example demonstrates the advantage of the lattice distance over the nested distance for certain class of problems.

1.2.3   Stochastic Dual Dynamic Programming for Optimal Power Flow Problems under Uncertainty

The efficient and secure operation of the power network is important in the delivery of electricity from suppliers to customers. The optimal power flow (OPF) problem serves as a foundation for achieving this objective and offers an approach to identifying the most economical and reliable power system configuration.

The OPF aims to find an optimal allocation, transmission, and distribution of resources in the power network that minimizes a certain cost function subject to physical constraints imposed by electrical laws and engineering limits. The power

flow equations, representing the relationship between voltages and power injections using alternating current (AC), are nonlinear and lead to nonconvex optimization problems. That is the reason that the AC OPF problems are strongly NP-hard (see Bienstock and Verma 2019).

The OPF problem requires a combination of operations research and power engineering to find a reliable solution strategy and ensure secure and stable power system operation. Therefore, an understanding of power flow dynamics and the building blocks of OPF, e.g., the admittance matrix, is essential to propose an effective algorithm for this class of problems. In this paper, I provide an extensive introduction to the formulation of the OPF problem, including the construction of the admittance matrix and treatment of phase-shifting and tap-changing transformers.

The most common approach in the literature dealing with the AC OPF problem relies on an approximation of power flow equations assuming direct current (DC). This approximation notably simplifies the problem from non-convex to linear optimization and enables a variety of effective algorithms that can possibly be used as a solution method. However, the DC OPF model doesn't take into account all physical properties of power flow, and the solution has to be modified to meet the requirements of the AC power system (see Larrahondo et al. 2021).

Apart from DC relaxation, there is rich literature on the relaxation of AC OPF problems. The most common include linear programming in Coffrin and Van Hentenryck (2014), Misra et al. (2018), quadratic programming in Coffrin et al. (2016), Marley et al. (2017), integer programming in Quiroga et al. (2019) or mixed-integer programming in Bienstock and Muñoz (2014).

In particular, convex relaxations have attracted significant attention in recent years. The results of Lavaei and Low (2012) on convex semi-definite programming (SDP) relaxations of AC OPF problems triggered a flurry of research in refined conic approximations in Bingane et al. (2021), Low (2014a) and further relaxations to second order cone programming in Jabr (2006), Kocuk et al. (2016b), Yang and

Nagarajan (2021). The main reason for the remarkable interest in conic relaxations is that they provide a bound on the global optimal value and may lead to global optimality. Furthermore, the infeasibility of the relaxation implies the infeasibility of the AC OPF problem.

Since the SDP relaxations are not always exact (e.g., Bukhsh et al. 2013b, Molzahn and Hiskens 2015c), numerous authors focus on tightening them and demonstrating under what conditions an exactly global optimal solution for AC OPF can be reached with that relaxation. Examples include branch-and-bound algorithms to iteratively partition the feasible set of relaxations in order to find a solution with a smaller gap (see Chen et al. 2016, Phan 2012). In Madani et al. (2015b) and Natarajan et al. (2013), penalization terms are incorporated into the objective to ensure the feasibility of solutions produced by relaxation. Josz et al. (2015), Molzahn and Hiskens (2015c) propose employing moment-based hierarchies to form conic relaxations that result in globally optimal solutions for AC-OPF problems. Andersen et al. (2014), Molzahn et al. (2013) leverage the sparsity of power networks through a tree decomposition of the problem. Further work in this direction uses valid inequalities as in Kocuk et al. (2016b), cutting planes in Kocuk et al. (2018), convex envelopes in Coffrin et al. (2017), and sequential and bound-tightening methods in Schetinin (2019), Wei et al. (2017). A comprehensive overview of this very active field of research can be found in Molzahn and Hiskens (2019), Zohrizadeh et al. (2020).

Despite the recent advances on convex relations of the AC OPF problem, most authors focus on the deterministic optimization model (e.g. Lara et al. 2018), as uncertain parameters, e.g., demand, can be very well predicted. However, we are witnessing the increasing penetration of renewable energy sources and the expansion of electric vehicles, bringing intermittency and uncertainty to the energy system. Therefore, there is an increased need to consider the uncertainty in the optimization model to obtain the actual representation of the power network operation.

The main approaches to consider uncertainty in the OPF problem include stochastic programming in Papavasiliou et al. (2018), robust optimization in Attarha et al. (2018), or chance-constrained optimization in Roald and Andersson (2018). However, most authors apply DC approximation of the OPF problem as in Mégel et al. (2016) or consider a two-stage formulation of the stochastic optimization problem as in Bucciarelli et al. (2018).

In the two-stage formulation, the operational planning is usually reduced to one stage, assuming perfect information. This implies the sacrifice of accuracy in the OPF problem in favor of computational efficiency, which can lead to the overloading of transmission lines or voltage violations that threaten the stability and reliability of the power system.

In order to fill the gap and contribute to this research area, I propose a general multi-stage stochastic formulation of the AC OPF problem. The proposed model may include the investment as well as the operational decisions over the given time horizon, enabling a wide range of applications.

Additionally, I assume that random variables are finitely supported Markov processes represented by a scenario lattice. It ensures computational tractability and avoids the exponential growth of nodes as the number of stages increases, which can be observed for scenario trees.

In order to propose an effective solution strategy for the formulated model, I use recent developments in convex relaxations of AC OPF problem driven by Lavaei and Low (2012). The selection of this relaxation is motivated by its capability to provide an accurate solution in reasonable computational time for a variety of applications.

However, the design of a successful algorithm for a multi-stage stochastic AC OPF problem requires further steps to effectively handle the multi-stage formulation and uncertainty. I have explored the latest advances in decomposition methods that have already been applied to the OPF problems, especially Benders decomposition, which gained significant attention in this field of research (see Lara et al. 2018, Mégel

et al. 2016). In numerous improvements and adaptations, Bender decomposition-based approaches demonstrate a remarkable decrease in computational time with a relatively minor accuracy tradeoff for deterministic OPF problems. Therefore, decomposition methods appear to deliver favorable results and seem well-suited for the proposed model.

The most successful method for solving sequential decision problems under uncertainty is the stochastic dual dynamic programming (SDDP) algorithm originally proposed by Pereira and Pinto (1991). The SDDP algorithm decomposes the multi-stage stochastic optimization problems into smaller subproblems and combines the cutting-plane approximations based on the dual variables with a sampling technique. The SDDP algorithm converges toward an optimal solution by iteratively improving the value function estimates.

Primarily, the algorithm required that the random process was stagewise independent. Since the method gained enormous interest and has been extensively researched, numerous improvements and enhancements to broader problem classes can be found in the literature. I refer to Füllner and Rebennack (2023) for an overview of extensions and applications of the SDDP algorithm. From the perspective of the proposed model, the most promising results include Löhndorf and Wozabal (2021a), Löhndorf et al. (2013) where the SDDP algorithm is extended to Markov processes.

Finally, I combine the convex relaxation of the AC OPF problem proposed by Lavaei and Low (2012) with the SDDP algorithm for Markov processes to solve multi-stage stochastic AC OPF problems. I demonstrate the convergence of the approach to the true solution as long as the tightness of the relaxation of the AC OPF problem is preserved in consecutive iterations. Additionally, I propose a method to recover a physically feasible solution from a solution of the relaxed AC OPF problem for the cases where the employed relaxation is not exact.

As a proof of concept, I provide a case study on storage siting, sizing, and operations for a modified version of the power network described in Barrows et al.

(2020). The formulated optimization problem consists of the first stage, representing the storage investments, and the later stages, covering the operational planning of the energy system over one week. The model considers the uncertainty of load and renewable production for wind and solar, as well as the alternating current nature of the power flow.

The proposed algorithm achieves an optimality gap below 3% compared to the globally optimal solution for the described case study. In comparison to the rolling deterministic planning, the stochastic approach demonstrates higher investment costs, leading to lower curtailment costs and 27% lower total costs. The presented case study contributes to the existing literature on storage integration problems (e.g. Mégel et al. 2016, Xiong and Singh 2016) illustrating that it is possible to encompass a wider range of complexities in the operational planning by considering multi-stage stochastic formulation of AC OPF instead of DC OPF.

In summary, this paper introduces an effective solution strategy for a general class of multi-stage stochastic AC-OPF problems built on the combination of recent developments in convex relaxations of AC OPF problems and the SDDP decomposition algorithm for Markovian stochastic optimization problems. The proposed model fills the existing gap in the literature by considering multi-stage formulation, uncertainty, and alternating nature of power flow simultaneously. Furthermore, the approach to recover a physically accurate solution and the convergence properties of the algorithm are demonstrated. In the end, the applicability and the performance of the recommended solution strategy are illustrated in the extensive case study.

1.2.4   Optimal Renewable Expansion and Storage Integration Planning under Uncertainty

The successful implementation of renewable energy sources in the power network is challenging due to their variability and demands appropriate modeling and planning. Different approaches to the expansion planning problem are considered in the litera-

ture to determine the optimal direction of changes in the electrical grid. Generation expansion, transmission expansion, or a mix of both can be distinguished among recent results collected and reviewed in Skolfield and Escobedo (2021). In this paper, I propose a generation expansion planning problem focusing on the extension and integration of renewable energy sources.

In 2021, renewable generation constituted an all-time high of 30% in global electricity generation, being the result of impressive progress over the past decade where renewables capacity increased by 130%, reaching 3064 GW. The main drivers of the growth are solar PV and wind power, which increased installation capacity 21-fold and over 4-fold between 2010 and 2021, respectively. The observed increase in renewables capacity is a result of significant cost reductions caused by technological developments, high learning rates, policy support, and innovative financing models. According to International Renewable Energy Agency (2021a), the cost of electricity from utility-scale solar photovoltaics fell 85%, followed by concentrating solar power (68%), onshore wind (56%) and offshore wind (48%) between 2010 and 2020. Those statistics present substantial improvement in the competitiveness of solar and wind technologies, leading to a situation where the existing coal-fired capacity is less profitable than the new renewable capacity. Therefore, I focus on the extension of solar and wind power capacity in the proposed generation expansion planning model.

The integration of a high share of renewable energy sources into the electricity grid leads to the necessity of exploiting flexibility sources and planning them ahead of time. The flexibility of a power system allows to cope with the variability and uncertainty introduced by variable renewable generation in different time scales, from the very short to the long term, avoiding curtailment of renewable energy and providing a reliable supply of the demanded energy to customers.

The main sources of flexibility are dispatchable power plants, energy storage, demand response, and interconnectors for cross-border trade (see International Re-

newable Energy Agency 2018).

Power plants that can ramp up or down fast, have a low minimum operating level, and have fast start-up and shutdown times can serve as a source of flexibility. For example, hydro generators and open-cycle gas turbines are considered to be among the most flexible conventional generators.

Energy storage also gains interest as an approach to maintaining the flexibility of the power system by storing and dispatching energy. The most common type of electricity storage is pumped hydropower, but batteries are getting more attention as an alternative solution due to advancements in storage technology and reductions in storage costs. Storage systems are mainly characterized by the following parameters: *power capability* - the amount of power that can be provided, *storage capacity* - the amount of energy that can be stored and discharged per cycle, and *storage efficiency* - the ratio of the total discharged energy to the total charged energy in one cycle.

Demand response represents techniques for load reduction during peak usage or decrease of renewable production. It comprises direct load control by utilities, voluntary load reduction (usually activated by price signals), and dynamic demand relying on automated regulation of power usage. Those techniques operate as a virtual peaking plant that can ramp up very quickly to the full capacity.

Interconnectors provide flexibility to the power system by allowing for the transfer of a production surplus to a deficit area. It requires technical network connection between areas by building suitable transmission lines and operational agreements between interconnected systems.

Among the listed sources of flexibility, energy storage seems to be a promising technology for the integration of renewable energy sources. It can help to mitigate fluctuations in renewable energy generation by storing the excess energy when generation is high and releasing it when generation is low. Thereby, it increases renewable energy utilization and reduces curtailment. Furthermore, energy storage

can improve the power network stability and resilience by providing grid-balancing services and backup power. Energy storage can also be used as a peak shaving tool, helping to manage electricity consumption and reduce energy costs. It means that energy storage can enhance the power system operations from technical and economic perspectives. Therefore, I include it in the proposed generation expansion planning model as a source of flexibility supporting the integration of renewable energy generation.

In this paper, a multi-stage stochastic optimization model is formulated to evaluate the generation expansion in the power network necessary to phase out fossil fuels. The optimization problem consists of the first stage, representing the investment planning, and the consecutive stages, reflecting days of the operational planning. In the first stage, the model identifies the optimal location and capacity of the energy storage and new renewable generation units focusing on solar and wind power plants. In the subsequent stages, the stability and flexibility of the network are assessed in the optimization of the daily power network operations in hourly resolution. The proposed model aims to find optimal decisions that minimize investment and operating costs over the given time horizon.

The main contribution of this paper is formulating the generation expansion planning problem that considers the uncertainty of the demand and renewable generation, alternating current of the power flow, and multi-stage planning of the power network operations simultaneously. In the literature, generation expansion planning models vary widely in scope and resolution of time and space, as researchers often focus more on one of the above aspects to manage complexity.

The effective evaluation of the impact of investment decisions on the power system requires including operational planning in the model. In order to cover the full physical complexity, the operation of the power network should take into account the alternating current nature of power flows. As the AC OPF problem is an NP-hard nonconvex optimization problem, planners usually use a linearized DC

approximation model, (e.g. Lara et al. 2018).

Further, the impact of solar and wind variability has been noticed in the last few years, especially in power networks with aggressive targets for renewable generation. Therefore, the intermittency and unpredictability of renewable generation can not be neglected in the generation expansion planning model, which aims to effectively integrate high renewable energy shares. There are stochastic models in the literature, e.g., Pineda et al. (2016), proposing a market-focused approach with uncertainty in demand and renewable generation. Still, authors use DC approximation of AC OPF and two-stage formulation.

Lastly, the multi-stage formulation can enhance the assessment of the power system's stability and reliability. There are researchers considering multi-stage models, e.g., Hinojosa and Velasquez (2016), formulating multi-stage DC-based security-constrained generation capacity expansion planning problem. However, again, they use DC approximation in the power system operations or consider a deterministic model.

The above arguments indicate that the proposed generation expansion planning model is innovative and fills the gap in the existing literature by simultaneously incorporating all complexities in the model.

In addition, I consider not only the physics law of AC power flow but also the representation of the reactive power for renewable energy sources, particularly wind power. I use the approach introduced in Gil-González et al. (2020) to model the reactive power for wind power plants, where the limits depend on the capacity and power generation at the respective point in time. As the renewable generation is assumed to be random, it implies that the bounds are changing with every realization of the random process. This approach is not widely adopted in the literature, as most authors employ DC approximation, where the reactive power is completely omitted.

The expansion of renewable generation is driven by ambitious climate targets

aiming to reduce greenhouse gas emissions and involves the profound transformation of the power network infrastructure. The progress of the energy transition can be measured with the share of renewable generation covering power demand. In relation to generation expansion planning, this measure can be used to find an optimal investment strategy to achieve a given target. To support decision-makers following global policies, I incorporate the constraint that guarantees a given ratio of renewable generation covering power demand on a daily basis in the proposed optimization model. Any deviation from the target is penalized with the defined cost in the objective function. A similar constraint has already been implemented in Lara et al. (2018) but for a deterministic model and applying DC approximation of the power flow.

The proposed generation expansion planning model is a nonconvex optimization problem where the nonconvexity appears in the operational stages due to the alternating current nature of power flows. Due to the complexity, the formulated problem requires powerful tools to solve it. In this paper, I apply the solution strategy proposed in Chapter 3, built on convex relaxation introduced by Lavaei and Low (2012) and the SDDP algorithm. I also provide a detailed explanation of the required problem reformulations and the algorithm adaptation to this particular class of problems.

Finally, I present a case study where the generation expansion planning model is implemented for the modified version of the IEEE RTS-GMLC network. The results include an analysis of the optimal investment decisions for two seasons, comparing required storage and new renewable capacities for different daily renewable generation targets.

In summary, this paper proposes the generation expansion planning model, which considers the uncertainty, alternating current of the power flows, and multi-stage formulation simultaneously in contrast to the existing results in the literature. The optimization model provides optimal storage and new renewable capacity required to

phase out fossil fuels and ensure a given share of renewable generation covering power demand, minimizing total costs. The proposed generation expansion planning model can support decision-makers in determining the optimal direction of changes in the power infrastructure so they can effectively participate in the energy transition.

1.3   Structure of the Thesis

As the contribution of this thesis, I provide a framework to handle energy planning problems that incorporate a multi-stage formulation, finitely supported Markov structure of random processes and the alternating current nature of power flows. In consecutive chapters, I focus on different aspects and challenges in this class of problems. In Section 2, I develop a theory for discrete approximation of the Markov process involved in the linear stochastic optimization problem. I introduce the lattice distance, which enables the measurement of the error in optimal values resulting from replacing a complex Markov process with a simpler scenario lattice. In Chapter 3, I propose an effective solution method for the OPF problems under uncertainty. The strategy is built upon the convex relaxation of the power flow equations and SDDP algorithm. Lastly, in Chapter 4, I demonstrate the application of the developed theory for generation expansion planning problems in the case study for the modified IEEE RTS-GMLC network. Finally, Chapter 5 concludes the thesis, summarizing the results and discussing further research ideas.

Chapter 2

A Stability Result for Linear Markovian Stochastic Optimization Problems

written in collaboration with Prof. David Wozabal[1]

In this paper, we propose a semi-metric for Markov processes that allows to bound optimal values of linear Markovian stochastic optimization problems. Similar to existing notions of distance for general stochastic processes, our distance is based on transportation metrics. As opposed to the extant literature, the proposed distance is problem-specific, i.e., dependent on the data of the problem whose objective value we want to bound. As a result, we are able to consider problems with randomness in the constraints as well as in the objective function and, therefore, relax an assumption in the extant literature. We derive several properties of the proposed semi-metric and demonstrate its use in a stylized numerical example.

2.1   Introduction

Stochastic optimization is concerned with the solution of optimization problems that involve random quantities as data. Consequently, the decisions $x(\xi)$ depend on the values of a random process ξ, making stochastic optimization a problem in function spaces. Mirroring the situation in deterministic optimization, only a few stochastic optimization problems lend themselves to analytical treatment and allow for closed-form solutions. In the following, we, therefore, focus on discrete-time problems that are solved numerically.

The theory of stochastic optimization as well as the development of solution methods made great advances in the last decades. In particular, there exists a sound theory for two-stage stochastic optimization problems, i.e., problems with only one decision stage in the future (see Birge and Louveaux (2011), Shapiro et al. (2009) for an overview). Consequently, two-stage stochastic optimization is nowadays routinely applied by researchers and industry practitioners alike. State-of-the-art methods are based on discrete representations of the possibly continuous source of randomness in the form of a finite set of samples or scenarios. This can either be achieved by sample average approaches (see Shapiro et al. (2009) for an introduction) or by explicitly choosing representative scenarios. In this paper, we will focus on the latter.

Despite the abovementioned successes, it became clear quite early that the effort required to solve stochastic optimization does not scale well in the problem's size. More specifically, it has been shown that stochastic optimization problems exhibit a non-polynomial increase in complexity as the number of random variables increases Hanasusanto et al. (2016). The problem underlying these difficulties is the numerical evaluation of high dimensional integrals, which is, in turn, related to the problem of optimal discretization of probability distributions.

The situation is even more complicated for multi-stage problems, where we deal with random processes resulting in additional random variables in every stage and the issue of finding discretizations for conditional distributions. Consequently, it was
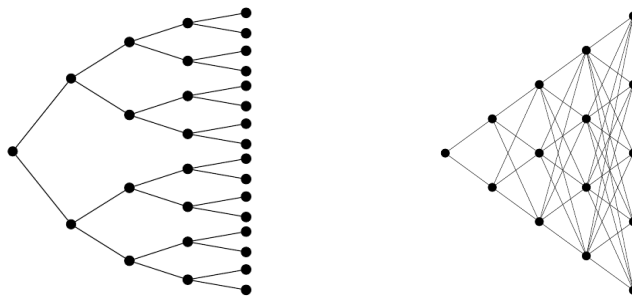
Figure 2.1: A scenario tree with 31 nodes representing 16 scenarios on the left and a scenario lattice with 15 nodes representing 120 scenarios on the right. The transition probabilities on the arcs are not depicted to keep the picture legible.

observed in Shapiro (2006, 2010) that solving multi-stage stochastic optimization problems is often practically intractable.

Notwithstanding these problems, there is a rich literature on multi-stage stochastic optimization. The majority of authors use scenario trees as a representation of discrete stochastic processes (see the left panel in Figure 2.1 for an illustration). In a scenario tree, nodes represent possible states of the world and are assigned to a point in time. All nodes at the same point in time are usually depicted at the same level of the tree. Possible transitions between nodes in consecutive stages are represented by probability-weighted arcs connecting the nodes. Consequently, the collection of transition probabilities between a node and the nodes of the next stage connected by arcs describes the distribution of the random process conditional on that node. Note that the requirement that the resulting graph is a tree implies that every node is allowed to have exactly one predecessor in the previous stage.

There are various ways to construct scenario trees for multi-stage stochastic programs (see Dupacová et al. (2000), Kaut and Wallace (2007) for surveys). In Høyland and Wallace (2001), Høyland et al. (2003), a recursive application of moment matching is presented. The approach is easy to understand and apply but suffers from an exponential explosion of nodes in the resulting trees as the number of stages increases. Furthermore, the method offers no theoretical insight regarding

the discretization error made when replacing the original process with the generated tree.

The papers Pennanen (2005, 2009) propose a method for the construction of scenario trees that is based on integration quadratures and ensures that the approximated problems based on scenario trees epi-converge to the true infinite-dimensional problem yielding convergence in optimal value as well as in optimal decisions. However, the results are asymptotic in nature, i.e., the approximation scheme doesn't offer guarantees for any given discrete approximation.

Another approach is based on the principle of bound-based constructions, see Casey and Sen (2005), Edirisinghe (1996), Frauendorfer (1996), Kuhn (2005). The idea is to construct two discrete stochastic programs that provide upper and lower bounds on the optimal value of the original problem.

The results in this paper extend a stream of literature that uses probability metrics to define notions of distance for stochastic processes and allows inference about the accuracy of approximating trees, see Dupacová et al. (2003), Heitsch and Römisch (2003, 2009), Pflug (2001), Pflug and Pichler (2012, 2014). The authors in Dupacová et al. (2003), Heitsch and Römisch (2003) consider a distance between discrete stochastic processes and assume that both processes are defined on the same probability space. This assumption is relaxed in Pflug and Pichler (2012, 2014) where a nested distance between value-and-information structures is developed, which can be applied to continuous processes. Heitsch and Römisch (2011), Heitsch et al. (2006) prove stability results using the sum of a L_r-distance and a filtration distance to bound objective values of a certain class of stochastic optimization problems.

Scenario trees are discrete approximations of general processes and, therefore, lend themselves to the construction of a general theory of stochastic optimization. However, the requirement that every node has only one predecessor makes it hard to construct scenario trees with many stages that model the conditional distributions

well, i.e., ensure that every node has a sufficient number of successors and, at the same time, avoid exponential growth of the number of nodes.

A possible way out of this dilemma is to restrict the type of stochastic optimization to problems with a Markovian structure where the random processes in the problem formulation are Markov processes Löhndorf et al. (2013) or, even more common, independent Pereira and Pinto (1991). In this setting, the *history* of random variables and decisions is condensed in the state variables of the problem, and there is no need to *remember* the whole history of the randomness and the decisions. This paves the way for leaner discretizations, which we call *scenario lattices* in this paper and which are similar to stochastic meshes used in option pricing Broadie and Glasserman (2004). In particular, a scenario lattice consists of the same building blocks as a scenario tree but relaxes the requirement that every node has only one predecessor and, therefore, solves the problem of the exponential explosion of the number of nodes as the number of stages grows (see the right panel in Figure 2.1). In the same way that a scenario tree is a natural representation of a general discrete stochastic process, a scenario lattice is a natural representation of a discrete Markov process.

Even though the abovementioned problem class is quite popular, there are no theoretical results on how to construct optimal scenario lattices. An exception is Bally and Pagès (2003a,b), who design an algorithm for the construction of scenario lattices for Brownian motions based on ideas of optimal quantization.

We mention that there is a large and well developed theory on the approximations of Markov decision processes (MDPs) that is concerned with similar questions as this article. Typical formulations of MDP problems feature finite state and action states as well as a stationary Markov process describing the randomness, which is potentially influenced by the actions taken by the decision maker.

The setting as well as the solution methods differ from our paper in several important ways. Firstly, methods for solving MDPs are almost exclusively based

on the discretization of the whole state space, leading to the well-known curse of dimensionality as the dimension of the state space grows. Consequently, methods to approximate MDPs either assume a finite or countable state and action space to start with (Bertsekas and Shreve 1978, Fox 1971, Langen 1981, Ren and Krogh 2002, White 1980, 1982) or discretize the state space to be able to solve the problem.

Furthermore, much of the work on approximations of MDPs deals with infinite horizon problems relying on the fact that optimal value functions are fixed points of the Bellman operator (Chow and Tsitsiklis 1991, Hinderer 2005, Ren and Krogh 2002, Saldi et al. 2017, White 1980, 1982).

Papers that deal with continuous state spaces usually impose (Lipschitz) continuity conditions on the probability transition kernels (Bertsekas and Shreve 1978, Dufour and Prieto-Rumeau 2012, 2013, 2015, Hinderer 2005, Müller 1997, Saldi et al. 2017), which we do not require.

The difference between our approach and the MDP literature is thus threefold: Firstly, we keep the *resource state* continuous in order to be able to solve the problems on the nodes of the scenario lattice by linear optimization. This avoids at least part of the curse of dimensionality usually encountered in dynamic programming. Second, unlike most of the literature on approximation of MDPs, we deal with finite horizon problems. Lastly, we do not assume any Lipschitz continuity of the Markov kernel.

With this paper, we contribute to the development of a theory for discrete approximations of Markov processes that can be used in stochastic programming. In particular, we propose a class of problem-specific semi-distances for Markov processes and show that the objective value of a certain class of linear stochastic optimization problems is Lipschitz continuous with respect to these distances. This lays the foundations for constructing scenario lattices approximating general Markov processes that, in turn, can be used to formulate approximating optimization problems. In particular, the results in this paper can be used to control the error that

results from replacing a stochastic optimization problem that is formulated using a complex (possibly continuous) Markov process with another, simpler problem using a compact scenario lattice instead of the original process. Furthermore, we discuss a LP formulation of our distance for discrete Markov processes, i.e., scenario lattices. We consider a multi-stage version of the well-known newsvendor problem to demonstrate how to use our results in practical problems.

Our approach is inspired by Pflug and Pichler (2012), who work on optimal scenario trees and general stochastic optimization problems. In contrast to Pflug and Pichler (2012), our approach is specialized to linear stochastic programs with a Markovian structure, which results in tighter bounds for this problem class and additionally allows for problems where the randomness does not only affect the objective function but also the feasible set. The latter makes it necessary to adopt a different technique of proof based on stability results for linear programs rather than the idea of transporting solutions from one problem to the other. While in the MDP literature there are papers that model differences in feasible sets in terms of the Hausdorff distance (Hinderer 2005), to the best of our knowledge, we are the first to propose stability results based on transportation distances that allow for problems where the feasible set depends on randomness in inequality constraints: Dupacová et al. (2003), Heitsch and Römisch (2003), Pflug and Pichler (2012, 2014) require the feasible set to be independent of randomness, while in Heitsch and Römisch (2011), Heitsch et al. (2006) the constraints involving random parameters are required to be equality constraints. Furthermore, we demonstrate that our distance yields tighter bounds than Pflug and Pichler (2012) for problems where the constraints do not depend on the random process.

This paper is structured as follows: In Section 2.2, we introduce some notation and discuss the problem setup. In Section 2.3, we define the problem-dependent lattice distance and establish some of its key properties. Section 2.4 contains the main results of the paper which allow to connect the lattice distance to optimal

values of linear stochastic programming problems, while Section 2.5 is devoted to the case of discretely supported processes representable by lattices and a numerical example. Section 2.6 concludes the paper.

2.2   Problem Description

We consider a class of discrete-time, finite horizon, and linear stochastic dynamic programming problems depending on a Markov process. The time periods in our problem are indexed by $t \in \mathbb{T} = \{0, 1, \ldots, T\}$, where the values at $t = 0$ represent the deterministic start state of the problem. We partition the state space in an *environmental state* ξ and a *resource state* S. The former is governed by a (possibly inhomogeneous) Markov process $\xi = (\xi_0, \xi_1, \ldots, \xi_T)$, $\xi_t : \Omega_t \to \mathbb{R}^{n_t}$ which is assumed to be independent of the decisions. Examples are prices, demand for a product, or weather-related variables such as temperature. The *resource state* S_t, on the other hand, describes the part of the state space that is influenced by the decision maker. Examples include inventory levels, states of machinery, and contractual obligations.

We equip the probability space Ω_t with the σ-algebra $\sigma_t = \sigma(\xi_t)$ generated by the random variable ξ_t and define the path space $\Omega = \Omega_0 \times \ldots \times \Omega_T$ and a corresponding σ-algebra $\mathcal{F} = \sigma_0 \otimes \ldots \otimes \sigma_T$. Note that we base our σ-algebras only on the random variables ξ_t and not on the whole history of random variables until t as it is usually done when working with scenario trees. Consequently, $\sigma_0, \sigma_1 \ldots, \sigma_T$ is not a filtration.

Furthermore, we define the paths for which the event $H \in \sigma_t$ occurs as

$$H_t^\Omega := \Omega_0 \times \Omega_1 \times \ldots \times \Omega_{t-1} \times H \times \Omega_{t+1} \times \ldots \times \Omega_T$$

and the corresponding σ-algebra as

$$\sigma_t^\Omega = \{\Omega_0 \times \ldots \times \Omega_{t-1} \times H \times \Omega_{t+1} \times \ldots \times \Omega_T : H \in \sigma_t\} = \left\{H_t^\Omega : H \in \sigma_t\right\}.$$

The distribution of ξ is described by a sequence of Markov kernels, and we write $P_t^{\omega_{t-1}}$ for the distribution of ξ_t given $\omega_{t-1} \in \Omega_{t-1}$. The kernel as a function from Ω_{t-1} to the set of probability measures on Ω_t is σ_{t-1}-measurable Pollard (2002). For a given sequence of Markov kernels, we denote $\omega = (\omega_0, \ldots, \omega_T)$ and define the distribution on Ω as

$$P(H) := \int_{\Omega_0} \ldots \int_{\Omega_T} \mathbb{1}_H(\omega) P_T^{\omega_{T-1}}(d\omega_T) \ldots P_1^{\omega_0}(d\omega_1) P_0(d\omega_0)$$

for every $H \in \mathcal{F}$.

We consider stochastic optimization problems that can be written as

$$V_0(S_0, \xi_0) = \begin{cases} \max_{x,S} & \mathbb{E} \left(\sum_{t=0}^{T} c_t(\xi_t)^\top x_t \right) \\ \text{s.t.} & (x_t, S_{t+1}) \in \mathcal{X}_t(S_t, \xi_t) \quad \forall t \in \mathbb{T} \end{cases} \tag{2.1}$$

with $x = (x_0, \ldots, x_t)$, $S = (S_1, \ldots, S_{T+1})$, $S_t \in \mathbb{R}^{k_t}$ and feasible sets

$$\mathcal{X}_t(S_t, \xi_t) = \left\{ (x_t, S_{t+1}) : \begin{array}{l} A_{1,t} x_t \leq b_{1,t}(\xi_t) + C_{1,t} S_t \\ A_{2,t} x_t = S_{t+1} \\ A_{2,t} x_t \leq b_{2,t+1} \\ x_t, S_{t+1} \geq 0 \end{array} \right\}, \tag{2.2}$$

which we assume to be compact. Note that the data of the problem depends on the stochastic process ξ via the functions $\xi_t \mapsto c_t(\xi_t)$ and $\xi_t \mapsto b_{1,t}(\xi_t)$, which we assume to be continuous.

We assume that for planning in stage t, the decision maker knows S_t, i.e., the system's resource state at the beginning of the period as well as ξ_t, i.e., the realization of the Markov process in period t. Given this information the feasible set for the decision x_t as well as the definition of S_{t+1} can be expressed using linear inequality constraints. The decisions x_t are auxiliary decision variables in stage t that are not part of the resource state. Note that in order for the problem to be feasible $b_{2,t+1} \geq 0$

has to hold. The combination of constraints in (2.1) ensures that

$$0 \leq S_{t+1} = A_{2,t} x_t \leq b_{2,t+1},$$

i.e., that the feasible region for S_{t+1} is box-constrained and therefore compact.

Remark 2.1. *Usually, we would expect a state transition equation of the form* $S_{t+1} = S_t + A x_t$. *However, since we want to make the proposed distance independent of the resource state, we formulate the state transition using* x_t. *More specifically, we assign* S_t *to a subset of variables in* x_t *in the first constraint. The state transition is subsequently modeled in the equality constraint using those variables instead of* S_t. *Alternatively, we could assign* S_{t+1} *to variables in* x_t *in the equality constraint and then formulate the state transition using the first inequality constraint. We refer to the example in Section 2.5 for an illustration of this principle.*

Because of its recursive structure, problem (2.1) can be equivalently written in terms of its dynamic programming equations using value functions, i.e.,

$$V_t(S_t, \xi_t) = \begin{cases} \max\limits_{x_t, S_{t+1}} & c_t(\xi_t)^\top x_t + \mathbb{E}\left(V_{t+1}(S_{t+1}, \xi_{t+1}) | \xi_t\right) \\ \text{s. t.} & (x_t, S_{t+1}) \in \mathcal{X}_t(S_t, \xi_t) \end{cases} \quad \forall t \in \mathbb{T} \quad (2.3)$$

and $V_{T+1}(S_{T+1}, \xi_{T+1}) \equiv 0$ or, more generally, a known piecewise linear concave function. Since ξ is a Markov process and V_t as well as the decisions (x_t, S_{t+1}) only depend on the current state (S_t, ξ_t), we call the problem a stochastic optimization problem with Markovian structure.

If we are dealing with discrete Markov processes, the expectations of the value functions V_t, which are concave functions of the resource state, can be written as a minimum of finitely many affine functions. We formalize this well-known fact in the following lemma whose proof can be found, for example, in Löhndorf et al. (2013), Philpott and Guan (2008), Shapiro (2011).

Lemma 2.1. *If* ξ *is finitely supported, then for every realization of* ξ_t, $S_{t+1} \mapsto$

$\mathbb{E}\left(V_{t+1}(S_{t+1}, \xi_{t+1})|\xi_t\right)$ *is a concave, polyhedral function. In particular, there are coefficients* $b^i_{3,t+1}(\xi_t) \in \mathbb{R}$ *and row vectors* $C^i_{3,t+1}(\xi_t) \in \mathbb{R}^k$ *for* $i = 1, \ldots, m_{t+1}(\xi_t)$ *such that*

$$\mathbb{E}\left(V_{t+1}(S_{t+1}, \xi_{t+1})|\xi_t\right) = \min_{i=1,\ldots,m_{t+1}(\xi_t)} b^i_{3,t+1}(\xi_t) + C^i_{3,t+1}(\xi_t)S_{t+1},$$

where $m_{t+1}(\xi_t)$ *is the number of affine functions required to model*

$$\mathbb{E}\left(V_{t+1}(S_{t+1}, \xi_{t+1})|\xi_t\right).$$

2.3   A Distance for Markov Processes

In order to introduce the concept of a distance between Markov processes, we first recall the Wasserstein or Kantorovich distance for distributions Kantorovich (1942), Villani (2003). Loosely speaking, the Wasserstein distance is defined as the total cost of passing from a given distribution to a desired one by *moving* probability mass accordingly.

Definition 2.1. *Let* $\xi : (\Omega, \mathcal{A}) \to \mathbb{R}^n$ *and* $\tilde{\xi} : (\tilde{\Omega}, \tilde{\mathcal{A}}) \to \mathbb{R}^n$ *be two random vectors with distributions* P *and* $\tilde{P}$, *respectively. The Wasserstein distance of order* r $(r \geq 1)$ *between* ξ *and* $\tilde{\xi}$ *is defined as*

$$W_r(\xi, \tilde{\xi}) = \begin{cases} \inf_{\pi} \left(\int_{\Omega \times \tilde{\Omega}} \|\xi(\omega) - \tilde{\xi}(\tilde{\omega})\|_r^r \, \pi\,(d\omega, d\tilde{\omega}) \right)^{\frac{1}{r}} \\ s.t. \quad \pi(H \times \tilde{\Omega}) = P(H) \quad \forall H \in \mathcal{A}, \\ \qquad \pi(\Omega \times \tilde{H}) = \tilde{P}(\tilde{H}) \quad \forall \tilde{H} \in \tilde{\mathcal{A}}, \end{cases} \tag{2.4}$$

where the infimum is taken over all probability measures π *on* $(\Omega \times \tilde{\Omega}, \mathcal{A} \otimes \tilde{\mathcal{A}})$.

Remark 2.2. *Note that, following Pflug and Pichler (2012), we define* W_r *as a distance between two random vectors* $\xi : \Omega \to \mathbb{R}^n$ *and* $\tilde{\xi} : \Omega \to \mathbb{R}^n$ *instead of between two distributions* P *and* $\tilde{P}$. *However, in order for* W_r *to be well defined, information*

on the probability measures P and $\tilde{P}$ on Ω and $\tilde{\Omega}$ is required, as can be seen from (2.4).

In particular, when changing P and $\tilde{P}$ while holding ξ and $\tilde{\xi}$ constant, the image measure of ξ and $\tilde{\xi}$ and therefore also W_r changes. By a slight abuse of notation, we consider ξ and $\tilde{\xi}$ to contain the information on the probability spaces (Ω, P) and $(\tilde{\Omega}, \tilde{P})$, i.e., as mappings $\xi : (\Omega, P) \to \mathbb{R}^n$ and $\tilde{\xi} : (\tilde{\Omega}, \tilde{P}) \to \mathbb{R}^n$ in the same way that Pflug and Pichler (2012) do, when defining nested distributions.

Remark 2.3. *The above problem is bounded, and an optimal transportation measure π exists due to the weak compactness of the set of transportation plans (see Villani (2003), Lemma 4.4). Furthermore, according to the famous Kantorovich-Rubinstein Theorem, for $r = 1$, the dual of (2.4) can be written as the following maximization problem*

$$W_1(\xi, \tilde{\xi}) = \begin{cases} \sup\limits_{f} & \left(\int f dP - \int f d\tilde{P} \right) \\ s.t. & \mathrm{Lip}(f) \leq 1, \end{cases}$$

where $Lip(f)$ is the Lipschitz constant of f.

Clearly, for a two-stage stochastic optimization problem

$$v(P) = \begin{cases} \inf\limits_{x} & f(x) + \mathbb{E}_P(Q(x,\xi)) \\ s.t. & x \in \mathcal{X} \end{cases} \quad, \quad Q(x,\xi) = \begin{cases} \inf\limits_{y} & g(y,\xi) \\ s.t. & y \in \mathcal{Y}(x) \end{cases}$$

with

$$|Q(x,\xi) - Q(x,\tilde{\xi})| \leq L \, \|\xi - \tilde{\xi}\|_1 \quad \forall x \in \mathcal{X}, \tag{2.5}$$

we have

$$v(P) - v(\tilde{P}) \leq \mathbb{E}_P(Q(\tilde{x}^*, \xi)) - \mathbb{E}_{\tilde{P}}(Q(\tilde{x}^*, \tilde{\xi})) \leq L \, W_1(\xi, \tilde{\xi})$$

where $\tilde{x}^*$ is the optimal solution for $v(\tilde{P})$. By symmetry, it follows that

$$|v(P) - v(\tilde{P})| \leq L \, W_1(\xi, \tilde{\xi}),$$

i.e., the objective value of the two-stage stochastic program is Lipschitz continuous with respect to W_1, as long as the cost-to-go function Q is Lipschitz in ξ. This was first recognized in Römisch and Schultz (1991).

The authors in Pflug and Pichler (2012, 2014) generalize these ideas to a multi-stage setting using the notion of nested distributions, which correspond to *generalized* scenario trees. Based on a modified transportation problem and an assumption similar to the uniform Lipschitz property in (2.5), they obtain a distance with respect to which the objective value of a general multi-stage problem is Hölder continuous, see Section 2.4 for more details.

We aim for a similar result for scenario lattices and problems of the form (2.1). Additionally, we relax one major assumption in the abovementioned approaches, namely that randomness enters the problem only in the objective function. Observe that the argument above hinges on the fact that the set $\mathcal{Y}$ does not depend on ξ. The same restriction applies to the results on multi-period problems in Pflug and Pichler (2012, 2014).

We begin with analyzing the following simple deterministic linear optimization problem, which is of a similar structure as (2.3), with the second last inequality constraint and the second term in the objective function, y, modeling the piecewise linear value function (see Lemma 2.1)

$$
\max_{x \in \mathbb{R}^n, y \in \mathbb{R}, z \in \mathbb{R}^k} \left\{ c_1^\top x + y : \begin{array}{l} A_1 x \leq b_1 \\ A_2 x = z \\ A_2 x \leq b_2 \\ \mathbb{1}_m y \leq b_3 + C_3 z \\ x, z \geq 0 \end{array} \right\}.
\tag{2.6}
$$

Furthermore, we define $\mathbb{1}_m \in \mathbb{R}^m$ as the column vector of ones, assume that C_3 has m rows and k columns, and assume that the other matrices and vectors are of fitting dimension.

First, we prove the following result which is motivated by Hoffman's lemma Hoffman (1952) and, in particular, its discussion in Shapiro et al. (2009), Theorem 7.11 and Theorem 7.12. For what follows, we adopt the notational convention that the addition of a vector $x = (x_1, \ldots, x_n)$ and a scalar $y \in \mathbb{R}$ is to be interpreted pointwise, i.e., results in the vector $(x_1 + y, \ldots, x_n + y)$ and, similarly, inequalities of the form $x \leq y$ are interpreted pointwise as well.

Lemma 2.2. *Let $V(b_1)$ be the optimal value of problem (2.6) dependent on the parameter b_1 and assume that there is a $\kappa \geq 0$ with*

$$\left\| C_3^\top \lambda \right\|_\infty \leq \kappa$$

for all $\mathbb{R}^m \ni \lambda \geq 0$ with $|\mathbb{1}_m^\top \lambda| \leq 2$. Then for any b_1, b_1' for which (2.6) is feasible

$$|V(b_1) - V(b_1')| \leq \gamma(A_1, A_2, \kappa, c_1) \left\| b_1 - b_1' \right\|_1. \tag{2.7}$$

where $\gamma(A_1, A_2, \kappa, c_1) = \max_{\lambda \in \mathrm{ext}(\Gamma)} ||\lambda_2||_\infty < \infty$ and $\mathrm{ext}(\Gamma)$ are the vertices of the polyhedron

$$\Gamma = \left\{ (\lambda_2, \lambda_3, \lambda_4, \lambda_6, \lambda_7) : \begin{array}{l} \left\| A_1^\top \lambda_2 + A_2^\top(\lambda_3 + \lambda_4) - \lambda_6 \right\|_\infty \leq 1 + \|c_1\|_\infty \\ \|\lambda_3 - \lambda_7\|_\infty \leq 1 + \kappa \\ \lambda_2, \lambda_4, \lambda_6, \lambda_7 \geq 0 \end{array} \right\}.$$

Proof. We start by rewriting (2.6) as

$$\max_{t \in \mathbb{R}, x \in \mathbb{R}^n, y \in \mathbb{R}, z \in \mathbb{R}^k} \left\{ t : \begin{array}{l} t - c_1^\top x - y \leq 0 \\ A_1 x \leq b_1 \\ A_2 x = z \\ A_2 x \leq b_2 \\ \mathbb{1}_m y \leq b_3 + C_3 z \\ x, z \geq 0 \end{array} \right\}. \tag{2.8}$$

Denote by $\mathcal{M}(b_1)$ the set of feasible points of problem (2.8) and consider a point

$\alpha = (x, y, z, t) \in \mathcal{M}(b_1)$. Note that for any $a \in \mathbb{R}^n$, $||a||_1 = \sup\limits_{||u||_\infty \leq 1} u^\top a$ and define $u = (u_1, u_2, u_3, u_4)$ with u_i corresponding to the respective entries in α, i.e., $u_1 \in \mathbb{R}^n$, $u_2 \in \mathbb{R}$ and so on. Therefore, we have

$$\text{dist}(\alpha, \mathcal{M}(b_1')) = \inf_{\alpha' \in \mathcal{M}(b_1')} ||\alpha - \alpha'||_1 = \inf_{\alpha' \in \mathcal{M}(b')} \sup_{||u||_\infty \leq 1} u^\top(\alpha - \alpha')$$

$$= \sup_{||u||_\infty \leq 1} \inf_{\alpha' \in \mathcal{M}(b_1')} u^\top(\alpha - \alpha').$$

By a change of variables defining $w = (w_1, w_2, w_3, w_4) = \alpha - \alpha'$ and using linear optimization duality with $\lambda = (\lambda_1, \lambda_2, \lambda_3, \lambda_4, \lambda_5, \lambda_6, \lambda_7)$, we have

$$\inf_{\alpha' \in \mathcal{M}(b_1')} u^\top(\alpha - \alpha') = \inf_{w \in \tilde{\mathcal{M}}(b_1')} u^\top w = \sup_{\lambda \in \tilde{\mathcal{M}}^*(u)} \lambda_1^\top(t - c_1^\top x - y)$$

$$+ \lambda_2^\top(A_1 x - b_1') + \lambda_4^\top(A_2 x - b_2) + \lambda_5^\top(\mathbb{1}_m y - b_3 - C_3 z) + \lambda_6^\top(-x) + \lambda_7^\top(-z),$$

where

$$\tilde{\mathcal{M}}(b_1') = \left\{ w : \begin{array}{l} t - c_1^\top x - y \leq w_4 - c_1^\top w_1 - w_2 \\ A_1 x - b_1' \leq A_1 w_1 \\ A_2 w_1 - w_3 = 0 \\ A_2 x - b_2 \leq A_2 w_1, \\ \mathbb{1}_m y - b_3 - C_3 z \leq \mathbb{1}_m w_2 - C_3 w_3 \\ -x \leq -w_1 \\ -z \leq -w_3 \end{array} \right\}$$

and

$$\tilde{\mathcal{M}}^*(u) = \left\{ \lambda : \begin{array}{l} -c_1 \lambda_1 + A_1^\top \lambda_2 + A_2^\top \lambda_3 + A_2^\top \lambda_4 - \lambda_6 = u_1 \\ -\lambda_1 + \mathbb{1}_m^\top \lambda_5 = u_2 \\ \lambda_3 - C_3^\top \lambda_5 - \lambda_7 = u_3 \\ \lambda_1 = u_4 \\ \lambda_1, \lambda_2, \lambda_4, \lambda_5, \lambda_6, \lambda_7 \geq 0 \end{array} \right\}.$$

Consequently we obtain that

$$\text{dist}(\alpha, \mathcal{M}(b_1')) = \sup_{||u||_\infty \leq 1, \lambda \in \tilde{\mathcal{M}}^*(u)} \lambda_1^\top (t - c_1^\top x - y) + \lambda_2^\top (A_1 x - b_1') \tag{2.9}$$

$$+ \lambda_4^\top (A_2 x - b_2) + \lambda_5^\top (\mathbb{1}_m y - b_3 - C_3 z) + \lambda_6^\top (-x) + \lambda_7^\top (-z).$$

The right-hand side of (2.9) has a finite optimal value (since the left-hand side of (2.9) is finite) and, hence, has an optimal solution $(\hat{u}, \hat{\lambda})$. It follows that

$$\text{dist}(\alpha, \mathcal{M}(b_1')) = \hat{\lambda}_1^\top (t - c_1^\top x - y) + \hat{\lambda}_2^\top (A_1 x - b_1') + \hat{\lambda}_4^\top (A_2 x - b_2)$$

$$+ \hat{\lambda}_5^\top (\mathbb{1}_m y - b_3 - C_3 z) + \hat{\lambda}_6^\top (-x) + \hat{\lambda}_7^\top (-z).$$

Since $\alpha \in \mathcal{M}(b_1)$ and $\hat{\lambda}_1, \hat{\lambda}_2, \hat{\lambda}_4, \hat{\lambda}_5, \hat{\lambda}_6, \hat{\lambda}_7 \geq 0$, we have

$$\text{dist}(\alpha, \mathcal{M}(b_1')) \leq \hat{\lambda}_2^\top (A_1 x - b_1') = \hat{\lambda}_2^\top (A_1 x - b_1) + \hat{\lambda}_2^\top (b_1 - b_1')$$

$$\leq \hat{\lambda}_2^\top (b_1 - b_1') \leq ||\hat{\lambda}_2||_\infty ||b_1 - b_1'||_1.$$

To find a bound for $||\hat{\lambda}_2||_\infty$, we analyze the extreme points of the feasible set

$$\Gamma' = \left\{ \lambda : \begin{array}{l} ||-c_1 \lambda_1 + A_1^\top \lambda_2 + A_2^\top \lambda_3 + A_2^\top \lambda_4 - \lambda_6||_\infty \leq 1 \\ ||-\lambda_1 + \mathbb{1}_m^\top \lambda_5||_\infty \leq 1 \\ ||\lambda_3 - C_3^\top \lambda_5 - \lambda_7||_\infty \leq 1 \\ ||\lambda_1||_\infty \leq 1 \\ \lambda_1, \lambda_2, \lambda_4, \lambda_5, \lambda_6, \lambda_7 \geq 0 \end{array} \right\}.$$

Since we know that $||\lambda_1||_\infty \leq 1$, we can replace the constraint

$$\left\| -\lambda_1 + \mathbb{1}_m^\top \lambda_5 \right\|_\infty \leq 1$$

with

$$|\mathbb{1}_m^\top \lambda_5| \leq 2$$

and the constraint

$$\left\| -c_1\lambda_1 + A_1^\top \lambda_2 + A_2^\top \lambda_3 + A_2^\top \lambda_4 - \lambda_6 \right\|_\infty \leq 1$$

with

$$\left\| A_1^\top \lambda_2 + A_2^\top (\lambda_3 + \lambda_4) - \lambda_6 \right\|_\infty \leq 1 + \left\| c_1 \right\|_\infty.$$

Then using the assumption that $\left\| C_3^\top \lambda_5 \right\|_\infty \leq \kappa$ we can substitute

$$\left\| \lambda_3 - C_3^\top \lambda_5 - \lambda_7 \right\|_\infty \leq 1$$

with the constraint

$$\| \lambda_3 - \lambda_7 \|_\infty \leq 1 + \kappa$$

to increase the feasible set of problem (2.9), and hence increase its optimal value. Consequently,

$$\max_{\lambda \in \Gamma'} \| \lambda_2 \|_\infty \leq \max_{\lambda \in \Gamma} \| \lambda_2 \|_\infty$$

with

$$\Gamma = \left\{ (\lambda_2, \lambda_3, \lambda_4, \lambda_6, \lambda_7) : \begin{array}{l} \| A_1^\top \lambda_2 + A_2^\top (\lambda_3 + \lambda_4) - \lambda_6 \|_\infty \leq 1 + \| c_1 \|_\infty \\ \| \lambda_3 - \lambda_7 \|_\infty \leq 1 + \kappa \\ \lambda_2, \lambda_4, \lambda_6, \lambda_7 \geq 0 \end{array} \right\}.$$

Note that the optimal value remains bounded when replacing Γ' with Γ, since if there would be a ray

$$R = \left\{ \lambda(\alpha) = \lambda^0 + \alpha \lambda^1 : \alpha \in [0, \infty) \right\}$$

in Γ such that $\| \lambda_2(\alpha) \|_\infty \xrightarrow{\alpha \to \infty} \infty$ and at the same time

$$\left\| A_1^\top \lambda_2(\alpha) + A_2^\top (\lambda_3(\alpha) + \lambda_4(\alpha)) - \lambda_6(\alpha) \right\|_\infty \leq 1 + \| c_1 \|_\infty, \quad \forall \alpha > 0,$$

this would imply that

$$\alpha||(A_1^\top \lambda_2^1 + A_2^\top(\lambda_3^1 + \lambda_4^1) - \lambda_6^1)||_\infty - ||A_1^\top \lambda_2^0 + A_2^\top(\lambda_3^0 + \lambda_4^0) - \lambda_6^0||_\infty$$

$$\leq \left\| A_1^\top \lambda_2(\alpha) + A_2^\top(\lambda_3(\alpha) + \lambda_4(\alpha)) - \lambda_6(\alpha) \right\|_\infty$$

$$\leq 1 + \|c_1\|_\infty, \quad \forall \alpha > 0$$

and therefore

$$||A_1^\top \lambda_2^1 + A_2^\top(\lambda_3^1 + \lambda_4^1) - \lambda_6^1||_\infty = 0. \tag{2.10}$$

In this case, we can define $\lambda^{1\prime} = (0, \lambda_2^1, \lambda_3^1, \lambda_4^1, 0, \lambda_6^1, \lambda_7^1)$ and a ray

$$R' = \left\{ 0 + \alpha\lambda^{1\prime} : \alpha \in [0, \infty) \right\}.$$

Clearly, points in R' fulfill the first constraint of Γ' by (2.10), the second one since the first and the fifth component of $\lambda^{1\prime}$ are zero, and the third since $\lambda_3^1 = \lambda_7^1$ has to hold for R to be in Γ. This means that R' is contained in Γ', contradicting the boundedness of the original problem. Hence, the modified problems remain bounded, and therefore, the maximum is taken at a vertex of the polyhedron Γ.

The polyhedral set Γ has a finite number of extreme points. Hence, $||\hat{\lambda}_2||_\infty$ can be bounded by $\gamma(A_1, A_2, \kappa, c_1)$ which depends on A_1, A_2, κ, c_1 and

$$\text{dist}(\alpha, \mathcal{M}(b_1')) \leq ||\hat{\lambda}_2||_\infty \, ||b_1 - b_1'||_1 \leq \gamma(A_1, A_2, \kappa, c_1) \, ||b_1 - b_1'||_1. \tag{2.11}$$

Assume that $\alpha = (x, y, z, t)$ is the optimal solution of problem (2.8) and $t = V(b_1)$. Let further $\alpha' \in \mathcal{M}(b_1')$ be a point minimizing the distance $\text{dist}(\alpha, \mathcal{M}(b_1'))$. Then (2.11) implies

$$|t - t'| \leq \gamma(A_1, A_2, \kappa, c_1) \, ||b_1 - b_1'||_1$$

and we obtain

$$V(b_1) - V(b_1') \leq V(b_1) - t' = t - t' \leq \gamma(A_1, A_2, \kappa, c_1) \, ||b_1 - b_1'||_1.$$

Analogously, we get

$$V(b_1') - V(b_1) \leq \gamma(A_1, A_2, \kappa, c_1) \left\| b_1 - b_1' \right\|_1$$

and finally (2.7). $\qquad\qquad\qquad\qquad\qquad\qquad\qquad\qquad\qquad\qquad\qquad\qquad\square$

Remark 2.4. *The matrix C_3 represents slopes of the linear functions modeling value function for discrete distributions (see Lemma 2.1). Applying Lemma 2.2 to the problem (2.3), C_3 may differ depending on the stage t and the state of the random process ξ_t. Therefore, we write $C_{3,t}(\xi_{t-1})$ for the matrix of slopes of the linear functions used in the representation of $\mathbb{E}\left(V_t(S_t, \xi_t)|\xi_{t-1}\right)$ and choose $\kappa_t(\xi_{t-1})$ as follows*

$$\kappa_t(\xi_{t-1}) = \max\left\{ \left\| C_{3,t}(\xi_{t-1})^\top \lambda \right\|_\infty : \lambda \geq 0, \ |\mathbb{1}_{m_t(\xi_{t-1})}^\top \lambda| \leq 2 \right\} = 2 \max_{i,j} |C_{3,t}^{ij}(\xi_{t-1})|$$

where $C_{3,t}^{ij}$ is the entry in the ith row and j^{th} column of the matrix $C_{3,t}$.

Remark 2.5. *For continuous distributions, the matrix C_3 doesn't exist. However, in our formulation of the problem $S_t \mapsto \mathbb{E}\left(V_t(S_t, \xi_t)|\xi_{t-1}\right)$ is a continuous function on the compact set of permissible S_t for every ξ_{t-1}, hence it is Lipschitz continuous with Lipschitz constant $L_t(\xi_{t-1})$ on this set. Therefore, in this case we use $\kappa_t(\xi_{t-1}) = 2L_t(\xi_{t-1})$ in the definition of the distance below.*

An alternative proof of the above lemma could be based on the Lipschitz continuity of the feasible set with respect to the Hausdorff metric as shown in Robinson (1975), Walkup and Wets (1969). However, the aforementioned papers do not provide any instruction for calculation of the Lipschitz constant, which makes it difficult to apply their results in concrete optimization problems. Our approach does not suffer from this problem since it allows to explicitly bound the variation in the objective as a function of the right-hand side data of the problem (2.6). Next, we will prove a similar result to bound the objective value when the objective coefficient c_1 changes.

Lemma 2.3. *If $V(c_1)$ is the optimal value of problem (2.6) in dependence on the objective value coefficient c_1, then*

$$|V(c_1) - V(\tilde{c}_1)| \leq \phi(A_1, b_1, A_2, b_2)||c_1 - \tilde{c}_1||_1$$

with $\phi(A_1, b_1, A_2, b_2) = \max_{x \in \text{ext}(\Phi)} ||x||_\infty$ and

$$\Phi = \{x \in \mathbb{R}^n : A_1 x \leq b_1, A_2 x \leq b_2, A_2 x \geq 0, x \geq 0\}.$$

Proof. Let (x^*, y^*) be an optimal solution to $V(c_1)$, then we have

$$V(c_1) = c_1^\top x^* + y^* = c_1^\top x^* + y^* - \tilde{c}_1^\top x^* + \tilde{c}_1^\top x^* =$$
$$= (c_1 - \tilde{c}_1)^\top x^* + \tilde{c}_1^\top x^* + y^* \leq ||c_1 - \tilde{c}_1||_1 ||x^*||_\infty + V(\tilde{c}_1).$$

By symmetry, this implies

$$|V(c_1) - V(\tilde{c}_1)| \leq \max(||x^*||_\infty, ||\tilde{x}^*||_\infty)||c_1 - \tilde{c}_1||_1$$

for an optimal solution $(\tilde{x}^*, \tilde{y}^*)$ to $V(\tilde{c}_1)$. Notice that the set of feasible points is invariant with respect to the parameter c_1. Hence, x^* and $\tilde{x}^*$ can be selected as extreme points of the same polyhedral set

$$\Phi = \{x \in \mathbb{R}^n : A_1 x \leq b_1, A_2 x \leq b_2, A_2 x \geq 0, x \geq 0\}.$$

Φ depends on A_1, b_1, A_2, b_2 and has a finite number of vertices. Therefore $||x^*||_\infty$ and $||\tilde{x}^*||_\infty$ can be bounded by a constant $\phi(A_1, b_1, A_2, b_2)$ for which

$$|V(c_1) - V(\tilde{c}_1)| \leq \phi(A_1, b_1, A_2, b_2)||c_1 - \tilde{c}_1||_1$$

finishing the proof. $\square$

Remark 2.6. *When applying the above lemma to the problem (3), $b_{1,t}(\xi_t) + C_{1,t} S_t$ corresponds to the second parameter of ϕ. Since we would like to avoid dependence of our distance on the resource state, we note that ϕ is increasing with respect to this*

parameter and replace $b_{1,t}(\xi_t) + C_{1,t}S_t$ *by* $b_{1,t}(\xi_t) + C_{1,t}^+ b_{2,t}$ *where* $C_{1,t}^+ = (\max(c_{i,j}, 0))_{i,j}$
and $c_{i,j}$ *are the entries in the matrix* $C_{1,t}$*. Since* $S_t \geq 0$ *and* $b_{2,t} \geq 0$*, we thereby increase the size of the polyhedron* Γ *and thus make the bound slightly looser but independent of* S_t*.*

Note that the problems in (2.3) fulfill the assumptions of Lemma 2.2 and Lemma 2.3. Equipped with these results, we define a transportation distance between two Markov processes. The distance is defined for *a given problem* of the form (2.1), i.e., we do not propose one distance but a whole family of problem-specific distances, which differ in the matrices and vectors used to define the constants γ and ϕ in Lemma 2.2 and Lemma 2.3. To avoid cluttered notation, we write

$$\gamma_t(\xi_t, \tilde{\xi}_t) = \gamma(A_{1,t}, A_{2,t}, \min\{\kappa_{t+1}(\xi_t), \tilde{\kappa}_{t+1}(\tilde{\xi}_t)\}, c_t(\xi_t))$$

and

$$\phi_t(\xi_t) = \phi(A_{1,t}, b_{1,t}(\xi_t) + C_{1,t}^+ b_{2,t}, A_{2,t}, b_{2,t+1}).$$

Furthermore, we omit the explicit dependence of ξ on ω wherever no confusion can arise, i.e., write ξ instead of $\xi(\omega)$.

Remark 2.7. *Note that to ensure measurability of* ϕ_t *and* γ_t *we have to use the universal sigma algebra, which is a natural extension of the Borel sigma algebra fitting for dynamic programming. See Bertsekas and Shreve (1978), Chapter 7 for an in-depth treatment of the subject and Bertsekas (2013), Appendix C for a short primer.*

In particular, we mention that the vertices of the polyhedra in the proofs of Lemma 2 and Lemma 3 change continuously with the right-hand sides of the linear inequality constraints almost everywhere. The functions γ_t *and* ϕ_t *are, therefore, Borel measurable due to the Borel measurability of the functions* c_t *and* b_t*.*

Furthermore, standard arguments yield that, by Borel measurability of the Markov

kernel, the functions

$$(S_t, \xi_{t-1}) \mapsto \mathbb{E}(V_t(S_t, \xi_t)|\xi_{t-1})$$

are lower semi-analytic. Hence, the function

$$f(S_t, S_t', \xi_{t-1}) = \frac{\mathbb{E}(V_t(S_t, \xi_t) - V_t(S_t', \xi_t)|\xi_{t-1})}{S_t - S_t'}$$

is lower semi-analytic on $\mathcal{Y} \times \mathbb{R}^{n_{t-1}}$ with $\mathcal{Y} = \left\{(x, y) \in \mathbb{R}^{k_t} \times \mathbb{R}^{k_t} : x \neq y\right\}$. It follows from Bertsekas (2013), Proposition C.1 that

$$\xi_{t-1} \mapsto \kappa_t(\xi_{t-1}) = \sup_{S_t \neq S_t'} f(S_t, S_t', \xi_{t-1})$$

is lower semi-analytic and, therefore, universally measurable.

Consequently, we interpret all integrals as integrals with respect to the unique extensions of measures with respect to the universal sigma algebra (see Bertsekas and Shreve 1978).

Definition 2.2. *Let ξ and $\tilde{\xi}$ be two Markov processes defined on probability spaces Ω and $\tilde{\Omega}$, respectively, and P and $\tilde{P}$ corresponding probability measures on Ω and $\tilde{\Omega}$. We define a lattice distance for the problem (2.1) as*

$$D_L(\xi, \tilde{\xi}) = \begin{cases} \inf_{\pi} \int_{\Omega \times \tilde{\Omega}} d(\xi(\omega), \tilde{\xi}(\tilde{\omega}))\pi(d\omega, d\tilde{\omega}) \\ s.t. \quad \pi_t^{\omega_{t-1}, \tilde{\omega}_{t-1}}(H_t \times \tilde{\Omega}_t) = P_t^{\omega_{t-1}}(H_t), \quad (t \in \mathbb{T}\backslash\{0\}) \\ \quad\quad \pi_t^{\omega_{t-1}, \tilde{\omega}_{t-1}}(\Omega_t \times \tilde{H}_t) = \tilde{P}_t^{\tilde{\omega}_{t-1}}(\tilde{H}_t), \quad (t \in \mathbb{T}\backslash\{0\}) \end{cases} \tag{2.12}$$

taking the infimum over all Markov probability measures π defined on $\mathcal{F} \otimes \tilde{\mathcal{F}}$. We assume that the constraints hold for almost all $(\omega_{t-1}, \tilde{\omega}_{t-1}) \in \Omega_{t-1} \times \tilde{\Omega}_{t-1}$, as well as all $H_t \times \tilde{H}_t \in \sigma_t \otimes \tilde{\sigma}_t$ and define

$$d(\xi, \tilde{\xi}) := \sum_{t=0}^{T} \min\left\{d_t(\xi_t, \tilde{\xi}_t), d_t(\tilde{\xi}_t, \xi_t)\right\}, \tag{2.13}$$

and

$$d_t(\xi_t, \tilde{\xi}_t) := \gamma_t(\xi_t, \tilde{\xi}_t) \|b_{1,t}(\xi_t) - b_{1,t}(\tilde{\xi}_t)\|_1 + \phi_t(\tilde{\xi}_t) \|c_t(\xi_t) - c_t(\tilde{\xi}_t)\|_1. \qquad (2.14)$$

Remark 2.8. *Note that similar to the convention discussed in Remark 2.2, we require the information on the measures $\tilde{P}$ and P on the underlying probability spaces to calculate the distance between the two Markov processes.*

Remark 2.9. *As will become clear in the proof of Theorem 2.3, both $d_t(\xi_t, \tilde{\xi}_t)$ and $d_t(\tilde{\xi}_t, \xi_t)$ can be used to construct bounds for the difference in stochastic optimization problems. We therefore use the minimum in (2.13) to improve the bounds and ensure symmetry of D_L.*

Note that the objective function in (2.12) is defined in terms of the unconditional transport plan π between the joint distributions P and $\tilde{P}$ while the constraints rely on the corresponding disintegration in the form of Markov kernels $\pi_t^{\omega_{t-1}, \tilde{\omega}_{t-1}}$, which are guaranteed to exist Pollard (2002) and relate to π via

$$\pi(H \times \tilde{H}) = \int_{\Omega \times \tilde{\Omega}} \mathbb{1}_{H \times \tilde{H}}(\omega, \tilde{\omega}) \ \ldots \pi_t^{\omega_{t-1}, \tilde{\omega}_{t-1}}(d\omega_t, d\tilde{\omega}_t) \ldots \pi_0(d\omega_0, d\tilde{\omega}_0)$$

for $H \times \tilde{H} \in \mathcal{F} \otimes \tilde{\mathcal{F}}$. However, since the disintegration of π into Markov kernels is only π-almost surely unique, the constraints in (2.12) have to be fulfilled π_{t-1} almost surely, where π_{t-1} is the unconditional marginal of π in stage $t-1$.

Remark 2.10. *Analogously to the Remark 2.3 and Pflug and Pichler (2012, 2014), the infimum in the above definition is attained due to weak-compactness of the set of transportation plans.*

Next, we show that there is always at least one feasible transport plan between any two Markov processes, i.e., there are no processes with infinite distance.

Proposition 2.1. *The defining optimization problem of D_L is always feasible. In particular, the product measure $\pi := P \otimes \tilde{P}$ is always part of the feasible set.*

Proof. Let $A \in \sigma_{t+1}$ and $B \in \tilde{\sigma}_{t+1}$ for given t and $C \in \mathcal{F}$ and $D \in \tilde{\mathcal{F}}$. We have

$$\int\limits_{C \times D} P_{t+1}^{\omega_t}(A) \cdot \tilde{P}_{t+1}^{\tilde{\omega}_t}(B) \pi(d\omega, d\tilde{\omega}) = \int\limits_{C} P_{t+1}^{\omega_t}(A) P(d\omega) \cdot \int\limits_{D} \tilde{P}_{t+1}^{\tilde{\omega}_t}(A) \tilde{P}(d\tilde{\omega})$$

$$= P(C \cap A_{t+1}^{\Omega}) \cdot \tilde{P}(D \cap B_{t+1}^{\tilde{\Omega}}) = \pi((C \cap A_{t+1}^{\Omega}) \times (D \cap B_{t+1}^{\tilde{\Omega}}))$$

$$= \pi((C \times D) \cap (A_{t+1}^{\Omega} \times B_{t+1}^{\tilde{\Omega}})) = \int\limits_{C \times D} \pi_{t+1}^{\omega_t, \tilde{\omega}_t}(A \times B) \pi(d\omega, d\tilde{\omega})$$

where the first equality follows from the properties of the product measure. Since the sets A, B, C, and D are chosen arbitrarily and $P_{t+1}^{\omega_t}(A) \cdot \tilde{P}_{t+1}^{\tilde{\omega}_t}(B)$ as well as $\pi_{t+1}^{\omega_t, \tilde{\omega}_t}(A \times B)$ are $\sigma_t \otimes \tilde{\sigma}_t$ measurable, it follows that they coincide π-almost everywhere, i.e.,

$$P_{t+1}^{\omega_t}(A) \cdot \tilde{P}_{t+1}^{\tilde{\omega}_t}(B) = \pi_{t+1}^{\omega_t, \tilde{\omega}_t}(A \times B).$$

For the particular choices $A = \Omega_{t+1}$ or $B = \tilde{\Omega}_{t+1}$, we get the conditions in problem (2.12). $\qquad \square$

Next, we show that D_L is a *semi-metric*, i.e., that it is non-negative and symmetric. Example 2.1 demonstrates that it does not fulfill the triangle inequality.

Proposition 2.2. *If either c_t or $b_{1,t}$ have a continuous inverse, D_L is a semi-metric on the equivalence classes of Markov processes that have the same distribution.*

Proof. From the non-negativity of the norms and the constants ϕ_t and γ_t, we obtain that $D_L \geq 0$. Clearly, $d(\xi, \tilde{\xi}) = d(\tilde{\xi}, \xi)$. If π^* is the optimal transportation plan for $D_L(\xi, \tilde{\xi})$, then $\tilde{\pi}^*(\tilde{\omega}, \omega) = \pi^*(\omega, \tilde{\omega})$ is the optimal transportation plan for $D_L(\tilde{\xi}, \xi)$. Therefore we have $D_L(\xi, \tilde{\xi}) = D_L(\tilde{\xi}, \xi)$.

To show

$$D_L(\xi, \tilde{\xi}) = 0 \Leftrightarrow \xi = \tilde{\xi} \text{ in distribution,}$$

we note that one direction is trivial, since $\xi = \tilde{\xi}$ in distribution implies that $D_L(\xi, \tilde{\xi}) = 0$.

(a) Process $\xi^{(1)}$ (b) Process $\xi^{(2)}$ (c) Process $\xi^{(3)}$
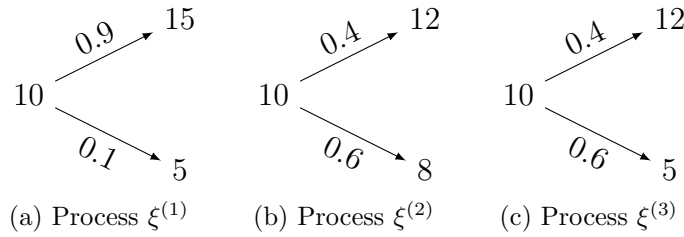
Figure 2.2: The three processes used in Example 2.1 to show that the triangle inequality of D_L does not hold.

If c_t or $b_{1,t}$ have continuous inverses, then $b_{1,t}(\xi_t) \neq b_{1,t}(\tilde{\xi}_t)$ or $c_t(\xi_t) \neq c_t(\tilde{\xi}_t)$ in distribution for any two processes ξ and $\tilde{\xi}$ that do not have the same distribution.

Under these circumstances, if $D_L(\xi, \tilde{\xi}) = 0$, similar to Villani (2009), we can without loss of generality assume that $\Omega = \tilde{\Omega}$ and find a measure π whose image measure on $\bigtimes_{t=1}^{T} \mathbb{R}^{n_t}$ is almost surely concentrated on the diagonal. This implies that ξ and $\tilde{\xi}$ have the same distribution. $\qquad\square$

Example 2.1. *In the following example, we demonstrate that the triangle inequality does not hold in general for D_L. To that end, consider a simple two-stage problem with the objective function in period t defined by*

$$c_t(\xi_t)^\top x_t = (\xi_t - 8, 0)x_t$$

where ξ_t is a one-dimensional random variable. The constraints in the form of (2.2) are described by

$$A_1 = (\ 1 \quad 0\ ), \quad b_1 = 0, \quad C_1 = 1, \quad A_2 = (\ 0 \quad 1\ ), \quad b_2 = 10.$$

Considering the three random processes presented in Figure 2.2 and using definition (2.12), we obtain the following values of the lattice distance between every pair of processes

$$D_L(\xi^{(1)}, \xi^{(2)}) = 59.8, \quad D_L(\xi^{(2)}, \xi^{(3)}) = 19.8, \quad D_L(\xi^{(1)}, \xi^{(3)}) = 88.$$

We refer to Section 2.5 for a detailed description on how to calculate the distances. Hence, we have

$$D_L(\xi^{(1)}, \xi^{(2)}) + D_L(\xi^{(2)}, \xi^{(3)}) = 59.8 + 19.8 = 79.6 < 88 = D_L(\xi^{(1)}, \xi^{(3)})$$

confirming that the triangle inequality does not hold.

2.4   Bounding Linear Markov Decision Problems

In this section, we show how the lattice distance D_L can be used to approximate linear stochastic programming problems with a Markovian structure as defined in (2.1). We start by showing that every Markov process can be approximated to an arbitrary precision by a discrete process in Theorem 2.1. We proceed by proving Theorem 2.3 in which we show that optimal values of problems in (2.1) are Lipschitz continuous with respect to D_L. These two results, in combination, imply that D_L can, in theory, be used to find discrete Markov processes (scenario lattices) that, when used in optimization problems, lead to an arbitrarily close approximation of the objective values.

In order to show Theorem 2.1, we require the following result demonstrating that distances between any pair of Markov processes can be approximated to an arbitrary precision by distances where one of the processes is replaced by a discrete approximation. For what follows, we denote by $\mathcal{L}^p(\Omega \times \tilde{\Omega}, \pi)$ the Lebesgue space of p-integrable functions.

Lemma 2.4. *Let*

$$\theta_t(\xi_t, \tilde{\xi}_t) = \min\{d_t(\xi_t, \tilde{\xi}_t), d_t(\tilde{\xi}_t, \xi_t)\} \tag{2.15}$$

and π be transportation plan that minimizes $D_L(\xi, \tilde{\xi})$ for two given processes ξ and $\tilde{\xi}$. If for all $0 \le t \le T$, $\theta_t(\xi_t, \tilde{\xi}_t) \in \mathcal{L}^p(\Omega_t \times \tilde{\Omega}_t, \pi_t)$ for some $p > 1$ and there is a

$x_{0t} \in \mathbb{R}^{n_t}$ *such that*

$$\int\limits_{\Omega \times \tilde{\Omega}} \theta_t(\xi_t, x_{0t}) \, \nu(d\omega, d\tilde{\omega}) < \infty \tag{2.16}$$

for all feasible transportation plans ν, then there is a sequence of discrete approximations $(\tilde{\xi}^k)_{k \in \mathbb{N}}$ such that $D_L(\xi, \tilde{\xi}^k) \xrightarrow{k \to \infty} D_L(\xi, \tilde{\xi})$.

Note that the condition $p > 1$ ensures that the space $\mathcal{L}^p(\Omega \times \tilde{\Omega}, \pi)$ is reflexive, which is used for the proof of Lemma 2.5 below, which in turn is required for the proof of Lemma 2.4.

Theorem 2.1. *Every Markov process ξ for which (2.16) holds can be approximated arbitrarily well in terms of D_L by a discrete process, i.e., there are discrete Markov processes $(\xi^k)_{k \in \mathbb{N}}$ such that $D_L(\xi, \xi^k) \xrightarrow{k \to \infty} 0$.*

Proof. Use ξ instead of $\tilde{\xi}$ in Lemma 2.4 and note that $\theta(\xi_t, \xi_t) = 0$ for the transportation plan that does not transport anything. Therefore the conditions of Lemma 2.4 are fulfilled and $D_L(\xi, \xi^k) \xrightarrow{k \to \infty} 0$ follows. $\qquad\qquad\qquad\square$

Note that this result is purely theoretical, showing that, loosely speaking, discrete Markov processes are *dense* with respect to D_L. In particular, the crude discretization used below to show Lemma 2.4 does not yield efficient approximations of Markov processes.

Remark 2.11. *We note that similar to the tree distance proposed in Pflug and Pichler (2012), the empirical distribution does not converge to the true distribution in D_L. This follows essentially by the same argument that is given in Pflug and Pichler (2016) in Proposition 1. Modifications of the distance based on non-parametric estimates addressing this issue as in Pflug and Pichler (2016) would be, in principle, possible but are out of the scope of this paper.*

To prove Lemma 2.4, we define discrete approximations $\tilde{\xi}^k$ of $\tilde{\xi}$. We start by noting that since θ_t is continuous, it is uniformly continuous on $B_t^k := B_t(0, k) \times$

$B_t(0,k)$, where $B_t(0,k)$ is the ball of radius k around 0 in $\mathbb{R}^{n_t}$. Now, for each k define a discrete random variable $\tilde{\xi}_t^k : \tilde{\Omega}_t \to \mathbb{R}^{n_t}$ with atoms $\tilde{\xi}_{t,m}^k$ and

$$E_{t,m}^k = \left\{ \tilde{\omega}_t \in \tilde{\Omega}_t : \tilde{\xi}_t^k(\tilde{\omega}_t) = \tilde{\xi}_{t,m}^k \right\}$$

such that

$$|\theta_t(\xi_t(\omega_t), \tilde{\xi}_t(\tilde{\omega}_t)) - \theta_t(\xi_t(\omega_t), \tilde{\xi}_t^k(\tilde{\omega}_t))| \leq k^{-1}, \ \forall \omega_t \ \forall \tilde{\omega}_t : \tilde{\xi}_t(\tilde{\omega}_t) \in B_t(0,k)$$

and $\tilde{\xi}_t^k(\tilde{\omega}_t) = x_{0t}$ for all $\tilde{\omega}_t$ such that $\tilde{\xi}_t(\tilde{\omega}_t) \notin B_t(0,k)$. Furthermore, define corresponding Markov kernels as

$$\tilde{P}_{t,k}^{\tilde{\xi}_{t-1,m}^k}(\tilde{\xi}_{t,j}^k) = \int\limits_{E_{t-1,m}^k} \tilde{P}_t^{\tilde{\omega}_{t-1}}(E_{t,j}^k) \ \tilde{P}_{t-1}(d\tilde{\omega}_{t-1})$$

and the functions

$$f_k^t(\nu) = \int\limits_{\Omega_t \times \tilde{\Omega}_t} \theta_t(\xi_t, \tilde{\xi}_t^k) \ \nu_t(d\omega_t, d\tilde{\omega}_t), \quad f_0^t(\nu) = \int\limits_{\Omega_t \times \tilde{\Omega}_t} \theta_t(\xi_t, \tilde{\xi}_t) \ \nu_t(d\omega_t, d\tilde{\omega}_t)$$

for $\nu_t \in \mathcal{L}^q(\Omega_t \times \tilde{\Omega}_t, \pi_t)$ with $q^{-1} + p^{-1} = 1$ the unconditional distributions of the transportation plan ν in stage t.

In Lemma 2.5, we will show that the approximations defined above epi-converge to the objective function of the optimization problem defining the lattice distance. Epi-convergence is the weakest notion of convergence of functions that allows to conclude that convergence of objective functions implies the convergence of optimal solutions and is defined as follows.

Definition 2.3 (epi-convergence)**.** *A sequence of functions $f_n : X \to \mathbb{R}$ defined on a metric space X epi-convergences to a function $f : X \to \mathbb{R}$, if for each $x \in X$*

$$\liminf_{n \to \infty} f_n(x_n) \geq f(x) \quad \text{for every } x_n \to x \text{ and}$$

$$\limsup_{n \to \infty} f_n(x_n) \leq f(x) \quad \text{for some } x_n \to x.$$

We write $f_n \xrightarrow{epi} f$.

We will additionally require the notion of barrelled spaces, which are exactly the spaces where the *uniform boundedness principle* is valid, which we will use in the proof of Lemma 2.4.

Definition 2.4 (barrel, barrelled space)**.** *A closed set $B \subseteq X$ in a real topological vector space X is a* barrel*, if and only if the following conditions hold*

1. *B is absolutely convex, i.e.,*

$$x_1, x_2 \in B \Rightarrow \lambda_1 x_1 + \lambda_2 x_2 \in B$$

   for $|\lambda_1| + |\lambda_2| = 1$.

2. *B is absorbing, i.e., for every $x \in X$ there is a $\alpha > 0$ with $x \in \alpha B$.*

A locally convex vector space is called barrelled*, if and only if every barrel is a neighborhood of zero.*

Theorem 2.2 (Uniform boundedness principle, Theorem III.2.1 in Bourbaki et al. (1987))**.** *Let X be a barrelled locally convex vector space and Y be an arbitrary locally convex vector space. A collection $\mathcal{F}$ of continuous linear functions $f : X \to Y$ is bounded pointwise, i.e.,*

$$\{f(x) : f \in \mathcal{F}\} \subseteq Y$$

is bounded for all $x \in X$, if and only if the functions are equi-continuous, i.e., for every neighborhood $V \subseteq Y$ of zero, there is a neighborhood of zero $U \subseteq X$, such that

$$f^{-1}(V) \subseteq U, \quad \forall f \in \mathcal{F}.$$

Lemma 2.5. *If the integrability conditions (2.16) hold for ξ and $\tilde{\xi}$, then*

$$\sum_{t=0}^{T} f_k^t \xrightarrow{epi} \sum_{t=0}^{T} f_0^t \quad as\ k \to \infty.$$

Proof. Define

$$f_{kn}^t(\nu) = \int\limits_{\Omega_t \times \tilde{\Omega}_t} \theta_t(\xi_t, \tilde{\xi}_t^k) \mathbb{1}_{B_t^n}(\xi_t, \tilde{\xi}_t) \, \nu_t(d\omega_t, d\tilde{\omega}_t)$$

$$f_{0n}^t(\nu) = \int\limits_{\Omega_t \times \tilde{\Omega}_t} \theta_t(\xi_t, \tilde{\xi}_t) \mathbb{1}_{B_t^n}(\xi_t, \tilde{\xi}_t) \, \nu_t(d\omega_t, d\tilde{\omega}_t).$$

Fix $\epsilon > 0$. By integrability of θ_t with respect to ν_t and an application of the dominated convergence theorem, it follows that there is a compact set $K_t \subset \mathbb{R}^{n_t} \times \mathbb{R}^{n_t}$ for every $t = 0, \dots, T$ such that

$$\int\limits_{\Omega_t \times \tilde{\Omega}_t} \theta_t(\xi_t, x_{0t}) \mathbb{1}_{K_t^c}(\xi_t, \tilde{\xi}_t) \, \nu_t(d\omega_t, d\tilde{\omega}_t) < \epsilon,$$

$$\int\limits_{\Omega_t \times \tilde{\Omega}_t} \theta_t(\xi_t, \tilde{\xi}_t) \mathbb{1}_{K_t^c}(\xi_t, \tilde{\xi}_t) \, \nu_t(d\omega_t, d\tilde{\omega}_t) < \epsilon.$$

Now choose $k \in \mathbb{N}$ such that $K_t \subseteq B_t^k$ and $k > \epsilon^{-1}$ and note that

$$|f_{kn}^t(\nu) - f_{0n}^t(\nu)| \leq \int\limits_{\Omega_t \times \tilde{\Omega}_t} |\theta_t(\xi_t, \tilde{\xi}_t^k) - \theta_t(\xi_t, \tilde{\xi}_t)| \mathbb{1}_{B_t^k}(\xi_t, \tilde{\xi}_t) \, \nu_t(d\omega_t, d\tilde{\omega}_t)$$

$$+ \int\limits_{\Omega_t \times \tilde{\Omega}_t} \theta_t(\xi_t, \tilde{\xi}_t) \mathbb{1}_{B_t^n \setminus B_t^k}(\xi_t, \tilde{\xi}_t) \, \nu_t(d\omega_t, d\tilde{\omega}_t)$$

$$+ \int\limits_{\Omega_t \times \tilde{\Omega}_t} \theta_t(\xi_t, x_{0t}) \mathbb{1}_{B_t^n \setminus B_t^k}(\xi_t, \tilde{\xi}_t) \, \nu_t(d\omega_t, d\tilde{\omega}_t) \leq 3\epsilon,$$

i.e., $f_{kn}^t \to f_{0n}^t$ uniformly for all n. Note further that

$$f_0^t = \lim_n f_{0n}^t = \lim_n \lim_k f_{kn}^t = \lim_k \lim_n f_{kn}^t = \lim_k f_k^t$$

where the two limits can be exchanged because of the uniform convergence shown above and the first equality follows by the monotone convergence theorem. As the

convergence holds for every $t = 0, \ldots, T$, we obtain that

$$\sum_{t=0}^{T} f_0^t = \lim_k \sum_{t=0}^{T} f_k^t.$$

$\mathcal{L}^p(\Omega \times \tilde{\Omega}, \pi)$ is reflexive, and therefore, the weak topology is barrelled (see Meise et al. (1997), Theorem 23.22). Since $\sum_{t=0}^{T} f_k^t \to \sum_{t=0}^{T} f_0^t$ weakly, the set $\left\{ \sum_{t=0}^{T} f_k^t, \sum_{t=0}^{T} f_0^t \right\}$ is weakly bounded and therefore weakly equi-continuous by the uniform boundedness principle. Since $\left\{ \sum_{t=0}^{T} f_{kn}^t : n \in \mathbb{N}_0 \right\}$ is equi-continuous, it is equi–lower semi-continuous and $\sum_{t=0}^{T} f_k^t \overset{epi}{\longrightarrow} \sum_{t=0}^{T} f_0^t$ (see Dolecki et al. (1983), Theorem 2.18). $\qquad\square$

Lemma 2.4. Because of the epi-convergence proved in Lemma 2.5, we obtain (see Attouch and Wets (1983), Theorem 2.5)

$$D_L(\xi, \tilde{\xi}^k) = \min_{\nu \in \Upsilon} \sum_{t=0}^{T} f_k^t(\nu) \to \min_{\nu \in \Upsilon} \sum_{t=0}^{T} f_0^t(\nu) = D_L(\xi, \tilde{\xi}).$$

Note that the feasible set Υ can w.l.o.g. be assumed the feasible set of $D_L(\xi, \tilde{\xi})$, since for every feasible transportation plan for $D_L(\xi, \tilde{\xi}^k)$ there exists a plan that is feasible for $D_L(\xi, \tilde{\xi})$ yielding the same objective. $\qquad\square$

Next, we prove the main result of the paper, establishing that the optimal value of the stochastic optimization problem associated with D_L is Lipschitz with respect to D_L. We first note the following useful lemma assuming that $i_t : \Omega_t \times \tilde{\Omega}_t \to \Omega_t$, $\tilde{i}_t : \Omega_t \times \tilde{\Omega}_t \to \tilde{\Omega}_t$ are natural projections for $t = 0, \ldots, T$.

Lemma 2.6. *For a measurable function $f : \Omega_t \to \mathbb{R}$ and measures P_t, $\tilde{P}_t$, π_t that fulfill the conditions in (2.12), we have*

$$\mathbb{E}_{\pi_t}(f \circ i_t) = \mathbb{E}_{P_t}(f).$$

Proof. The result clearly holds for functions $f = \mathbb{1}_A$ with $A \in \Omega_t$, and therefore, by the usual argument, also for general measurable functions. $\qquad\square$

Theorem 2.3. *Let ξ and $\tilde{\xi}$ be Markov processes and V_0 be the value function for a stochastic optimization problem of the form* (2.1), *then*

$$|V_0(S_0, \xi_0) - \tilde{V}_0(S_0, \tilde{\xi}_0)| \leq D_L(\xi, \tilde{\xi}).$$

Proof. We start by choosing $\epsilon > 0$ arbitrarily. If the process ξ is continuous, we define an ϵ-exact approximation of the value functions. To this end, we note that since for every ξ_{t-1}, $S_t \mapsto \mathbb{E}(V_t(S_t, \xi_t)|\xi_{t-1})$ is a continuous function on the compact set of permissible decisions S_t, it is Lipschitz continuous with Lipschitz constant $L_t(\xi_{t-1})$. By concavity of $S_t \mapsto \mathbb{E}(V_t(S_t, \xi_t)|\xi_{t-1})$ there exists a supergradient $C_{3,t}^{S_t}(\xi_{t-1})$ and by continuity there is an open neighborhood $\mathcal{U}(S_t)$ of S_t such that

$$|\mathbb{E}(V_t(S, \xi_t)|\xi_{t-1}) - b_{3,t}^{S_t}(\xi_{t-1}) - C_{3,t}^{S_t}(\xi_{t-1})S| \leq \epsilon, \quad \forall S \in \mathcal{U}(S_t).$$

with $b_{3,t}^{S_t}(\xi_{t-1}) = \mathbb{E}(V_t(S_t, \xi_t)|\xi_{t-1})$.

By compactness, the set of feasible S_t can be covered by a finite open cover $\mathcal{U}^i = \mathcal{U}(S_t^i)$ with corresponding $b_{3,t}^i(\xi_{t-1})$ and $C_{3,t}^i(\xi_{t-1})$ for $i = 1, \ldots, m_t(\xi_{t-1})$ such that

$$|\mathbb{E}(V_t(S, \xi_t)|\xi_{t-1}) - \min_i b_{3,t}^i(\xi_{t-1}) + C_{3,t}^i(\xi_{t-1})S| \leq \epsilon, \quad \forall \text{ feasible } S.$$

Clearly, it follows that

$$\hat{\kappa}_t(\xi_{t-1}) := \max_{i,j} |C_{3,t}^{i,j}(\xi_{t-1})| \leq 2L_t(\xi_{t-1}) \tag{2.17}$$

and therefore $\hat{\kappa}_t(\xi_{t-1}) \leq \kappa_t(\xi_{t-1}) = 2L_t(\xi_{t-1})$. An analogous argument holds for process $\tilde{\xi}$. Note that if ξ or $\tilde{\xi}$ are discrete, we can choose $\epsilon = 0$ and $\hat{\kappa}_t = \kappa_t$ or $\hat{\tilde{\kappa}}_t = \tilde{\kappa}_t$, since the value function approximation constructed above can be made exact due to Lemma 2.1.

Defining

$$\delta_t^1(\xi_t, \tilde{\xi}_t) = \gamma(A_{1,t}, A_{2,t}, \min\{\hat{\kappa}_{t+1}(\xi_t), \hat{\tilde{\kappa}}_{t+1}(\tilde{\xi}_t)\}, c_t(\xi_t))\|b_{1,t}(\xi_t) - b_{1,t}(\tilde{\xi}_t)\|_1$$

$$\delta_t^2(\xi_t, \tilde{\xi}_t) = \phi(A_{1,t}, b_{1,t}(\tilde{\xi}_t) + C_{1,t}^+ b_{2,t}, A_{2,t}, b_{2,t+1})\|c_t(\xi_t) - c_t(\tilde{\xi}_t)\|_1$$

as well as $\delta_t(\xi_t, \tilde{\xi}_t) = \delta_t^1(\xi_t, \tilde{\xi}_t) + \delta_t^2(\xi_t, \tilde{\xi}_t)$, we note that

$$
\begin{aligned}
V_T(S_T, \xi_T) &= \max\left\{c_T(\xi_T)^\top x_T : (x_T, S_{T+1}) \in \mathcal{X}_T(S_T, \xi_T)\right\} \\
&\geq \max\left\{c_T(\xi_T)^\top x_T : (x_T, S_{T+1}) \in \mathcal{X}_T(S_T, \tilde{\xi}_T)\right\} - \delta_T^1(\xi_T, \tilde{\xi}_T) \\
&\geq \max\left\{c_T(\tilde{\xi}_T)^\top x_T : (x_T, S_{T+1}) \in \mathcal{X}_T(S_T, \tilde{\xi}_T)\right\} - \delta_T(\xi_T, \tilde{\xi}_T) \\
&= \tilde{V}_T(S_T, \tilde{\xi}_T) - \delta_T(\xi_T, \tilde{\xi}_T),
\end{aligned}
\tag{2.18}
$$

where first inequality follows from Lemma 2.2 and second from Lemma 2.3 and Remark 2.6. Note that since $V_{T+1} \equiv 0$, $\kappa_{T+1}(\xi_T) = \tilde{\kappa}_{T+1}(\tilde{\xi}_T) = 0$. Exchanging the order of steps in which Lemma 2.2 and Lemma 2.3 are applied yields

$$\tilde{V}_T(S_T, \tilde{\xi}_T) - \delta_T(\tilde{\xi}_T, \xi_T) \leq V_T(S_T, \xi_T)$$

and exchanging the roles of V_T and $\tilde{V}_T$ finally results in

$$|\tilde{V}_T(S_T, \tilde{\xi}_T) - V_T(S_T, \xi_T)| \leq \min\left\{\delta_T(\xi_T, \tilde{\xi}_T), \delta_T(\tilde{\xi}_T, \xi_T)\right\} =: \Delta_T(\xi_T, \tilde{\xi}_T).$$

Proceeding to the next stage, we assume w.l.o.g. that

$$\min\{\hat{\kappa}_T(\xi_{T-1}), \hat{\tilde{\kappa}}_T(\tilde{\xi}_{T-1})\} = \hat{\tilde{\kappa}}_T(\tilde{\xi}_{T-1}).$$

Then for all $\xi_{T-1} \in \Omega_{T-1}, \tilde{\xi}_{T-1} \in \tilde{\Omega}_{T-1}$ we have

$$V_{T-1}(S_{T-1}, \xi_{T-1}) = \begin{cases} \max & c_{T-1}(\xi_{T-1})^\top x_{T-1} + \mathbb{E}_{P_T}(V_T(S_T, \xi_T)|\xi_{T-1}) \\ \text{s.t.} & (x_{T-1}, S_T) \in \mathcal{X}_{T-1}(S_{T-1}, \xi_{T-1}) \end{cases}$$

$$= \begin{cases} \max & c_{T-1}(\xi_{T-1})^\top x_{T-1} + \mathbb{E}_{\pi_T}(V_T(S_T, \xi_T) \circ i_T|\xi_{T-1}, \tilde{\xi}_{T-1}) \\ \text{s.t.} & (x_{T-1}, S_T) \in \mathcal{X}_{T-1}(S_{T-1}, \xi_{T-1}) \end{cases}$$

$$\geq \begin{cases} \max & c_{T-1}(\xi_{T-1})^\top x_{T-1} + \mathbb{E}_{\pi_T}(\tilde{V}_T(S_T, \tilde{\xi}_T) \circ \tilde{i}_T - \Delta_T|\xi_{T-1}, \tilde{\xi}_{T-1}) \\ \text{s.t.} & (x_{T-1}, S_T) \in \mathcal{X}_{T-1}(S_{T-1}, \xi_{T-1}) \end{cases}$$

$$= \begin{cases} \max & c_{T-1}(\xi_{T-1})^\top x_{T-1} + \mathbb{E}_{\tilde{P}_T}(\tilde{V}_T(S_T, \tilde{\xi}_T)|\tilde{\xi}_{T-1}) \\ \text{s.t.} & (x_{T-1}, S_T) \in \mathcal{X}_{T-1}(S_{T-1}, \xi_{T-1}) \end{cases}$$

$$- \mathbb{E}_{\pi_T}(\Delta_T|\xi_{T-1}, \tilde{\xi}_{T-1})$$

$$\geq \begin{cases} \max & c_{T-1}(\xi_{T-1})^\top x_{T-1} + \tilde{\gamma} - \epsilon \\ \text{s.t.} & (x_{T-1}, S_T) \in \mathcal{X}_{T-1}(S_{T-1}, \xi_{T-1}) \\ & \mathbb{1}_{m_T(\tilde{\xi}_{T-1})}\tilde{\gamma} \leq \tilde{b}_{3,T}(\tilde{\xi}_{T-1}) + \tilde{C}_{3,T}(\tilde{\xi}_{T-1})S_T \end{cases}$$

$$- \mathbb{E}_{\pi_T}(\Delta_T|\xi_{T-1}, \tilde{\xi}_{T-1})$$

$$\geq \begin{cases} \max & c_{T-1}(\xi_{T-1})^\top x_{T-1} + \tilde{\gamma} \\ \text{s.t.} & (x_{T-1}, S_T) \in \mathcal{X}_{T-1}(S_{T-1}, \tilde{\xi}_{T-1}) \\ & \mathbb{1}_{m_T(\tilde{\xi}_{T-1})}\tilde{\gamma} \leq \tilde{b}_{3,T}(\tilde{\xi}_{T-1}) + \tilde{C}_{3,T}(\tilde{\xi}_{T-1})S_T \end{cases}$$

$$- \epsilon - \mathbb{E}_{\pi_T}(\Delta_T|\xi_{T-1}, \tilde{\xi}_{T-1}) - \delta^1_{T-1}(\xi_{T-1}, \tilde{\xi}_{T-1})$$

$$\geq \begin{cases} \max & c_{T-1}(\tilde{\xi}_{T-1})^\top x_{T-1} + \tilde{\gamma} \\ \text{s.t.} & (x_{T-1}, S_T) \in \mathcal{X}_{T-1}(S_{T-1}, \tilde{\xi}_{T-1}) \\ & \mathbb{1}_{m_T(\tilde{\xi}_{T-1})}\tilde{\gamma} \leq \tilde{b}_{3,T}(\tilde{\xi}_{T-1}) + \tilde{C}_{3,T}(\tilde{\xi}_{T-1})S_T \end{cases}$$

$$- \epsilon - \mathbb{E}_{\pi_T}(\Delta_T|\xi_{T-1}, \tilde{\xi}_{T-1}) - \delta_{T-1}(\xi_{T-1}, \tilde{\xi}_{T-1})$$

$$\geq \begin{cases} \max & c_{T-1}(\tilde{\xi}_{T-1})^\top x_{T-1} + \tilde{\gamma} + \epsilon \\ \text{s.t.} & (x_{T-1}, S_T) \in \mathcal{X}_{T-1}(S_{T-1}, \tilde{\xi}_{T-1}) \\ & \mathbb{1}_{m_T(\tilde{\xi}_{T-1})}\tilde{\gamma} \leq \tilde{b}_{3,T}(\tilde{\xi}_{T-1}) + \tilde{C}_{3,T}(\tilde{\xi}_{T-1})S_T \end{cases}$$

$$- 2\epsilon - \mathbb{E}_{\pi_T}(\Delta_T|\xi_{T-1}, \tilde{\xi}_{T-1}) - \delta_{T-1}(\xi_{T-1}, \tilde{\xi}_{T-1})$$

$$\geq \tilde{V}_{T-1}(S_{T-1}, \tilde{\xi}_{T-1}) - 2\epsilon - \mathbb{E}_{\pi_T}(\Delta_T|\xi_{T-1}, \tilde{\xi}_{T-1}) - \delta_{T-1}(\xi_{T-1}, \tilde{\xi}_{T-1})$$

where the second equality follows by Lemma 2.6, the first inequality from (2.18), the following equality again from Lemma 2.6 and the subsequent inequalities follow from Lemma 2.2 and Lemma 2.3 and (2.17). As in the derivation of (2.18), we can exchange the order in which Lemma 2.2 and Lemma 2.3 are applied to get the above inequality with $\delta_{T-1}(\xi_{T-1}, \tilde{\xi}_{T-1})$ replaced by $\delta_{T-1}(\tilde{\xi}_{T-1}, \xi_{T-1})$. Exchanging the roles of V_{T-1} and $\tilde{V}_{T-1}$ we obtain

$$|\tilde{V}_{T-1}(S_{T-1}, \tilde{\xi}_{T-1}) - V_{T-1}(S_{T-1}, \xi_{T-1})| \leq \mathbb{E}_{\pi_T}(\Delta_T(\xi_T, \tilde{\xi}_T) | \xi_{T-1}, \tilde{\xi}_{T-1})$$
$$+ \Delta_{T-1}(\xi_{T-1}, \tilde{\xi}_{T-1}) + 2\epsilon.$$

Proceeding by backward induction, and noting that the distance D_L is non-decreasing when replacing $\hat{\kappa}_t(\xi_{t-1})$ by $\kappa_t(\xi_{t-1})$ and $\hat{\tilde{\kappa}}_t(\xi_{t-1})$ by $\tilde{\kappa}_t(\tilde{\xi}_{t-1})$, we arrive at

$$|\tilde{V}_0(S_0, \tilde{\xi}_0) - V_0(S_0, \xi_0)| \leq D_L(\xi, \tilde{\xi}) + 2T\epsilon$$

and since $\epsilon > 0$ was arbitrary, the result follows.   □

Remark 2.12. *Linear stochastic optimization problems without randomness in the constraints are special cases of the problems for which Pflug and Pichler (2012) provide stability results analogous to Theorem 2.3. Hence, a comparison of the two types of results for this problem class is of interest.*

The authors in Pflug and Pichler (2012) show that for their nested distance D_T, a convex set $\mathbb{X}$, and a general objective function $h : \mathbb{X} \times \Omega \to \mathbb{R}$

$$|\min_{x \in \mathbb{X}} \mathbb{E}(h(x, \xi)) - \min_{x \in \mathbb{X}} \mathbb{E}(h(x, \tilde{\xi}))| \leq L\, D_T(\xi, \tilde{\xi})$$

assuming that there is a constant L such that

$$|h(x, \xi) - h(x, \tilde{\xi})| \leq L\, \|\xi - \tilde{\xi}\|_1, \quad \forall x \in \mathbb{X}, \quad \forall (\omega, \tilde{\omega}) \in \Omega \times \tilde{\Omega}.$$

Defining $\mathcal{G}_t = \sigma(\xi_0, \ldots, \xi_t)$, $\tilde{\mathcal{G}}_t = \sigma(\tilde{\xi}_0, \ldots, \tilde{\xi}_t)$ as the σ-algebras generated by the history of the processes, the distance D_T for arbitrary stochastic processes is defined

as

$$
D_T(\xi, \tilde{\xi}) =
\begin{cases}
\displaystyle\inf_{\pi} \int\limits_{\Omega \times \tilde{\Omega}} \|\xi - \tilde{\xi}\|_1 \, \pi\,(d\omega, d\tilde{\omega}) \\[2ex]
s.t. \quad \pi(A \times \tilde{\Omega} | \mathcal{G}_t \otimes \tilde{\mathcal{G}}_t) = P\,(A\,|\mathcal{G}_t)\,, \quad \forall A \in \mathcal{G}_T \\[1ex]
\qquad \pi(\Omega \times \tilde{A} | \mathcal{G}_t \otimes \tilde{\mathcal{G}}_t) = \tilde{P}(\tilde{A}|\tilde{\mathcal{G}}_t), \quad \forall \tilde{A} \in \tilde{\mathcal{G}}_T.
\end{cases}
\tag{2.19}
$$

In this paper, we treat the special case $h\,(x, \xi) = \sum_{t=0}^{T} c_t\,(\xi_t)^\top x_t$ for which L can be calculated as $L = \max_t L_{c_t}\phi_t$ assuming that the functions c_t are Lipschitz with constants L_{c_t} and ϕ_t is the function calculated in Lemma 2.3. Note that ϕ_t is deterministic in the case of a deterministic feasible set.

It is easy to see that for two Markov processes, the permissible transportation plans π for D_T and for D_L are equivalent. Assume that π^* is an optimal transportation plan for D_T, then we have

$$
\begin{aligned}
D_L(\xi, \tilde{\xi}) &\leq \int\limits_{\Omega \times \tilde{\Omega}} \sum_{t=0}^{T} \phi_t \|c_t\,(\xi_t) - c_t(\tilde{\xi}_t)\|_1 \, \pi^*\,(d\omega, d\tilde{\omega}) \\
&\leq \int\limits_{\Omega \times \tilde{\Omega}} \sum_{t=0}^{T} \phi_t L_{c_t} \|\xi_t - \tilde{\xi}_t\|_1 \, \pi^*\,(d\omega, d\tilde{\omega}) \\
&\leq L \int\limits_{\Omega \times \tilde{\Omega}} \|\xi - \tilde{\xi}\|_1 \, \pi^*\,(d\omega, d\tilde{\omega}) = L\, D_T(\xi, \tilde{\xi}).
\end{aligned}
$$

The above calculations show that our bound is tighter than D_T for problems where both bounds are applicable, i.e., linear stochastic optimization problems with deterministic feasible set $\mathbb{X}$.

2.5   Implementation for Finite Scenario Lattices

In this section, we focus on the computation of D_L for two finitely supported Markov processes. In Section 2.5.1, we detail all necessary steps to compute D_L, provide a formal algorithm for the computation, and discuss computational issues. In Section

2.5.2, we discuss a simple example demonstrating the bounding property of D_L and provide a comparison to the tree distance of Pflug and Pichler (2012).

2.5.1   Computation of D_L

In this section, we show that similar to the case of the classical Wasserstein distance and Pflug and Pichler (2012), the distance can be computed by solving a linear optimization problem to find the optimal transport plan π.

We represent two discrete Markov processes ξ and $\tilde{\xi}$ by scenario lattices. To that end, at every stage $t \in \mathbb{T}$ we define the probability spaces

$$\Omega_t = \left\{ i \in \mathbb{N} : 1 \leq i \leq N_t \right\}, \ \tilde{\Omega}_t = \left\{ \tilde{i} \in \mathbb{N} : 1 \leq \tilde{i} \leq M_t \right\}$$

where N_t and M_t are the number of atoms of the unconditional distributions P_t and $\tilde{P}_t$, respectively. The conditional transition from a given state i $(\tilde{i})$ at time $(t-1)$ to a state j $(\tilde{j})$ at time t is described by a conditional probability $P_t^i(j)$ and $\tilde{P}_t^{\tilde{i}}(\tilde{j})$, respectively.

The optimal transport plan π is a Markov process on Ω, which is fully described by the conditional probabilities

$$\pi \left((\omega_t, \tilde{\omega}_t) = (i, \tilde{i}) \middle| \bigtimes_{s=1}^{t-1} (\omega_s, \tilde{\omega}_s) \right) = \pi_t^{\omega_{t-1}, \tilde{\omega}_{t-1}}(i, \tilde{i}), \quad \forall (i, \tilde{i}) \in \Omega_t \times \tilde{\Omega}_t.$$

The measure π can therefore be represented by a set of non-negative matrices $\pi_t^{\omega_{t-1}, \tilde{\omega}_{t-1}} \in \mathbb{R}^{|\Omega_t| \times |\tilde{\Omega}_t|}$ with $\pi_t^{\omega_{t-1}, \tilde{\omega}_{t-1}}(i, \tilde{i})$ the element in row i and column $\tilde{i}$ for $(i, \tilde{i}) \in \Omega_t \times \tilde{\Omega}_t$ and

$$\sum_{(i, \tilde{i}) \in \Omega_t \times \tilde{\Omega}_t} \pi_t^{\omega_{t-1}, \tilde{\omega}_{t-1}}(i, \tilde{i}) = 1.$$

We furthermore denote by π_t the unconditional distributions at time t.

To be able to compute the lattice distance as a linear program, we define

$$\tau_t^{\omega_{t-1}, \tilde{\omega}_{t-1}}(i, \tilde{i}) = \pi_t^{\omega_{t-1}, \tilde{\omega}_{t-1}}(i, \tilde{i}) \pi_{t-1}(\omega_{t-1}, \tilde{\omega}_{t-1}), \quad \forall (i, \tilde{i}) \in \Omega_t \times \tilde{\Omega}_t$$

as well as $\pi_{t-1}(\omega_{t-1}, \tilde{\omega}_{t-1})$ as decision variables. For given $(\omega_{t-1}, \tilde{\omega}_{t-1})$ and $(i, \tilde{i})$, the constraints in the definition of D_L can therefore be written as linear constraints in these variables as

$$\tau_t^{\omega_{t-1}, \tilde{\omega}_{t-1}}(\{i\} \times \tilde{\Omega}_t) = P_t^{\omega_{t-1}}(i)\ \pi_{t-1}(\omega_{t-1}, \tilde{\omega}_{t-1}),$$

$$\tau_t^{\omega_{t-1}, \tilde{\omega}_{t-1}}(\Omega_t \times \{\tilde{i}\}) = \tilde{P}_t^{\tilde{\omega}_{t-1}}(\tilde{i})\ \pi_{t-1}(\omega_{t-1}, \tilde{\omega}_{t-1})$$

where $\tau_t^{\omega_{t-1}, \tilde{\omega}_{t-1}}(\{i\} \times \tilde{\Omega}_t) = \sum_{\tilde{\omega}_t \in \tilde{\Omega}_t} \tau_t^{\omega_{t-1}, \tilde{\omega}_{t-1}}(i, \tilde{\omega}_t)$ and $\tau_t^{\omega_{t-1}, \tilde{\omega}_{t-1}}(\Omega_t \times \{\tilde{i}\})$ is defined analogously.

Hence, given two discrete processes ξ and $\tilde{\xi}$ as well as $\theta_t(\xi_t(\omega_t), \tilde{\xi}_t(\tilde{\omega}_t))$, $D_L(\xi, \tilde{\xi})$ can be computed as the following linear optimization problem in the variables $\tau_t^{\omega_{t-1}, \tilde{\omega}_{t-1}}(i, \tilde{i})$ and $\pi_t(\omega_t, \tilde{\omega}_t)$

$$D_L(\xi, \tilde{\xi}) = \begin{cases} \min & \sum_{t=1}^{T} \sum_{\omega_t, \tilde{\omega}_t} \theta_t(\xi_t(\omega_t), \tilde{\xi}_t(\tilde{\omega}_t))\ \pi_t(\omega_t, \tilde{\omega}_t) \\ \text{s.t.} & \tau_t^{\omega_{t-1}, \tilde{\omega}_{t-1}}(\{i\} \times \tilde{\Omega}_t) = P_t^{\omega_{t-1}}(i)\pi_{t-1}(\omega_{t-1}, \tilde{\omega}_{t-1}) \\ & \tau_t^{\omega_{t-1}, \tilde{\omega}_{t-1}}(\Omega_t \times \{\tilde{i}\}) = \tilde{P}_t^{\tilde{\omega}_{t-1}}(\tilde{i})\pi_{t-1}(\omega_{t-1}, \tilde{\omega}_{t-1}) \\ & \pi_t(\omega_t, \tilde{\omega}_t) = \sum_{\omega_{t-1}, \tilde{\omega}_{t-1}} \tau_t^{\omega_{t-1}, \tilde{\omega}_{t-1}}(\omega_t, \tilde{\omega}_t) \\ & \pi_{t-1}(\omega_{t-1}, \tilde{\omega}_{t-1}) = \sum_{\omega_t, \tilde{\omega}_t} \tau_t^{\omega_{t-1}, \tilde{\omega}_{t-1}}(\omega_t, \tilde{\omega}_t) \end{cases} \quad (2.20)$$

where the constraints hold for all $(\omega_{t-1}, \tilde{\omega}_{t-1}) \in \Omega_{t-1} \times \tilde{\Omega}_{t-1}$ and for all $(i, \tilde{i}) \in \Omega_t \times \tilde{\Omega}_t$ for all $t \in \mathbb{T} \setminus \{0\}$ and $\pi_0(1, 1) := 1$. Note that the third set of constraints ensures that the unconditional probabilities in π_t sum to one, while the last set of constraints ensures that the probability mass of $\pi_{t-1}(\omega_{t-1}, \tilde{\omega}_{t-1})$ is distributed amongst the successors of $(\omega_{t-1}, \tilde{\omega}_{t-1})$, i.e., that the stages are properly connected.

Note that, since we model the conditional probabilities $\pi_t^{\omega_{t-1}, \tilde{\omega}_{t-1}}(i, \tilde{i})$ only dependent on the state of the process in $(t-1)$, the feasible measures π are automatically Markov.

Since (2.20) is a linear program, it can be efficiently solved. However, in order to do so, the $\theta_t(\xi_t, \tilde{\xi}_t)$ have to be computed. Since $\theta_t(\xi_t, \tilde{\xi}_t)$ only depends on the values

of the two processes ξ and $\tilde{\xi}$ and are thus independent of the probabilities π, they can be obtained offline.

In order to compute $\theta_t(\xi_t, \tilde{\xi}_t)$, the constants $\gamma_t(\xi_t(\omega_t), \tilde{\xi}_t(\tilde{\omega}_t))$ and $\phi_t(\xi_t(\omega_t))$ and $\phi_t(\tilde{\xi}_t(\tilde{\omega}_t))$ are required. These quantities are maxima of $||\cdot||_\infty$ over the vertices of the polyhedra Γ_t and Φ_t defined in Lemma 2.2 and Lemma 2.3 and dependent on the constant problem data $A_{1,t}$, $A_{2,t}$, $b_{2,t+1}$, $C_{1,t}$, as well as the random data $b_{1,t}$, c_t, and κ_t.

Candidates x^+ for vertices of a polyhedron $\Lambda = \left\{ x \in \mathbb{R}^k : Ax \leq b \right\}$ with $A \in \mathbb{R}^{m \times k}$ can be found choosing a subset $I \subseteq \{1, \ldots, m\}$ with $|I| = k$ and solving $A^I x^+ = b^I$ where $A^I \in \mathbb{R}^{k \times k}$ and b^I are the submatrices of A and b with rows $i \in I$, respectively. x^+ is a vertex of Λ if it fulfills $Ax^+ \leq b$.[2]

The number of vertices grows exponentially with the number of constraints in the linear problems on the nodes. However, the type of problems that are solved using the decomposition approaches described in Section 2.2 usually have a large number of stages but rather small nodal problems. Furthermore, in most problems, the data on the left-hand side of the problem $A_{1,t}$, $A_{2,t}$, $b_{2,t+1}$, $C_{1,t}$ does not vary with the stage or the randomness and some of the right-hand sides remain constant as well. Hence, one can precompute the value of $||x^+||_\infty$ for all vertices where the right-hand side does not change and store the factorization of the left-hand side matrix for all the vertices where the right-hand side is random in order to efficiently compute x^+ for varying b. This, together with the limited problem size on the nodes, makes the computation of γ_t and ϕ_t computationally relatively cheap even for larger scenario lattices.

We provide pseudocode for the calculation of D_L in Algorithm 1. The algorithm loops over the stages t of the problem and iteratively computes the constants γ_t and ϕ_t.

In line 2, we write polyhedra defined in Lemma 2.2 and Lemma 2.3 as a system

---

[2]Note that m has to be necessarily greater than k, since otherwise optimization problems defining γ_t and ϕ_t would be unbounded.

Algorithm 1 Computation of D_L

Require: Data $A_{1,t}$, $A_{2,t}$, $b_{2,t}$, $C_{1,t}$, functions c_t, $b_{1,t}$, κ_t for all $t \in \mathbb{T}$

1: **for** $t \in \mathbb{T}$ **do**
2:      Define A_γ, b_γ, A_ϕ, b_ϕ such that $\Gamma_t = \{x : A_\gamma x \le b_\gamma\}$ and $\Phi_t = \{x : A_\phi x \le b_\phi\}$
3:      $M_\gamma^D \leftarrow -\infty$, $M_\phi^D \leftarrow -\infty$, $\mathcal{I}_\gamma \leftarrow \emptyset$, $\mathcal{I}_\phi \leftarrow \emptyset$
4:      **for** $I \subset \{1, \ldots, N_{\gamma,t}\}$ with $|I| = K_{\gamma,t}$ **do**   ▷ deterministic vertices LU for γ
5:          **if** $b_\gamma^I(\xi_t, \tilde{\xi}_t) \equiv b_\gamma^I \in \mathbb{R}^{K_{\gamma,t}}$ **then**   ▷ rhs deterministic
6:              x_γ^I solves $A_\gamma^I x_\gamma^I = b_\gamma^I$
7:              **if** $A_\gamma x_\gamma^I \le b_\gamma$ **then** $M_\gamma^D \leftarrow \max(M_\gamma^D, ||x_{\gamma,2}^I)||_\infty)$
8:          **else**   ▷ rhs stochastic
9:              Store LU factorization of A_γ^I in $(P_\gamma^I, L_\gamma^I, U_\gamma^I)$
10:             $\mathcal{I}_\gamma \leftarrow \mathcal{I}_\gamma \cup \{I\}$
11:         **end if**
12:     **end for**
13:     **for** $I \subset \{1, \ldots, N_{\phi,t}\}$ with $|I| = K_{\phi,t}$ **do**   ▷ deterministic vertices LU for ϕ
14:         **if** $b_\phi^I(\xi_t) \equiv b_\phi^I \in \mathbb{R}^{K_{\phi,t}}$ **then**   ▷ rhs deterministic
15:             x_ϕ^I solves $A_\phi^I x_\phi^I = b_\phi^I$
16:             **if** $A_\phi x_\phi^I \le b_\phi$ **then** $M_\phi^D \leftarrow \max(M_\phi^D, ||x_\phi^I||_\infty)$
17:         **else**   ▷ rhs stochastic
18:             Store LU factorization of A_ϕ^I in $(P_\phi^I, L_\phi^I, U_\phi^I)$
19:             $\mathcal{I}_\phi \leftarrow \mathcal{I}_\phi \cup \{I\}$
20:         **end if**
21:     **end for**
22:     **for** $\omega_t \in \Omega_t$ **do**   ▷ compute $\phi_t(\xi_t)$
23:         $\phi_t(\xi_t(\omega_t)) \leftarrow M_\phi^D$
24:         **for** $I \in \mathcal{I}_\phi$ **do**
25:             Use $(P_\phi^I, L_\phi^I, U_\phi^I)$ to solve $A_\phi^I x_\phi^I = b_\phi^I(\xi_t(\omega_t))$
26:             **if** $A_\phi x_\phi^I \le b_\phi$ **then** $\phi_t(\xi_t(\omega_t)) \leftarrow \max(\phi_t(\xi_t(\omega_t)), ||x_\phi^I||_\infty)$
27:         **end for**
28:     **end for**
29:     **for** $\tilde{\omega}_t \in \tilde{\Omega}_t$ **do**
30:         $\phi_t(\tilde{\xi}(\tilde{\omega}_t)) \leftarrow M_\phi^D$
31:         **for** $I \in \mathcal{I}_\phi$ **do**   ▷ compute $\phi_t(\tilde{\xi}_t)$
32:             Use $(P_\phi^I, L_\phi^I, U_\phi^I)$ to solve $A_\phi^I x_\phi^I = b_\phi^I(\tilde{\xi}_t(\tilde{\omega}_t))$
33:             **if** $A_\phi x_\phi^I \le b_\phi$ **then** $\phi_t(\tilde{\xi}_t(\tilde{\omega}_t)) \leftarrow \max(\phi_t(\tilde{\xi}_t(\tilde{\omega}_t)), ||x_\phi^I||_\infty)$
34:         **end for**
35:         **for** $\omega_t \in \Omega_t$ **do**
36:             $\gamma_t(\xi_t(\omega_t), \tilde{\xi}_t(\tilde{\omega}_t)) \leftarrow M_\gamma^D$
37:             **for** $I \in \mathcal{I}_\gamma$ **do**   ▷ compute $\gamma_t(\xi_t(\omega_t), \tilde{\xi}_t(\tilde{\omega}_t))$
38:                 Use $(P_\gamma^I, L_\gamma^I, U_\gamma^I)$ to solve $A_\gamma^I x_\gamma^I = b_\gamma^I(\xi_t(\omega_t), \tilde{\xi}_t(\tilde{\omega}_t))$
39:                 **if** $A_\gamma x_\gamma^I$ $\le$ b_γ **then** $\gamma_t(\xi_t(\omega_t), \tilde{\xi}_t(\tilde{\omega}_t))$ $\leftarrow$
    $\max(\gamma_t(\xi_t(\omega_t), \tilde{\xi}_t(\tilde{\omega}_t)), ||x_{\gamma,2}^I||_\infty)$
40:             **end for**
41:             Compute $\theta_t(\xi_t(\omega_t), \tilde{\xi}_t(\tilde{\omega}_t))$ according to (2.14) and (2.15).
42:         **end for**
43:     **end for**
44: **end for**
45: Compute $D_L(\xi, \tilde{\xi})$ according to (2.20)

---

of linear inequalities with single vectors and matrices A_γ, b_γ, A_ϕ, and b_ϕ. This is merely for notational convenience in the rest of the algorithm. We assume that there are in all $N_{\gamma,t}$ and $N_{\phi,t}$ inequalities defining Γ_t and Φ_t, respectively.

We define $K_{\gamma,t}$ and $K_{\phi,t}$ as dimensions of Γ_t and Φ_t. In lines 4-12 and 13-21 we iterate over all sets of size $K_{\gamma,t}$ and $K_{\phi,t}$ of linear inequalities defining the polyhedra. The solution to the corresponding system of linear equalities defines a vertex if it fulfills all the rest of the constraints. We evaluate the norm of those vertices that do not depend on random data and keep track of the maximum while we store the LU factorization of the systems whose right-hand sides are random. Note that for the computation of γ_t, we only require the norm of the components that correspond to λ_2 in Lemma 2.2, which we denote by $x_{\gamma,2}^I$ for a specific set of inequality constraints I. We also remark that for γ_t all vertices except the origin depend on the randomness unless either κ_t is independent of the randomness (stagewise independence) or the objective is deterministic.

In lines 23-29, we compute $\phi_t(\xi_t)$ by solving the linear systems $\mathcal{I}_\phi$ for all possible realizations of ξ_t using the stored LU factorizations. In line 37-44 we compute $\phi_t(\tilde{\xi}_t)$ for the realizations of $\tilde{\xi}_t$ and additionally compute $\gamma_t(\xi_t, \tilde{\xi}_t)$.

Given these quantities we easily obtain $\theta_t(\xi_t, \tilde{\xi}_t)$ in line 43 and finally D_L in line 47. Note that if either Γ_t or Φ_t are independent of the stage or at least identical in some stages, the algorithm can be modified by changing the outer loop in line 1 in an obvious way to avoid repetitive computations.

2.5.2 The flower girl Problem

As a demonstration, we consider a multi-stage extension of the classical newsvendor problem – the problem of a flower girl selling flowers, facing a random demand and a random sales price with the possibility to store excess flowers for the next periods. The problem has $(T+1)$ stages, with stage $t = 0$ being the deterministic start state. In every stage t, we start with the inventory level S_t limited by the storage capacity

$\bar{S}_t$. After the demand ξ_t^1 and the price ξ_t^2 become known in stage t, the flower girl sells x_t^2 flowers and places an order x_t^1 for flowers to be delivered from a wholesaler for a price p on the next day. If the available quantity exceeds the demand, the flower girl adds the excess to her inventory for sale in $(t+1)$. Due to the perishable nature of flowers, a fraction of $k \in (0,1)$ of the stored flowers are spoilt on the next day. The order in stage t has to be placed without knowing the random demand ξ_{t+1}^1. On the next day, the flowers can be sold at a market price ξ_{t+1}^2 not known on day t. The flower girl starts in period $t=0$ without any stock and no demand, i.e., $S_0 = 0$ and $\xi_0^1 = 0$.

The decisions in every stage consist of the number of flowers to order for the next stage x_t^1, the number of flowers to sell x_t^2, and the inventory level of the next day x_t^3. Note that, as described in Remark 2.1, the environmental state variable S_{t+1} is represented by x_t^3 so as to make the feasible set fit (2.2).

The storage equation consequently is

$$x_t^3 = (1-k) \cdot (S_t - x_t^2) + x_t^1, \quad \forall t = 0, \ldots, T.$$

The sales decisions are constrained by the random demand as well as the storage level, i.e.,

$$x_t^2 \leq \min \left\{ \xi_t^1, S_t \right\}, \quad \forall t = 0, \ldots, T, \quad a.s.$$

Furthermore, we impose the following constraints

$$x_t^3 = S_{t+1}, \quad x_t^3 \leq \bar{S}_{t+1}, \quad x_t^1, x_t^2, x_t^3, S_{t+1} \geq 0, \quad \forall t = 0, \ldots, T.$$

The flower girl maximizes her expected profit, which is given by

$$\mathbb{E} \left(\sum_{t=0}^{T} \xi_t^2 x_t^2 - p x_t^1 \right).$$

For our numerical example, we consider the three-stage version of the problem, i.e., the problem with $T = 2$. Further, we choose $k = 0.1$, $p = 5$ and the vector of

storage capacities $\bar{S} = (\bar{S}_0, \bar{S}_1, \bar{S}_2, \bar{S}_3) = (0, 11, 9, 0)$. To rewrite the problem to the form in (2.1), we define $c_t(\xi_t) = (-p, \xi_t^2, 0)^\top$ and the vectors and matrices appearing in the constraints as

$$A_{1,t} = \begin{pmatrix} 0 & 1 & 0 \\ 0 & 1 & 0 \\ -1 & (1-k) & 1 \\ 1 & -(1-k) & -1 \end{pmatrix}, \quad b_{1,t}(\xi_t) = \begin{pmatrix} \xi_t^1 \\ 0 \\ 0 \\ 0 \end{pmatrix}, \quad C_{1,t} = \begin{pmatrix} 0 \\ 1 \\ (1-k) \\ -(1-k) \end{pmatrix},$$

$$A_{2,t} = \begin{pmatrix} 0 & 0 & 1 \end{pmatrix}, \quad b_{2,t} = \begin{pmatrix} \bar{S}_t \end{pmatrix}.$$

As the function c_t and the matrices $A_{1,t}$, $A_{2,t}$ and $C_{1,t}$ have the same form for all stages, we can ignore the index t.

Next, we find the constants $\kappa_t(\xi_{t-1})$, which depend on the slopes of the value functions. Note that, in every period t, the flower girl can either sell all flowers for the price ξ_t^2 or hold them for sale in future periods, in which case part of the flower will perish. In the last period $\kappa_{T+1}(\xi_T) = 0$, since the flowers are worthless at the end of planning while in period $(T-1)$, stored flowers can be sold in period T, i.e., $\kappa_T(\xi_{T-1}) = 2\mathbb{E}(\xi_T^2|\xi_{T-1})$. In periods $t < (T-1)$, flowers can either be sold in period $t+1$ or carried on to period $t+2$, in which case they have to be evaluated using the respective value function. This yields the approximation

$$\kappa_t(\xi_{t-1}) = 2\mathbb{E}(\max\{\xi_t^2, (1-k)\kappa_{t+1}(\xi_t)\}|\xi_{t-1}).$$

This logic can be recursively applied to find all the constants κ_t.

Putting everything together, the problem can be formulated as

$$
V_t\left(S_t, \xi_t\right) = \begin{cases}
\max_{x_t, S_{t+1}} & c(\xi_t)^\top x_t + \mathbb{E}\left(V_{t+1}\left(S_{t+1}, \xi_{t+1}\right) | \xi_t\right) \\
\text{s.t.} & A_1 x_t \leq b_{1,t}(\xi_t) + C_1 S_t \\
& A_2 x_t = S_{t+1} \\
& A_2 x_t \leq b_{2,t+1} \\
& x_t, S_{t+1} \geq 0
\end{cases}
$$

$$
= \begin{cases}
\max_{x_t, S_{t+1}} & c(\xi_t)^\top x_t + \gamma \\
\text{s.t.} & A_1 x_t \leq b_{1,t}(\xi_t) + C_1 S_t \\
& A_2 x_t = S_{t+1} \\
& A_2 x_t \leq b_{2,t+1} \\
& \mathbb{1}_{m_{t+1}(\xi_t)} \gamma \leq b_{3,t+1}(\xi_t) + C_{3,t+1}(\xi_t) S_{t+1} \\
& x_t, S_{t+1} \geq 0.
\end{cases}
$$

We consider the two Markov processes ξ and $\tilde{\xi}$ presented in Figure 2.3a and Figure 2.3b with transition probabilities

$$
P_1 = \begin{pmatrix} 0.5523 & 0.0871 & 0.3605 \end{pmatrix}, P_2 = \begin{pmatrix} 0.5489 & 0.0005 & 0.2901 & 0.1606 \\ 0.4576 & 0.0004 & 0.2067 & 0.3353 \\ 0.3953 & 0.0403 & 0.2681 & 0.2962 \end{pmatrix},
$$

$$
\tilde{P}_1 = \begin{pmatrix} 0.6374 & 0.3626 \end{pmatrix}, \tilde{P}_2 = \begin{pmatrix} 0.5529 & 0.2855 & 0.1626 \\ 0.4364 & 0.2838 & 0.2797 \end{pmatrix}.
$$

To bound the difference in the optimal values, we calculate $D_L(\xi, \tilde{\xi})$. As detailed in Algorithm 1, the constant $\gamma_t(\xi_t, \tilde{\xi}_t)$ can be obtained by maximizing $\|\lambda_2\|_\infty$ over the extreme points of the polyhedron

$$
\Gamma = \left\{ (\lambda_2, \lambda_3, \lambda_4, \lambda_6, \lambda_7) : \begin{array}{c} \left\| A_1^\top \lambda_2 + A_2^\top (\lambda_3 + \lambda_4) - \lambda_6 \right\|_\infty \leq 1 + \|c_t(\xi_t)\|_\infty \\ \|\lambda_3 - \lambda_7\|_\infty \leq 1 + \min\left\{ k_{t+1}(\xi_t), \tilde{\kappa}_{t+1}(\tilde{\xi}_t) \right\} \\ \lambda_2, \lambda_4, \lambda_6, \lambda_7 \geq 0 \end{array} \right\}.
$$

(a) First Markov Process ξ (b) Second Markov Process $\tilde{\xi}$
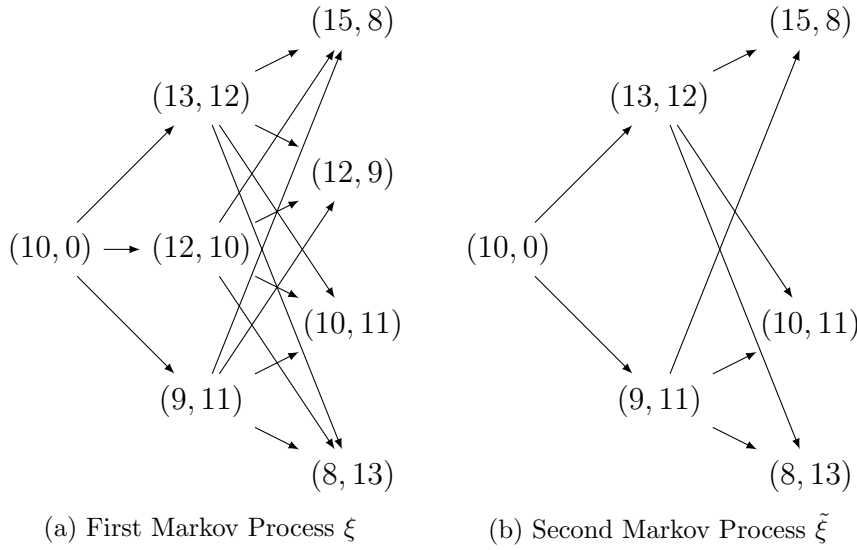
Figure 2.3: Depiction of the two Markov processes used for the numerical calculation of the flower girl example.

Similarly, the constant $\phi_t(\xi_t) = \phi(A_1, b_{1,t}(\xi_t) + C_1^+ b_{2,t}, A_2, b_{2,t+1})$ can be found by maximizing $\|x\|_\infty$ over the extreme points of the polyhedron

$$\Phi = \left\{ x : A_1 x \leq b_{1,t}(\xi_t) + C_1^+ b_{2,t}, A_2 x \leq b_{2,t+1}, A_2 x \geq 0, x \geq 0 \right\}.$$

Having calculated γ_t and ϕ_t, we proceed by computing $\theta_t(\xi_t, \tilde{\xi}_t)$ using (2.13) and (2.14). Then, we can determine the joint distribution π that minimizes the distance between processes by solving the linear optimization problem (2.20).

The resulting optimal transportation plan yields a distance of $D_L(\xi, \tilde{\xi}) = 7.03$. The optimal value of our problem for ξ is equal to 126.59, and for $\tilde{\xi}$, the optimal value equals 129.16, resulting in a difference of 2.58. Hence, our bound overestimates the difference in the optimal values by 4.45.

Lastly, we compare the performance of D_L to the performance of the nested distance defined in Pflug and Pichler (2012, 2014). For this calculation, it is necessary to simplify the problem to make the constraints independent of the randomness. To this end, we fix the demand at each stage. In particular, we assume that the

demand is equal to 0, 11, and 9 in the stages $t = 0$, 1, and 2, respectively. For this simplified setup, we obtain $D_L(\xi, \tilde{\xi}) = 3.94$ and $D_T(\xi, \tilde{\xi}) = 4.31$ demonstrating that for our problem D_L provides a tighter bound than D_T (see also Remark 2.12).

2.6   Conclusions

Stochastic optimization problems with a Markovian structure strike a good balance between the complexity of the underlying randomness and the expressiveness of the corresponding problem class. In particular, since scenario lattices offer leaner discretization structures than scenario trees, the unfavorable computational properties of general stochastic optimization problems can be, in part, mitigated.

In this paper, we define a family of problem-dependent semi-distances for linear stochastic optimization problems with a Markovian structure that can be used to bound objective values. We also show that every Markov process can, in theory, be approximated to arbitrary precision in terms of the defined distances. Therefore, the concepts in this paper can be used to find arbitrary precise discrete approximation of complicated problems, possibly with continuous state spaces.

Furthermore, we contribute to the literature on transportation distances by an approach that is capable of dealing with randomness in the constraints. This necessitates a different technique of proof since the transport of solutions between problems becomes impossible in this framework. We, therefore, base our results on stability results for linear programs.

In this paper, we laid the foundations for a theory-driven method to generate scenario lattices. Further research is required to find computationally efficient ways to do so and to evaluate the outcomes of real-world problems.

Chapter 3

Stochastic Dual Dynamic Programming for Optimal Power Flow Problems under Uncertainty

written in collaboration with Prof. David Wozabal[1]

Planning in the power sector has to take into account the physical laws of alternating current (AC) power flows as well as uncertainty in the data of the problems, both of which greatly complicate optimal decision-making. We propose a computationally tractable framework to solve multi-stage stochastic optimal power flow (OPF) problems in AC power systems. Our approach uses recent results on dual convex semi-definite programming (SDP) relaxations of OPF problems in order to adapt the stochastic dual dynamic programming (SDDP) algorithm for problems with a Markovian structure. We show that the usual SDDP lower bound remains valid and that the algorithm converges to a globally optimal solution of the stochastic AC-OPF problem as long as the SDP relaxations are tight. To test the practical viability of our approach,

we set up an extensive case study of a storage siting, sizing, and operations problem. We show that the convex SDP relaxation of the stochastic problem is usually tight and discuss ways to obtain near-optimal physically feasible solutions when this is not the case. The algorithm finds a physically feasible policy with a small optimality gap and yields a significant added value of 27% over a rolling deterministic policy, which leads to overly optimistic policies and underinvestment in flexibility. This demonstrates that the standard industry practice of assuming direct current and deterministic problems should be abandoned in favor of models that consider realistic AC flows and stochasticity in the data.

3.1   Introduction

The power sector is instrumental in the efforts to transition to a clean, carbon-neutral energy system. In the process of this transition, power systems worldwide experience transformational change as new sources of demand like electric mobility or electric heating are gaining importance, and production is increasingly shifting to variable renewable sources of electricity (VRES).

The latter development especially increases the stress on existing power systems since VRES capacities are often located far from demand centers and consequently induce flows that existing transmission systems were not designed for. Furthermore, the output of wind energy and solar PV, the most common forms of renewable power generation, is intermittent and depends on environmental factors outside the control of plant owners and transmission system operators.

As a result, there are numerous challenges in the design and operation of future power systems, and it is presently unclear how to best resolve them in a manner that leads to reliable electricity systems that are at the same time emission-free and cost-efficient. In particular, the question of how and to which extent existing grid

infrastructure has to be updated and what role grid-level electricity storage should play is central.

In order to answer these questions, one has to consider the physical laws of power flow and solve optimal power flow (OPF) problems, i.e., optimization problems that incorporate explicit rules governing physical flows in their constraints or objective functions. The goal of OPF problems is to optimize the steady-state operating point of transmission and distribution networks in order to deliver electricity from suppliers to consumers as efficiently as possible. This fundamental problem was formulated for the first time by Carpentier (1962), and since then, substantial progress has been made in the understanding of this problem class. See Frank et al. (2012a,b) for excellent surveys of the recent literature.

While direct current (DC) networks can be incorporated relatively easily in optimization models through a set of linear constraints, networks with alternating current (AC) require non-linear constraints that make the resulting AC-OPF problems non-convex and ultimately NP-hard (e.g. Lavaei and Low 2012).

However, real-world power systems use alternating current since AC power can be easily *stepped up and down* between different voltage levels, enabling the parallel operation of a long-distance, high-voltage transmission system and a distribution grid, which provides safe low-voltage electricity to end consumers.

Many standard planning tools, used, for example, by network operators, ignore the complexities of AC power flow and employ DC relaxations. While these approximations work well for the high-voltage transmission systems, where the X/R ratio is high enough to ensure de-facto decoupling of active and reactive power flow loops, they lead to large deviations from physical realities in lower voltage grids (see, e.g., Larrahondo et al. 2021, Stott et al. 2009).

There are many tractable approximations that can be used to solve AC-OPF problems including various linear programming-based relaxations and approximations (e.g., Coffrin and Van Hentenryck 2014), local search algorithms (e.g., Wu

et al. 2018a), and a variety of conic relaxations (e.g., Low 2014a,b).

In classic power systems planning, the only sources of uncertainty are conventional demand and power plant outages. Since in large networks, the former can be very well predicted, and the latter is a rare event that is taken care of by redundancies in network design, traditional OPF problem formulations are usually deterministic. However, the transition to carbon-neutral power systems that rely on many distributed resources and encompass an increasing share of load from electric heating and electric mobility introduces new sources of uncertainty, changing the nature of OPF problems and necessitating a more explicit treatment of randomness.

In particular, the large-scale introduction of VRES introduces uncertainty on the supply side, which is absent from classical power systems planning. Furthermore, as the potential for demand response by small dispersed consumers keeps increasing with the introduction of smart grids, electric heating, and electric mobility, the resulting flexibilities can be used by grid operators. Making use of this flexibility entails dealing with resources that are only partly controllable and whose availability and operational state have to be considered uncertain.

In this paper, we propose a general multi-stage stochastic optimization framework for AC-OPF problems that explicitly models AC power flow and, at the same time, is computationally tractable. In particular, we show that recent advances in convex relaxations of AC-OPF problems and decomposition methods for Markovian stochastic optimization problems can be combined to generate high-quality, physically accurate solutions for multi-stage stochastic AC-OPF problems.

Since even linear two-stage stochastic optimization, the most well-behaved subclass of stochastic optimization problems, is NP-hard (Hanasusanto et al. 2016), solving stochastic multi-stage AC-OPF problems seems hopeless at first glance.

Nevertheless, some attempts have been made to solve stochastic AC-OPF problems in the extant literature. However, most approaches consider two-stage stochastic optimization problems (e.g. Bai et al. 2017, Bucciarelli et al. 2018) and most

authors additionally use DC approximations (e.g., Bienstock et al. 2014, Pandzic et al. 2015). These models typically combine an investment decision on the first stage with operational decisions, possible over a longer period of time, in the second stage.

However, multi-stage stochastic programming, where uncertainty gradually *reveals itself* over several stages, is important for operational planning in systems containing assets that *link* several time periods, such as electricity storage. Models that merge operational planning into a single stage implicitly assume perfect information, which is overly optimistic and typically leads to underinvestment in storage and line capacity.

The literature on multi-stage stochastic optimization in OPF problems is extremely scarce. The authors in Papavasiliou et al. (2018) solve a multi-stage stochastic OPF problem based on *stochastic dual dynamic programming* (SDDP) using DC relaxations. Yang and Nagarajan (2021) use second-order-cone relaxation and adapt SDDP for a specific multi-stage $(N-1)$ contingency planning problem with random disruptions. The paper that comes closest to our approach is Rosemberg et al. (2021), which considers standard instances of a long-term hydro-planning problem and tests different convex relaxations to obtain approximations of optimal dispatch decisions. However, the authors use a highly abstracted tactical planning version of the problem in monthly time steps and do not provide many details on their implementation of the SDDP algorithm and how to recover from physically infeasible solutions. Furthermore, the considered problems deal with high voltage transmission grids with high X/R ratios, where the non-convexities of power flow problems generally play less of a role.

In our approach, we utilize recent advances in convex semi-definite programming (SDP) relaxations of AC-OPF problems that have been shown to allow for fast and accurate solutions to deterministic problems. In particular, the seminal paper Lavaei and Low (2012) uses the dual of a relaxed SDP formulation of a specific

AC-OPF problem and demonstrates that after some small modifications to the admittance matrix, which do not change the problem in a practically meaningful way, the approximation is tight for a large range of problems. These results triggered a flurry of research, which is comprehensively reviewed in Molzahn and Hiskens (2019), Zohrizadeh et al. (2020).

Another important building block of our approach is the advances in decomposition methods for multi-stage stochastic optimization that make it possible to solve large convex Markovian problems with many stages in a relatively short time. One of the most successful algorithmic frameworks in this regard is SDDP, which decomposes stochastic optimization problems along its stages and was originally proposed for problems with stage-wise independent randomness in Pereira and Pinto (1991). Since then, the original SDDP algorithm has been considerably refined and is now very well understood. In particular, Löhndorf and Wozabal (2021a), Löhndorf et al. (2013), Philpott and de Matos (2012) extend the original SDDP method to Markovian processes.

Convergence of SDDP is studied in Philpott and Guan (2008) for the linear case and in Girardeau et al. (2015) for a fairly general class of convex problems. Furthermore, Löhndorf et al. (2013) relax some of the restrictions of the original version of the method and Shapiro (2011) studies probabilistic stopping criteria. Terça and Wozabal (2020) show how to compute sensitivities for stochastic optimization problems solved using SDDP and propose an asymptotic approximation error of lattice-based approximations.

Finally, Lan (2020) shows that the complexity of SDDP only grows polynomially in the number of stages and therefore curbs the *curse of dimensionality* for stochastic optimization problems where the main difficulty are not large decision problems in the stages but rather the fact that there are many decision stages.

The contribution of this paper can be summarized as follows:

1. We propose an SDDP decomposition algorithm for a general class of multi-

stage stochastic AC-OPF problems by combining recent results on SDDP for Markovian multi-stage stochastic optimization problems based on scenario lattices with results on convex SDP relaxation of AC-OPF problems. The result is a general framework that can be used to solve a large class of multi-stage AC-OPF problems.

2. We show that the proposed algorithm converges to the true solution if the relaxation of the AC-OPF problems is exact in the forward pass and the backward pass of the algorithm. Furthermore, we show that the gap between the SDDP upper and lower bound can be used as a certificate of convergence as long as physically feasible voltages can be found in the forward pass. To that end, we propose a method to compute such physically feasible solutions as *projections* of the solutions of the relaxed AC-OPF problem to the feasible set of the non-convex problem in cases where the employed convex relaxation is not tight.

3. We provide a proof of concept in the form of an extensive storage siting, sizing, and operations problem in a modified version of the network proposed in Barrows et al. (2020). We model renewable production by wind and solar and loads as random and decide about storage investments in the first stage and about operation for a consecutive week of planning in the later stages.

   The results illustrate that the problem can be solved in a reasonable time with an optimality gap of below 3% relative to the globally optimal policy. We furthermore demonstrate that the stochastic approach yields significantly different policies than rolling deterministic planning, which leads to lower investment in storage and consequently more curtailment of production and loads as well as higher cost, resulting in a significant value of the stochastic solution of 27%.

The rest of the manuscript is organized as follows: In Section 3.2, we give a

short, yet self-contained, introduction to AC-OPF problems and their formulation as semi-definite programs, which is complemented by an appendix that provides more details on the construction of admittance matrices. In Section 3.3, we integrate the dual of a relaxed AC-OPF problem with the SDDP algorithm and give sufficient conditions for convergence to the true solutions of the non-convex problem. Section 3.4 is devoted to the storage siting, sizing, and operations problem, which explores the computational aspects of the proposed approach in a medium-sized application example. Finally, Section 3.5 concludes the paper and discusses avenues for further research. All proofs are relegated to A.

Notation: We work on a standard probability space $(\Omega, \mathcal{F})$ and define a filtration $\{\emptyset, \Omega\} = \mathcal{F}_0 \subseteq \mathcal{F}_1 \subseteq \cdots \subseteq \mathcal{F}_T \subseteq \mathcal{F}$ such that all random quantities ξ_t that realize in period t are measurable with respect to $\mathcal{F}_t$, denoted by $\xi_t \triangleleft \mathcal{F}_t$. We denote by $\mathbb{S}^d$ the set of symmetric $(d \times d)$ matrices. Furthermore, $x \circ y$ denotes the element-wise multiplication of two vectors x and $y \in \mathbb{R}^d$, while $A \bullet B = \text{tr}(AB)$ with $\text{tr}(A)$ the trace of a matrix A. Lastly, we use the notation $[d] = \{1, \ldots, d\}$ for $d \in \mathbb{N}$, denote complex conjugation by *, and the conjugate transpose by ^{H}.

3.2   Problem Description

This section specifies a class of fairly general finite-horizon multi-stage AC-OPF problems. Section 3.2.1 briefly introduces the relevant principles of AC power flow. For an in-depth treatment of the fundamentals of power flow, we refer to Glover et al. (2008), while Frank and Rebennack (2016) give a compact yet excellent introduction to the subject of optimal power flow problems. In Section 3.2.2, these principles are applied to power system modeling. Section 3.2.3 uses these preparations to define a multi-stage stochastic AC-OPF problem in its extensive form. Finally, in the spirit of Lavaei and Low (2012), Section 3.2.4 introduces an SDP formulation of the AC-OPF problem, which naturally lends itself to a convex approximation.

3.2.1   Alternating Current Power Flow

In a direct current circuit, the voltage remains constant over time. In this setting, all features of the system relevant to this paper can be explained with the *water analogy*, where *electric charge* is equated to water flowing between reservoirs of different elevations, which correspond to nodes of the electrical circuit. Gravity induces a potential between the reservoirs, which corresponds to *voltage $V \in \mathbb{R}$* and represents the potential energy per unit of water/charge, while the flow of water equals *electric current $I \in \mathbb{R}$*. Lastly, the limited diameter of the pipes connecting the reservoirs introduces an opposition to flow, which has an effect that is analogous to *electric resistance $R \in \mathbb{R}$*. Note that V is a *difference in potential*, i.e., voltages relate to different nodes of a circuit. If voltages are associated with single nodes, they are to be interpreted as differences to the system reference, usually *ground*, i.e., the lowest possible voltage level of no electric potential at all.

Bearing in mind this analogy, Ohm's law, $V = IR$, stating that for a given *voltage/pressure*, the induced *current/flow* is inversely proportional to the resistance, makes intuitive sense. Furthermore, it is easy to comprehend *Kirchhoffs current law*, which states that the current flowing into a node from connected nodes equals the current flowing out of the node (no current/water is lost) as well as the *Kirchhoffs' voltage law*, which requires voltages (elevation differences) to sum to zero when going around a closed loop in the network. These ingredients are sufficient to *solve* DC networks, i.e., given an input voltage and resistances of components, calculate all unknown voltages and currents using linear equations that can be easily incorporated in convex optimization problems.

Alternating current networks differ from the DC situation in that voltages follow a sinusoidal pattern $v(t) = V^A \sin(2\pi w t + \phi)$ over time t, where V^A is the peak voltage, ϕ is the phase angle, and w is the frequency in Hertz (if time is measured in seconds). This pattern is induced by AC voltage sources, which typically come in the form of generators that transform mechanical energy into electric energy by

rotating a coiled wire in a magnetic field in a circular motion with constant angular speed, as illustrated in Figure 3.1. Since moving a conductor in a magnetic field produces a voltage in the conductor that is proportional to the speed at which the coil crosses the magnetic field lines, i.e., the horizontal speed of the conductor in the right panel of Figure 3.1, the induced voltage follows a sinusoidal pattern. Note that as the two parts of the coil change positions, the voltage differences change sign due to *Flemming's right-hand rule.*
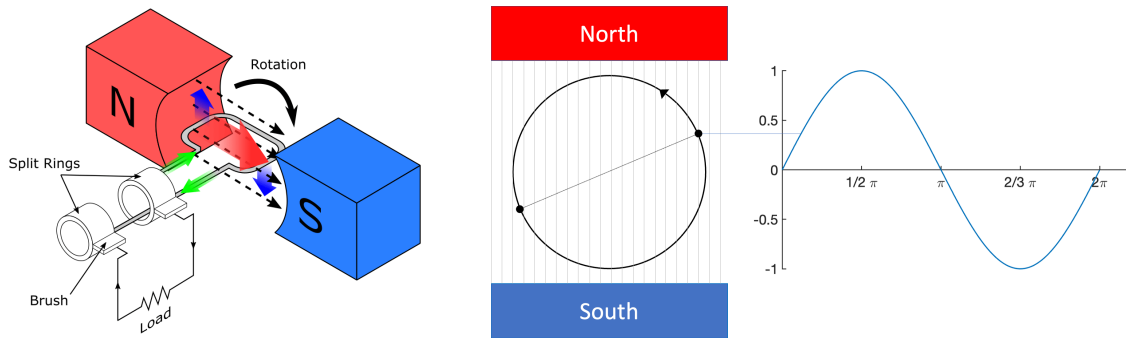
Figure 3.1:   The left panel shows a simplified design of an AC generator where a looped conductor is rotated in a magnetic field by an external force (image by courtesy of `www.saVRee.com`). The right panel shows a cut through the generator on the right with the two dots representing the wire and the induced sinusoidal voltage wave on the right.

Since voltages and currents fluctuate in AC systems, they are usually described in terms of either their peak values V^A or, more commonly, their *root mean square* (RMS) values, which, in the case of the voltage, are defined as

$$V^{RMS} = \sqrt{\int_0^1 \left(V^A \sin(2\pi wt + \phi)\right)^2 dt} = V^A \sqrt{\int_0^1 \sin(2\pi wt)^2 dt} = \frac{V^A}{\sqrt{2}}.$$

The definition of I^{RMS} for currents $i(t)$ is analogous.

While in the DC network, the only *opposition to current flow* is resistance, the pulsating nature of AC voltage induces another type of opposition, which is called *reactance.* Reactance is caused by the charge being stored either in magnetic fields that form around coils in electric components such as motors or transformers

(*inductive reactance*) or on the plates of a capacitor (*capacitive reactance*). In the case of the more common inductive reactance, the magnetic field lines cross the coil as the voltage in the network rises and the field builds up, inducing a current in the opposite direction of the current supplied by the voltage source. This is a manifestation of the same electromagnetic principle by which a voltage is induced when a coil moves through the magnetic field in a generator.

Both inductive and capacitive reactance thus *disturb* the current flow $i(t)$ and cause it to be *out of phase* with the voltage that is produced by the voltage source as shown in Figure 3.2. In reality, loads are never purely resistive, inductive, or capacitive but rather present themselves as a mixture of these effects which together result in a cumulative phase shift $\phi \in [-\pi/2, \pi/2]$ of the current $i(t)$ relative to the voltage $v(t)$. However, the current can always be decomposed by projection on a purely resistive component (in phase with the voltage) and a component that is purely reactive/capacitive (completely out of phase) in the Hilbert space of square-integrable functions.
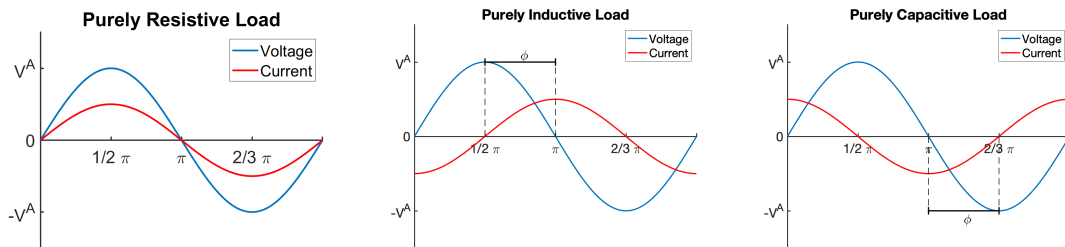
Figure 3.2: Three types of loads represent the different opposition to current flow in AC circuits, assuming the phase angle of the voltage to be equal to zero. The first panel shows a purely resistive load with voltage and current in phase, and the second panel shows a purely inductive load with a negative phase angle of $\phi = -\pi/2$ (the current *leads* the voltage), while the last panel shows a purely capacitive load with a positive phase angle of $\phi = \pi/2$ (the current *lags* the voltage).

As in DC networks, in AC networks, the instantaneous power at time t is the product of voltage and current, i.e., $p(t) = v(t)i(t)$. Assuming without loss of generality that the phase angle of the voltage is zero and $i(t) = I^A \sin(2\pi wt + \phi)$,

results in a cumulative power production of

$$P = V^A I^A \int_0^1 \sin(2\pi wt) \sin(2\pi wt + \phi) dt$$

$$= V^A I^A \left(\cos(\phi) \int_0^1 \sin(2\pi wt)^2 dt + \sin(\phi) \int_0^1 \sin(2\pi wt) \cos(2\pi wt) dt \right) \quad (3.1)$$

$$= V^A I^A \cos(\phi) \int_0^1 \sin(2\pi wt)^2 dt = V^{RMS} I^{RMS} \cos(\phi)$$

in one unit of time, which is called *active power* and represents the amount of useful electrical work delivered to the system. Note that due to the phase shift, the second term in (3.1) occurs, which represents the wastage of energy due to reactance in the network and which at times produces *negative power flows*, reducing the overall useful energy in the circuit. Taking the absolute value of these flows results in $V^{RMS} I^{RMS} \sin(\phi)$, which is called *reactive power Q*.

These relationships are frequently described by representing voltages, currents, and powers as complex numbers. Taking the example of currents, the idea is to represent $i(t) = I^A \sin(2\pi wt + \phi_I)$ by the complex number $I = I^{RMS} e^{i\phi_I}$, which encodes both the magnitude and the phase angle. Using this notation and setting the phase angle of the voltage to ϕ_V, we can write active and reactive power as

$$P = \mathfrak{Re}(VI^*) = \mathfrak{Re}(V^{RMS} I^{RMS} e^{i(\phi_V - \phi_I)}), \ Q = \mathfrak{Im}(VI^*), \quad (3.2)$$

which are the real and imaginary part of complex power $S = VI^* = P + iQ$, respectively. Note that the *apparent power* $|S|$ is the amount of energy that has to be put into the system, e.g., in the form of mechanical energy turning the generator. Hence, active, reactive, and apparent power are related by the *pythagorean relationship* $|S|^2 = P^2 + Q^2$, which is usually referred to as the *power triangle*, imagining the components P, Q, and S as the sides of a right-angled triangle with angle $\phi = (\phi_V - \phi_I)$ between the hypotenuse $|S|$ and the side P. We remark that reactive power Q has no physical manifestation but merely represents the loss of power induced by reactance according to the abovementioned relationship.

Note that Ohm's law, which relates voltages, currents, and resistance, can be generalized to AC circuits by writing $V = IZ$ where Z is the complex *impededance* $Z = |Z|e^{i\phi} = R + iX$ with R being classic resistance and X being the reactance. Multiplying complex current with impedence therefore does not only have a scaling effect (as in the DC case), but, by the choice of a non-zero reactance, also causes a rotation by ϕ which allows to model the phase-shifting effect of reactance. Equivalently, we can write $I = VY$, where $Y = Z^{-1}$ is called the *admittance*.

We conclude our introduction to AC power flow by noting the fact that relevant quantities in AC networks, such as active and reactive power in (3.2), depend in non-convex ways on the phase angles through the sine and cosine functions, and make AC-OPF problems non-convex and usually NP-hard (Lavaei and Low 2012).

3.2.2 Network Modeling

Electrical power systems are modeled as a network of n buses $\mathcal{N} = \{1, 2, \ldots, n\}$ which are interconnected by branches (lines) $\mathcal{L} \subseteq \mathcal{N} \times \mathcal{N}$. A bus corresponds to a node in a circuit and represents a load center (such as a lower voltage subnetwork), a generation unit, or a connection point to a higher voltage grid.

We associate to every bus $k \in \mathcal{N}$ a voltage $V_k \in \mathbb{C}$ relative to the system reference, usually ground, a current I_k which is absorbed/produced in the bus, and a shunt admittance y_k which models the admittance to the bus. Furthermore, each branch $(l, m) \in \mathcal{L}$ has an associated series admittance $y_{lm} \in \mathbb{C}$ modeling the impedance of the branch.

Note that by Kirchhoff's current law and Ohm's law, we get for every node $k \in \mathcal{N}$

$$0 = y_k(V_k - V_{k0}) + \sum_{i \neq k} y_{ki}(V_k - V_i) \Leftrightarrow I_k = y_k V_k + \sum_{i \neq k} y_{ki}(V_k - V_i),$$

where V_{k0} is the bus voltage and the first term, therefore, is the flow of current into/out of the bus while the second term is the flow from other buses. In order

to represent these relationships in a parsimonious form, we organize voltages and currents in vectors $V = (V_1, \ldots, V_n)^\top$ and $I = (I_1, \ldots, I_n)^\top$ and define a so-called *admittance matrix* Y with elements

$$(Y)_{kj} = \begin{cases} y_k + \sum_{i \neq k} y_{ki}, & k = j \\ -y_{kj}, & k \neq j, \end{cases}$$

so that we can express the relationship between currents and voltage vectors as $I = YV$.

In a real network, the computation of the admittance matrix is complicated by the need to account for shunt admittances of lines and possibly the existence of phase-shifting transformers with off-nominal turn ratios. We refer to Appendix B for details.

With these preparations, we can state AC-OPF problems entirely in terms of voltage and power, writing

$$S = V \circ I^* = V \circ Y^* V^*, \quad P = \mathfrak{Re}(S), \quad Q = \mathfrak{Im}(S) \tag{3.3}$$

for the vector of complex, active, and reactive powers at the buses of the network.

In order to describe flow on lines, let $e_k \in \mathbb{R}^n$ be the standard basis vectors and define the *partial admittance matrices* $Y_{lm} = (e_l e_l^\top - e_l e_m^\top) y_{lm}$, which allow to write the currents I_{lm} and powers S_{lm}, P_{lm}, and Q_{lm} flowing on line $(l, m) \in \mathcal{L}$ as

$$I_{lm} = y_{lm}(V_l - V_m) = e_l^\top Y_{lm} V, \quad S_{lm} = V_l I_{lm}^* = V^\top Y_{lm}^* V^*, \tag{3.4}$$

$$P_{lm} = \mathfrak{Re}(S_{lm}), \quad Q_{lm} = \mathfrak{Im}(S_{lm}). \tag{3.5}$$

Similarly, we define the matrices $Y_k = e_k e_k^\top Y$ containing only the k-th row of Y such that $I_k = e_k^\top Y_k V$.

Lastly, we remark that in power system analysis, electrical quantities are usually expressed in a *per unit system* as a ratio of the actual SI quantity to a base quantity. The per unit values are easier to interpret, as they usually lie within a narrow

numerical range close to 1. Furthermore, the per unit system improves the numerical stability of power flow calculations and reduces serious calculation errors, e.g., when referring quantities from one side of a transformer to the other.

3.2.3   A Stochastic Optimal Power Flow Problem

Optimal power flow problems are optimization problems that include the physical rules for power flow in their constraints or objectives. Classic formulations minimize the cost of electricity generation while maintaining the power system within safe operating limits.

We propose a general formulation of a finite horizon multi-stage stochastic AC-OPF problem. To this end, we assume that the part of the problem that is not directly concerned with modeling the power flow can be formulated as an SDP, thus covering most convex problem formulations of interest. We refer to Section 3.4 for a concrete instance of the proposed model class.

We denote the set of time periods by $t \in \mathcal{T} = \{1, \ldots, T\}$ and organize the non-electrical decision variables that model decisions taken in stage t into the symmetric, positive semi-definite matrix $X_t \in \mathbb{S}^{d_t}$, which may, for example, contain investment, operational, as well as trading and financial decisions.

We define the objective function as the expected cost over all stages

$$\mathbb{E}\left[\sum_{t \in \mathcal{T}} F_t \bullet X_t\right],$$

where $F_t : \Omega \to \mathbb{S}^{d_t}$ are random symmetric matrices with $F_t \triangleleft \mathcal{F}_t$. Note that the formulation above does not only cover risk-neutral decision-making but, by a suitable definition of variables and constraints, can also accommodate the most common risk measures (see, e.g., Föllmer and Schied 2004, Pflug and Römisch 2007).

We impose the following set of $s_t \in \mathbb{N}$ constraints in every stage of the problem

$$A_{ti}^1 \bullet X_{t-1} + A_{ti}^2 \bullet X_t \leq a_{ti}, \quad \forall i \in [s_t],\ t \in \mathcal{T}, \tag{3.6}$$

where $A_{ti}^1, A_{ti}^2 : \Omega \to \mathbb{S}^{d_t}$ and $a_{ti} : \Omega \to \mathbb{R}$ are random data with $A_{ti}^1, A_{ti}^2, a_{ti} \triangleleft \mathcal{F}_t$. As in standard stochastic optimization formulations, for example, for two-stage stochastic optimization problems (Birge and Louveaux 2011), (3.6) serves two purposes: Firstly, it models the constraints on decision variables in one stage of the problem, and secondly, it can be used to relate the variables in stage $t-1$ with the variable in stages t, thereby defining the dynamics of the problem on the level of the decisions. In this sense, the matrices A_{ti}^1 take the role of the *recourse matrix* in classic multi-stage linear stochastic programming.

Apart from X_t, the model also contains the voltages V_{tk}, the complex powers S_{tk}, the active powers P_{tk}, and the reactive powers Q_{tk} for bus k in time period t as decision variables. In order to model the physical behavior of the electrical system, we impose the following constraint

$$S_t = V_t \circ Y_t^* V_t^*, \quad P_t = \mathfrak{Re}(S_t), \quad Q_t = \mathfrak{Im}(S_t), \tag{3.7}$$

which relates voltages and powers on all buses of the network. In order to connect the decisions X_t to these variables, we impose the constraints

$$P_{tk} = A_{tk}^P \bullet X_t + a_{tk}^P, \qquad\qquad \forall k \in \mathcal{N}, t \in \mathcal{T} \tag{3.8}$$

$$Q_{tk} = A_{tk}^Q \bullet X_t + a_{tk}^Q, \qquad\qquad \forall k \in \mathcal{N}, t \in \mathcal{T}, \tag{3.9}$$

where $A_{ti}^P, A_{ti}^Q : \Omega \to \mathbb{S}^{d_t}$ and $a_{ti}^P, a_{ti}^Q : \Omega \to \mathbb{R}$ are random. The above constraints model inflows and outflows of power in the form of (possibly random) generation or random load and ensure that the electric variables modeling the power flow are in line with the decisions X_t, which determine how much power is injected/withdrawn in each bus.

Furthermore, we make the upper bounds for active power P_{tlm}, apparent power S_{tlm}, and voltage differentials between buses that are connected by branches (l, m)

dependent on the decisions X_t

$$|P_{tlm}| \leq B_{tlm}^P \bullet X_t + b_{tlm}^P, \qquad \forall (l,m) \in \mathcal{L}, t \in \mathcal{T} \qquad (3.10)$$

$$|S_{tlm}|^2 \leq B_{tlm}^S \bullet X_t + b_{tlm}^S, \qquad \forall (l,m) \in \mathcal{L}, t \in \mathcal{T} \qquad (3.11)$$

$$|V_{tl} - V_{tm}|^2 \leq B_{tlm}^V \bullet X_t + b_{tlm}^V, \qquad \forall (l,m) \in \mathcal{L}, t \in \mathcal{T}, \qquad (3.12)$$

with random symmetric coefficient matrices B_{tlm}^P, B_{tlm}^S, B_{tlm}^V and random parameters b_{tlm}^P, b_{tlm}^S, and b_{tlm}^V. Note that as these quantities are highly dependent on one another, most power flow models feature only one set of the above constraints.

Putting everything together, we arrive at the following multi-stage stochastic optimization problem for which we assume all constraints hold almost surely.

$$
\begin{aligned}
\min \quad & \mathbb{E}\left[\sum_{t \in \mathcal{T}} F_t \bullet X_t\right] \\
\text{s.t.} \quad & (3.4), (3.7), \quad \forall t \in \mathcal{T} && \text{(power flow)} \\
& P_t, Q_t, V_t, P_{tlm}, S_{tlm} \lhd \mathcal{F}_t, \quad \forall t \in \mathcal{T}, (l,m) \in \mathcal{L} && \text{(non-anticipativity)} \\
& (3.8), (3.9), (3.10), (3.11), (3.12) && \text{(connection with } X_t) \\
& (3.6), X_t \succeq 0, \ X_t \lhd \mathcal{F}_t, \quad \forall t \in \mathcal{T}. && \text{(constraints on } X_t)
\end{aligned}
$$
$$\tag{3.13}$$

Note that the measurability constraints enforce the non-anticipativity of the decisions.

3.2.4   An SDP Reformulation

In this section, we will cast (3.13) as an SDP. To achieve this, we need to write the problem entirely in terms of real numbers and reformulate power flow constraints.

Following the approach in Lavaei and Low (2012), we write

$$
M_k = \begin{pmatrix} e_k e_k^\top & 0 \\ 0 & e_k e_k^\top \end{pmatrix}, \quad
M_{lm} = \begin{pmatrix} (e_l - e_m)(e_l - e_m)^\top & 0 \\ 0 & (e_l - e_m)(e_l - e_m)^\top \end{pmatrix}.
$$

Furthermore, for a matrix $A \in \mathbb{C}^{n \times n}$, we define $\mathbb{A}, \hat{\mathbb{A}} \in \mathbb{R}^{2n \times 2n}$ as

$$
\mathbb{A} = \frac{1}{2} \begin{pmatrix} \mathfrak{Re}(A + A^\top) & \mathfrak{Im}(A^\top - A) \\ \mathfrak{Im}(A - A^\top) & \mathfrak{Re}(A + A^\top) \end{pmatrix}, \quad \hat{\mathbb{A}} = -\frac{1}{2} \begin{pmatrix} \mathfrak{Im}(A + A^\top) & \mathfrak{Re}(A - A^\top) \\ \mathfrak{Re}(A^\top - A) & \mathfrak{Im}(A + A^\top) \end{pmatrix},
$$

which we use to define matrices $\mathbb{Y}_k$, $\hat{\mathbb{Y}}_k$, $\mathbb{Y}_{lm}$, and $\hat{\mathbb{Y}}_{lm}$. We then define $\tilde{y} = [\mathfrak{Re}(y)^\top, \mathfrak{Im}(y)^\top]^\top \in \mathbb{R}^{2n}$ for $y \in \mathbb{C}^n$ and note that for $A \in \mathbb{C}^n$ and $y_1, y_2 \in \mathbb{C}^n$, we get

$$
\widetilde{Ay_1} = \begin{pmatrix} \mathfrak{Re}(A) & -\mathfrak{Im}(A) \\ \mathfrak{Im}(A) & \mathfrak{Re}(A) \end{pmatrix} \tilde{y}_1, \text{ and } \mathfrak{Re}(y_1^\top y_2) = \widetilde{(y_1^*)} y_2. \tag{3.14}
$$

To reformulate the problem, define $\tilde{V}_t$ as a real-valued version of the voltage vector and $W_t = \tilde{V}_t \tilde{V}_t^\top \in \mathbb{R}^{2n \times 2n}$. The idea of the employed SDP reformulation is to transfer the problem into the real numbers by using $\tilde{V}_t$ and then reformulate such that relevant quantities can be written as the product $\bullet$ of W_t with matrices that are derived from the admittance matrix. We demonstrate this principle using the example of active power at time t in node k, which we can write as

$$
P_{tk} = \mathfrak{Re}(V_{tk}^* I_{tk}) = \mathfrak{Re}\left(V_t^H e_k e_k^\top I_t\right) = \mathfrak{Re}\left(V_t^H Y_k V_t\right) = \tilde{V}_t^\top \begin{pmatrix} \mathfrak{Re}(Y_k) & -\mathfrak{Im}(Y_k) \\ \mathfrak{Im}(Y_k) & \mathfrak{Re}(Y_k) \end{pmatrix} \tilde{V}_t
$$

$$
= \tilde{V}_t^\top \mathbb{Y}_k \tilde{V}_t = \operatorname{tr}(\tilde{V}_t^\top \mathbb{Y}_k \tilde{V}_t) = \operatorname{tr}(\mathbb{Y}_k \tilde{V}_t \tilde{V}_t^\top) = \operatorname{tr}(\mathbb{Y}_k W_t) = \mathbb{Y}_k \bullet W_t,
$$

where the fourth equality gets rid of complex numbers and uses (3.14), the fifth uses $x^\top A x = \frac{1}{2} x^\top (A + A^\top) x$, while the subsequent steps use the properties of the trace operator.

The following lemma from Lavaei and Low (2012) executes this program for all relevant electrical quantities. We give a detailed proof in Appendix A.1.

Lemma 3.1. *For every time $t \in \mathcal{T}$, every node $k \in \mathcal{N}$, and every branch $(l, m) \in \mathcal{L}$*

the following relationships hold:

$$Q_{tk} = \hat{\mathbb{Y}}_k \bullet W_t, \qquad\qquad\qquad |V_{tk}|^2 = M_k \bullet W_t$$

$$|I_{tlm}|^2 = \mathbb{Y}_{lm}^\top \mathbb{Y}_{lm} \bullet W_t, \qquad\qquad\qquad P_{tlm} = \mathbb{Y}_{lm} \bullet W_t$$

$$|S_{tlm}|^2 = (\mathbb{Y}_{tlm} \bullet W_t)^2 + (\hat{\mathbb{Y}}_{lm} \bullet W_t)^2, \qquad |V_{tl} - V_{tm}|^2 = M_{lm} \bullet W_t.$$

Using the above result, we can reduce the power flow part of the problem to a decision about a positive semi-definite matrix W_t with rank one. Since every such matrix can be uniquely factored as $W_t = \tilde{V}_t \tilde{V}_t^\top$ for a vector $\tilde{V}_t \in \mathbb{R}^{2n}$, the voltages and hence all the other electrical variables can be recovered from W_t.

Using the identities in Lemma 3.1, we can now reformulate the multi-stage stochastic programming problem as

$$
\begin{aligned}
\min \quad & \mathbb{E}\left[\sum_{t \in \mathcal{T}} F_t \bullet X_t \right] \\
\text{s.t.} \quad & \mathbb{Y}_k \bullet W_t = A_{tk}^P \bullet X_t + a_{tk}^P, && \forall k \in \mathcal{N}, \ \forall t \in \mathcal{T} \\
& \hat{\mathbb{Y}}_k \bullet W_t = A_{tk}^Q \bullet X_t + a_{tk}^Q, && \forall k \in \mathcal{N}, \ \forall t \in \mathcal{T} \\
& M_k \bullet W_t = A_{tk}^V \bullet X_t + a_{tk}^V, && \forall k \in \mathcal{N}, \ \forall t \in \mathcal{T} \\
& \mathbb{Y}_{lm} \bullet W_t \le B_{tlm}^P \bullet X_t + b_{tlm}^P, && \forall (l, m) \in \mathcal{L}, \ \forall t \in \mathcal{T} \\
& \begin{bmatrix} -B_{tlm}^S \bullet X_t - b_{tlm}^S & \mathbb{Y}_{lm} \bullet W_t & \hat{\mathbb{Y}}_{lm} \bullet W_t \\ \mathbb{Y}_{lm} \bullet W_t & -1 & 0 \\ \hat{\mathbb{Y}}_{lm} \bullet W_t & 0 & -1 \end{bmatrix} \preceq 0, && \forall (l, m) \in \mathcal{L}, \ \forall t \in \mathcal{T} \\
& M_{lm} \bullet W_t \le B_{tlm}^V \bullet X_t + b_{tlm}^V, && \forall (l, m) \in \mathcal{L}, \ \forall t \in \mathcal{T} \\
& A_{ti}^1 \bullet X_{t-1} + A_{ti}^2 \bullet X_t \le a_{ti}, && \forall i \in [s_t], \ \forall t \in \mathcal{T} \\
& X_t \succeq 0, \ W_t \succeq 0, \ W_t \lhd \mathcal{F}_t, \ X_t \lhd \mathcal{F}_t, \ \mathrm{rank}(W_t) = 1, && \forall t \in \mathcal{T}. \\
&&& (\mathcal{P}^{nc})
\end{aligned}
$$

where due to the Schur's complement formula the constraint imposing negative

semi-definiteness is equivalent to $(B_{tlm}^S \bullet X_t + b_{tlm}^S) \geq 0$ and

$$0 \leq B_{tlm}^S \bullet X_t + b_{tlm}^S - [-\mathbb{Y}_{lm} \bullet W_t, -\hat{\mathbb{Y}}_{lm} \bullet W_t][-\mathbb{Y}_{lm} \bullet W_t, -\hat{\mathbb{Y}}_{lm} \bullet W_t]^\top$$

$$= B_{tlm}^S \bullet X_t + b_{tlm}^S - (\mathbb{Y}_{lm} \bullet W_t)^2 - (\hat{\mathbb{Y}}_{lm} \bullet W_t)^2 = B_{tlm}^S \bullet X_t + b_{tlm}^S - |S_{tlm}|^2,$$

which is constraint (3.11) on apparent power.

Note that except for the rank constraint, which makes the problem non-convex, $(\mathcal{P}^{nc})$ is a convex SDP. Therefore, we define the problem $(\mathcal{P}^c)$ as the convex problem, resulting from removing the rank constraint from $(\mathcal{P}^{nc})$. Clearly, $(\mathcal{P}^c)$ approximates $(\mathcal{P}^{nc})$ from below, i.e., is an *optimistic* approximation of the AC-OPF problem.

3.3   A Solution by Markovian Stochastic Dual Dynamic Programming

In this section, we show how the Markovian stochastic AC-OPF problems $(\mathcal{P}^c)$ can be solved using SDDP type composition methods and discuss under which circumstances the gap between the non-convex problem $(\mathcal{P}^{nc})$ and $(\mathcal{P}^c)$ vanishes.

In Section 3.3.1, we propose a dynamic programming formulation of a Markovian version of $(\mathcal{P}^c)$. Section 3.3.2, discusses a Markovian SDDP algorithm and provides details on how value functions can be trained. Finally, in Section 3.3.3, we show how the dual solution can be used to check for a positive duality gap in the relaxed AC-OPF problems.

3.3.1   A Markovian Formulation

In this section, we will reformulate the extensive form of the stochastic programming problem in $(\mathcal{P}^c)$ to a dynamic programming formulation. For this purpose, we denote by ξ_t all the random elements in the problem formulation that are measurable with respect to $\mathcal{F}_t$. Note that while potentially all data of the problem $(\mathcal{P}^c)$ may be

random, in actual applications, this is usually only the case for a small subset of variables.

In order to obtain numerical solutions, we introduce the following running assumption.

Assumption 3.1 (Finite Support). *The process $\xi = (\xi_1, \ldots, \xi_T)$ is finitely supported.*

Remark 3.1. *Note that in many instances, the randomness in stochastic optimization problems is most naturally modeled as continuously distributed. In these cases, one can approximate the original stochastic process by a discrete process and then solve the problem based on the approximation. There is a large literature that deals with qualitative and quantitative bounds on the error induced by this approach (e.g. Heitsch and Römisch 2009, Kiszka and Wozabal 2022, Löhndorf and Wozabal 2021a, Pflug and Pichler 2014, Shapiro et al. 2009). Here, we will ignore this complication and assume that Assumption 3.1 is either naturally fulfilled or, alternatively, that the problem can be closely approximated by a problem based on a finitely supported process ξ.*

The most general representation of a discrete time and discrete value stochastic process is a scenario tree, an example of which is displayed in Figure 3.3 (left). However, in a scenario tree where every node has more than one successor, the number of nodes necessarily grows exponentially in the number of stages. To deal with this complication, scenario trees typically have only a few stages or contain nodes with only one successor, which effectively leads to deterministic sub-problems at these nodes.

The complexity of a scenario tree can be reduced substantially if the data process is Markovian. In particular, all histories $(\xi_1, \ldots, \xi_t)$ of the process that lead to the same state ξ_t continue in identical sub-trees that can be combined without the loss of information. In line with the terminology often used in mathematical finance, we refer to such *recombining* scenario trees as *scenario lattices*.
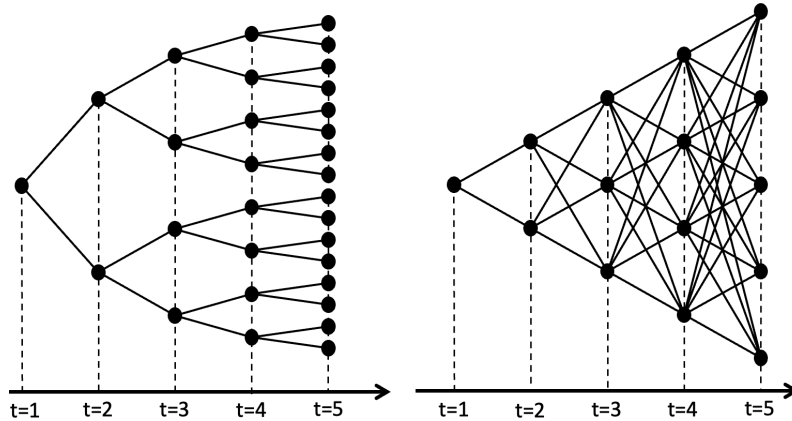
Figure 3.3: A tree with 31 nodes representing 16 scenarios on the left and a lattice with 15 nodes representing 120 scenarios on the right.

An example of a scenario lattice is depicted in Figure 3.3 (right). Formally, a scenario lattice is a graph organized in a finite number of layers. Each layer is associated with a discrete point in time and contains a finite number of nodes. Successive layers are connected by arcs. A node represents a possible state of the stochastic process, and an arc indicates the possibility of a state transition between the two connected nodes. Each arc connecting node i in stage t with node j in stage $t+1$ is associated with a probability weight p_{tij}, and the weights of outgoing arcs of a node add up to one. Note that this definition also covers inhomogeneous Markov processes where conditional distributions change over time. A scenario tree differs from a scenario lattice by the additional requirement that every node in t has only one predecessor in $(t-1)$. We denote the number of nodes of a scenario lattice in stage t by N_t, and ξ_{tj}, $j \in [N_t]$ as the state of the lattice process at node j in stage t and refer to Kiszka and Wozabal (2022) for a more in-depth treatment of scenario lattices and their properties.

In order to use scenario lattices in stochastic programming, we additionally need the decisions in stage t that do not *explicitly* depend on the whole history of the problem, but only *implicitly* via the current state of the problem. To formalize this concept, we define the state of the problem at time t as ξ_t and X_{t-1} with ξ_t as

the *environmental state*, which evolves randomly independent of the decisions, and X_{t-1} as the *resource state*, which can be directly controlled by the decision maker. Summarizing, to avoid the exponential explosion of complexity in the number of stages, we assume that the problem is Markovian in the stochastic process as well as in the decisions as detailed in the following assumption.

Assumption 3.2 (Markovian Stochastic Programming Problem). *1. The stochastic process ξ_t is Markovian, i.e., $\mathbb{E}[\xi_{t+1}|\mathcal{F}_t] = \xi_t$.*

2. The decision X_t depends on $(X_1, \ldots, X_{t-1})$ only via its dependence on X_{t-1}.

We note that Assumption 3.2 is natural in most situations, and for the problems where this is not the case, it can always be enforced by a state space expansion.

Using Assumption 3.2, we represent $(\mathcal{P}^c)$ by its dynamic programming equations

$$C_t(\xi_{tj}, X_{t-1}) = \begin{cases} \min & F_t \bullet X_t + \mathbb{E}[C_{t+1}(\xi_{t+1}, X_t)|\xi_t = \xi_{tj}] \\ \text{s.t.} & (X_t, W_t) \in \mathcal{X}_t(\xi_{tj}, X_{t-1}), \end{cases} \tag{3.15}$$

where $\mathcal{X}_t(\xi_{tj}, X_{t-1})$ is the feasible set for stage t, and all random elements take the values stored at lattice node ξ_{tj} and C_{T+1} is a given SDP representable convey function that acts as a boundary condition for the problem.

If the expected cost-to-go functions

$$(\xi_{tj}, X_t) \mapsto \mathcal{C}_{t+1}(\xi_{tj}, X_t) := \mathbb{E}[C_{t+1}(\xi_{t+1}, X_t)|\xi_t = \xi_{tj}]$$

are known explicitly, the problems in (3.15) reduce to deterministic AC-OPF problems that depend on the current state and relate to the next stage via $\mathcal{C}_{t+1}$, which in turn depends on the decisions taken at time t.

The following proposition relates the solution of the dynamic programming equations (3.15) with the solution of the original stochastic optimization problem.

Proposition 3.1. *If Assumptions 3.1 and 3.2 hold and for all $t \in \mathcal{T}$, all realizations of $(\xi_1, \ldots, \xi_t)$, and all optimal solutions X_{t-1} of C_{t-1}, there are optimal solutions*

(X_t, W_t) *such that W_t has rank 1, then the optimal values and solutions for* (3.15) *are also optimal for the original problem* $(\mathcal{P}^{nc})$.

3.3.2   A Solution by Stochastic Dual Dynamic Programming

While stochastic optimization problems that use scenario trees to discretize randomness can be solved via their deterministic equivalent by assigning one decision vector to each node of the tree, this property is lost when using scenario lattices.

In particular, since the lattice does not contain information on the history of the process, optimal decisions do not only depend on the environmental state ξ_t but also on the resource state X_{t-1}, which is not uniquely defined for a node but depends on the history of the decision process. Hence, in order to solve the problem, one has to obtain the cost functions $\mathcal{C}_t$, which effectively define the optimal policy via the problems (3.15).

In order to obtain cost functions, we propose to use SDDP, which is a sampling-based decomposition algorithm that allows to learn increasingly accurate approximations of $\mathcal{C}_t$. The algorithm goes back to the seminal work of Pereira and Pinto (1991) and has been extensively used to solve problems in energy planning.

The main idea of SDDP is to approximate the cost-to-go functions $\mathcal{C}_t$ by a piecewise affine model $\bar{\mathcal{C}}_t$. This is based on the fact that since the problems (3.15) are convex and X_{t-1} only enters the right-hand sides of the constraints, the functions $\mathcal{C}_t(\xi_t, X_{t-1})$ are convex and can be approximated below by a maximum of affine functions whose slopes are the subgradients of $\mathcal{C}_t$ at finitely many trial points X_{t-1}.

The SDDP algorithm alternates between simulating the decision policy (forward pass) based on the current approximations $\bar{\mathcal{C}}_t$ and recursively updating the piecewise affine models $\bar{\mathcal{C}}_t$ (backward pass). In order to describe the algorithm in more detail, we define the approximated problem on lattice node j in period t in the l-th iteration as

$$\bar{C}_{tl}(\xi_{tj}, X_{t-1}) =$$

$$
\begin{cases}
\min \quad F_t \bullet X_t + \theta \\
\text{s.t.} \quad \mathbb{Y}_k \bullet W_t = A_{tk}^P \bullet X_t + a_{tk}^P, & \forall k \in \mathcal{N} \quad [\lambda_k] \\
\quad\quad\ \hat{\mathbb{Y}}_k \bullet W_t = A_{tk}^Q \bullet X_t + a_{tk}^Q, & \forall k \in \mathcal{N} \quad [\gamma_k] \\
\quad\quad\ M_k \bullet W_t = A_{tk}^V \bullet X_t + a_{tk}^V, & \forall k \in \mathcal{N} \quad [\mu_k] \\
\quad\quad\ \mathbb{Y}_{lm} \bullet W_t \leq B_{tlm}^P \bullet X_t + b_{tlm}^P, & \forall (l,m) \in \mathcal{L} \quad [\lambda_{lm}] \\
\quad\quad\ \begin{bmatrix} -B_{tlm}^S \bullet X_t - b_{tlm}^S & \mathbb{Y}_{lm} \bullet W_t & \hat{\mathbb{Y}}_{lm} \bullet W_t \\ \mathbb{Y}_{lm} \bullet W_t & -1 & 0 \\ \hat{\mathbb{Y}}_{lm} \bullet W_t & 0 & -1 \end{bmatrix} \preceq 0, & \forall (l,m) \in \mathcal{L} \quad [r_{lm}] \\
\quad\quad\ M_{lm} \bullet W_t \leq B_{tlm}^V \bullet X_t + b_{tlm}^V, & \forall (l,m) \in \mathcal{L} \quad [\mu_{lm}] \\
\quad\quad\ A_{ti}^1 \bullet Z_{t-1} + A_{ti}^2 \bullet X_t \leq a_{ti}, & \forall i \in [s_t] \quad [\sigma_i] \\
\quad\quad\ Z_{t-1} = X_{t-1}, & \quad\quad\quad [\Phi] \\
\quad\quad\ e_{ti} + E_{ti} \bullet X_t \leq \theta, & \forall i \in [l-1] \quad [\nu_i] \\
\quad\quad\ X_t \succeq 0, \ W_t \succeq 0,
\end{cases}
$$

where the decision variables are X_t, W_t and Z_{t-1}, the dual multipliers of the constraints are indicated in square brackets, and realizations for random data are taken from node ξ_{tj}.

Note that θ, together with the second last constraint, models the piecewise affine approximation of the value function at lattice node j that has been constructed in the first $(l-1)$ iterations. Also note that Z_{t-1} is introduced purely for notational convenience to extract a subgradient of the function $X_{t-1} \mapsto \bar{C}_{tl}(\xi_{tj}, X_{t-1})$ as the dual multiplier Φ of the constraint $Z_{t-1} = X_{t-1}$.

In our general formulation, the resource state of the problem consists of the entire X_t, which is typically not required because only a few variables are relevant for the decision on the next stage. However, in order to simplify the exposition, we do not explicitly distinguish between environmental state variables and decisions that are

taken in period t.

Algorithm 2 Markov Chain SDDP

Require: Lattice ξ, number of iterations L, start state X_0
 1: $l \leftarrow 1$ $\triangleright$ initialize
 2: **while** [**do**main loop]$l \leq L$
 3:     $\hat{\xi}_1^l \leftarrow \xi_1, \hat{X}_0^l = X_0$
 4:     **for** [**do**forward pass]$t \in [T]$
 5:         Get solutions $\hat{X}_t^l$ for $\bar{C}_{tl}(\hat{\xi}_t^l, \hat{X}_{t-1}^l)$
 6:         Sample $\hat{\xi}_{t+1}^l$ given $\hat{\xi}_t^l$ from ξ_t
 7:     **end for**
 8:     **for** [**do**backward pass]$t \in T : 2$
 9:         **for** $j \in [N_t]$ **do**
10:             Get objective o_{tlj} and dual Φ_{tlj} for $\bar{C}_t(\xi_{tj}, \hat{X}_{t-1}^l)$
11:         **end for**
12:         **for** [**do**generate new cuts]$i \in [N_{t-1}]$
13:             $e_{t-1,il} \leftarrow \sum_{j \in [N_t]} p_{t-1,ij} o_{tlj}, E_{t-1,il} \leftarrow \sum_{j \in [N_t]} p_{t-1,ij} \Phi_{tlj}$
14:         **end for**
15:     **end for**
16:     $l \leftarrow l + 1$
17: **end while**

We summarize SDDP in Algorithm 2 defining L as the number of iterations. The algorithm takes a scenario lattice ξ and a start state X_0 as inputs. In the forward passes (lines 4 to 6), the algorithm simulates a path from the lattice process and solves the problems $\bar{C}_{tl}$ at the sampled lattice nodes using the value function approximations trained so far. In the backward pass (lines 8 to 14), the algorithm solves the problems on all the nodes at the resource states sampled in the forward pass and extracts an affine cut that is added to the representation of the respective value functions at the nodes of the lattice one stage earlier by multiplying with the corresponding conditional probabilities in line 13.

Note that we do not incorporate a convergence check but stop after a predetermined number of L iterations. Alternatively, one can periodically estimate the optimality gap

$$\text{gap}_l = U_l - \bar{C}_{1l}(\xi_1, X_0),$$

where

$$U_l = \mathbb{E}\left[\sum_{t=1}^{T} F_t \bullet X_{tl}\right]$$

is the expected value of the policy X_{tl} that results from solving the nodal problems using the value function approximations $\bar{C}_{tl}$ to represent future costs. Note that the cost functions approximation $\bar{C}_{1l}$ is a lower bound for the convex relaxation of the AC-OPF problem and, therefore, also for the original non-convex problem. On the other hand, U_l is an upper bound of the optimal value for the relaxed problem because the decisions X_{tl} are based on approximations of the real value functions, and the resulting policies are, therefore, suboptimal. Hence, for any iteration l, gap_l is an upper bound on the optimality gap of the SDDP policy for the relaxed AC-OPF problem.

In order to obtain an estimate of this gap, one can sample U_l by computing K forward passes based on independent samples $(\hat{\xi}_t^k)_{k\in[K],t\in\mathcal{T}}$ from the lattice and recording their objective values, i.e.,

$$\hat{U}_l^K = K^{-1}\sum_{k=1}^{K}\sum_{t=1}^{T}\hat{F}_t^k \bullet \hat{X}_t^k,$$

where $\hat{X}_t^k$ is the sampled decision and $\hat{F}_t^k$ is the objective value coefficient which belongs to the sampled node $\hat{\xi}_t^k$. An unbiased estimate of the gap is therefore $\widehat{\text{gap}}_l^K = \hat{U}_l^K - \bar{C}_{1l}(\xi_1, X_0)$.

Note that $\widehat{\text{gap}}_l^K$ is a random quantity since it is based on a sampled upper bound $\hat{U}_l^K$. See Shapiro (2011) for a discussion on how to use confidence bands around U_l^k in convergence checks. Further, note that $\widehat{\text{gap}}_l^K$ is potentially underestimating the gap between the SDDP policy and the costs of the *true* non-convex AC-OPF problem since $\hat{U}_K^l$ might be smaller than the cost of the non-convex AC-OPF problem.

Our discussion of the convergence properties is based on Girardeau et al. (2015), who show that SDDP converges almost surely to the true solution of the problem if the problem is convex, the feasible set of decisions is compact, and the problems

have relatively complete recourse. We, therefore, make the following assumption.

Assumption 3.3. *($\mathcal{P}^{nc}$) has relatively complete recourse and a compact feasible set.*

Based on this, we summarize the convergence results for SDDP in the following proposition.

Proposition 3.2. *For a problem ($\mathcal{P}^{nc}$) fulfilling Assumptions 3.1 – 3.3, the following holds:*

1. *The cost function approximation for the first stage $\bar{C}_{1l}(\xi_1, X_0)$ is a valid lower bound for the objective value of the multi-stage stochastic AC-OPF problem ($\mathcal{P}^c$) and therefore also for ($\mathcal{P}^{nc}$).*

2. *As $L \to \infty$, Algorithm 2 converges, i.e., $\widehat{gap}_l^K \to 0$ and the optimal solutions obtained using the cost functions approximations $\bar{\mathcal{C}}_t$ converge to the optimal solutions of ($\mathcal{P}^c$).*

3. *For any given l, if the problems in the K forward passes defining $\hat{U}_l^K$ yield physically feasible solutions for the non-convex problems on the nodes, then $\widehat{gap}_l^K$ is an unbiased estimate of an upper bound on the gap between the SDDP policy and the true objective of ($\mathcal{P}^{nc}$).*

4. *If there is a $\bar{l}$ such that for all $l \geq \bar{l}$ all nodal problems in forward and backward passes yield physically implementable solutions, then the optimal objective values calculated by Algorithm 2 converge to the true value of ($\mathcal{P}^{nc}$).*

Point 3 of Proposition 3.2 establishes that even if the convex relaxations of the AC-OPF problems in the nodes are not tight, one could use a computationally more expensive method to ensure physically feasible solutions to solve problems $\bar{C}_{tL}$ in the forward pass to make sure that $\widehat{\text{gap}}_l^K$ is a valid estimate of the optimality gap for the non-convex problem. In the next section, we will discuss this point in more detail and propose a method how to obtain such a physically feasible policy by modifying the forward simulations in convergence checks.

3.3.3   Dualization of Nodal Problems and Reconstruction of Voltages

Following Lavaei and Low (2012), we solve the dual of the nodal problems to compute $\bar{C}_{tl}$ in Algorithm 2 instead of the primal as this allows to check whether the relaxation of the original non-convex problem on the nodes is tight. In particular, the solutions W_t of the primal problem usually do not have rank 1, even if there is an optimal rank 1 solution. Luckily, in most cases, the dual solution of $\bar{C}_{tl}$ allows for the construction of a voltage vector that is part of an optimal solution of the original non-convex primal problem.

For the dual approach to work, we have to ensure that there is no duality gap between primal and dual nodal problems. Unlike in linear programming, for SDPs, a Slater condition has to be fulfilled to show strong duality. Unfortunately, it is not possible to verify this condition for problem $\bar{C}_{tl}$ in general. However, as is shown in Section 3.4, the constraints related to power flow are generally unproblematic in this regard and, in particular, allow for inner points of the feasible sets. Therefore, we make the following abstract assumption, which ensures a strong duality between the primal and dual problems.

Assumption 3.4 (Slater's Condition). *The problems $\bar{C}_{tl}$ have finite optimal values, and the feasible sets of the dual problem have an interior point.*

In order to dualize, we write out the Lagrangian of $\bar{C}_{tl}(\xi_{tj}, X_{t-1})$. To that end, we denote the elements of the symmetric matrix r_{lm} by

$$r_{lm} = \begin{pmatrix} r_{lm}^1 & r_{lm}^2 & r_{lm}^3 \\ r_{lm}^2 & r_{lm}^4 & 0 \\ r_{lm}^3 & 0 & r_{lm}^5 \end{pmatrix}$$

and define the following functions of the collection of dual variables denoted by α

$$h_t(\alpha) = \sum_{k \in \mathcal{N}} \left(-\lambda_k a_k^P - \gamma_k a_k^Q - \mu_k a_k^V \right) - \sum_{(l,m) \in \mathcal{L}} \left(\lambda_{lm} b_{lm}^P + r_{lm}^1 b_{lm}^S + r_{lm}^4 + r_{lm}^5 + \mu_{lm} b_{lm}^V \right)$$

$$- \sum_{i \in [s_t]} \sigma_i a_i + \Phi X_{t-1} + \sum_{i \in [l]} \nu_i e_{tnl}$$

$$G_t(\alpha) = \sum_{k \in \mathcal{N}} \left(\lambda_k \mathbb{Y}_k + \gamma_k \hat{\mathbb{Y}}_k + \mu_k M_k \right) + \sum_{(l,m) \in \mathcal{L}} \left(\lambda_{lm} \mathbb{Y}_{lm} + 2 r_{lm}^2 \mathbb{Y}_{lm} + 2 r_{lm}^3 \hat{\mathbb{Y}}_{lm} + \mu_{lm} M_{lm} \right)$$

$$H_t(\alpha) = F_t - \sum_{k \in \mathcal{N}} \left(\lambda_k A_k^P + \gamma_k A_k^Q + \mu_k A_k^V \right) - \sum_{(l,m) \in \mathcal{L}} \left(\lambda_{lm} B_{lm}^P + r_{lm}^1 B_{lm}^S + \mu_{lm} B_{lm}^V \right)$$

$$+ \sum_{i \in [s_t]} \sigma_i A_{ti}^2 + \sum_{i \in [l]} \nu_i E_{tnl}.$$

With the help of these functions, we can write the Lagrangian as

$$\mathcal{L}(W_t, X_t, Z_t, \theta, \alpha) = h_t(\alpha) + G_t(\alpha) \bullet W_t + H_t(\alpha) \bullet X_t + Z_{t-1} \bullet (-\Phi + A_{ti}^1 \sigma_i) + \theta \left(1 - \sum_{i \in [l]} \nu_i \right)$$

which by minimax duality leads to the following dual problems on the nodes

$$\bar{C}_{tl}(X_{t-1}, \xi_{tj}) = \begin{cases} \max_{\alpha} & \mathbb{E}\left[h(\alpha) \right] \\ \text{s.t.} & G_t(\alpha) \succeq 0, \ H_t(\alpha) \succeq 0 \\ & r_{lm} \succeq 0, \quad \forall (l,m) \in \mathcal{L} \\ & \sum_{i \in [l]} \nu_i = 1 \\ & \Phi = A_{ti}^1 \sigma_i, \quad \forall i \in [s_t], \end{cases} \qquad (3.16)$$

where the first and second inequalities are enforced by the fact that the primal variables W_t and X_t are symmetric and positive semi-definite.

Note that (3.16) is also the dual problem of the non-convex formulation of the AC-OPF problem on the lattice nodes, which include the rank condition on W_t (Lavaei and Low 2012). This implies that $\bar{C}_{tl}$ is the bidual of the original non-convex AC-OPF problem on the node and, consequently, the tightest convex approximation.

The following proposition gives a sufficient condition that ensure zero duality gap in the AC-OPF problems and allows to construct a physically feasible voltage

vector from the solution of the dual problem.

Proposition 3.3 (Lavaei and Low (2012))**.** *Let α and W_t be optimal dual and primal solutions of problem $\bar{C}_{tl}(\bar{\xi}_{tn}, X_{t-1})$. If*

$$\dim(\ker(G_t(\alpha))) = \dim(\{x \in \mathbb{R}^{2n} : G_t(\alpha)x = 0\}) \leq 2, \tag{3.17}$$

then

1. *the problem $\bar{C}_{tl}(\xi_{tj}, X_{t-1})$ has a rank one optimal solution $W_t^\star$ implying that AC-OPF problem is solved without duality gap;*

2. *a physically feasible voltage vector $V_t^\star$ can be constructed from an arbitrary vector $\mathcal{K} = (\mathcal{K}_1, \mathcal{K}_2)^\top$ in the null space of G_t and conditions on real or imaginary parts of voltages on two buses.*

Remark 3.2. *For the second point, note that, for some g_1 and $g_2 \in \mathbb{R}$, we can write*

$$\tilde{V}_t^\star = g_1 \mathcal{K} + g_2 \mathcal{K}_\perp$$

where $\mathcal{K}_\perp = (-\mathcal{K}_2^\top, \mathcal{K}_1^\top)^\top$ (see Appendix A.4). To determine g_1 and g_2, we need two conditions. As a first condition, we can use that the voltage angle at the swing bus n_0 equals 0 by convention, i.e.,

$$0 = g_1 \mathcal{K}_{2,n_0} + g_2 \mathcal{K}_{1,n_0} \Leftrightarrow g_1 = -g_2 \frac{\mathcal{K}_{1,n_0}}{\mathcal{K}_{2,n_0}}.$$

As a second condition, we can use any binding voltage, power, or current constraint on a bus $\bar{m}$. We proceed for the case of a binding upper bound on the squared absolute value of voltage and remark that formulas for the other cases can be derived analogously.

Assuming $|V_{t,\bar{m}}^\star|^2 = \bar{V}_{\bar{m}}^2$, where $\bar{V}_{\bar{m}}$ is the upper bound on the absolute value of the voltage on node $\bar{m}$, yields

$$|\bar{V}_{\bar{m}}|^2 = (g_1 \mathcal{K}_{1\bar{m}} - g_2 \mathcal{K}_{2\bar{m}})^2 + (g_1 \mathcal{K}_{2\bar{m}} + g_2 \mathcal{K}_{1\bar{m}})^2$$

Substitution for g_1 and solving for g_2 results in

$$g_2 = \bar{V}_{\bar{m}} \left(\left(\frac{\mathcal{K}_{1,n_0}^2}{\mathcal{K}_{2,n_0}^2} + 1 \right) \left(\mathcal{K}_{1\bar{m}}^2 + \mathcal{K}_{2\bar{m}}^2 \right) \right)^{-1/2}.$$

If condition (3.17) is not fulfilled, then the AC-OPF problem might not be solvable efficiently. In order to check condition (3.17), it is sufficient to verify that the multiplicity of the eigenvalue 0 is less than 2. In our numerical case study in Section 3.4, we find that (3.17) is fulfilled in most problems solved in the forward and backward pass of the SDDP algorithm. However, the condition is somewhat hard to check numerically since the eigenvalues are never exactly zero due to finite floating point precision and the implementation of interior point solvers for SDPs. One option to deal with these issues is to set numerical thresholds for considering eigenvalues to be zero, as is done for example in Molzahn et al. (2013).

We propose a different approach to ensure that the solution of the dual of the relaxed OPF problem yields a physically feasible voltage vector and to construct a valid optimality gap between the SDDP policy and an optimal solution of ($\mathcal{P}^{nc}$). To this end, we first solve the equations in Remark 3.2 for all the binding constraints and check if there is a $\tilde{V}_t^\star$, which yields voltages that do not violate any voltage bounds and, up to a certain accuracy, yield the same powers on the nodes as computed with the dual solution. If this is the case, we conclude that there is a physically feasible voltage vector that reproduces the solution of the dual problem.

If, on the other hand, we get a difference in powers or violations of voltage bounds on the buses for all voltage vectors obtained from bindings constraints, we infer that there is a duality gap between the real problem and its convex SDP relaxation. In this case, we find a physically feasible voltage vector that reproduces the powers on the buses as close as possible by solving the non-convex problem

$$
\begin{aligned}
\min_{V_t} \quad & ||\mathfrak{Re}(V_t \circ Y^* V_t^*) - P_t||_\chi^\chi + ||\mathfrak{Im}(V_t \circ Y^* V_t^*) - Q_t||_\chi^\chi \\
\text{s.t.} \quad & \underline{V}^2 \leq |V_t|^2 \leq \bar{V}^2,
\end{aligned}
\tag{3.18}
$$

where $\chi \geq 1$ and P_t and Q_t are the vectors of active and reactive powers implicitly used by the dual solution with $P_{tn} = \mathbb{Y}_n \bullet W_t$ and $Q_{tn} = \hat{\mathbb{Y}}_n \bullet W_t$.

While the above problem is non-convex, it has only a few variables and can be solved quickly with standard software. Furthermore, the computations have to be only performed in those forward passes that are used for convergence checks, i.e., in relatively few problems. In our numerical experiments, we choose $\chi > 1$ to make the objective function differentiable and aid gradient-based solvers (see Section 3.4).

We then recalculate the cost by re-solving the primal problems $\bar{C}_{tl}$ with fixed $\hat{W}_t = \hat{V}_t \hat{V}_t^\top$, where $\hat{V}_t$ is the optimal solution of (3.18). Fixing $\hat{W}_t$ yields a convex SDP that is always feasible due to Assumption 3.3 and necessarily yields an objective value larger than $\bar{C}_{tl}$. In this way, we obtain a physically feasible decision policy and thus an unbiased upper bound $\hat{U}_L^K$ for the true optimal cost in the calculation of $\widehat{\mathrm{gap}}_L^K$, which therefore is a valid estimate of the optimality gap of the SDDP policy relative to $(\mathcal{P}^{nc})$.

3.4   A Problem of Storage Siting, Sizing, and Operation

In this section, we present a numerical example demonstrating the performance of the proposed framework for a medium-sized problem of siting, sizing, and operation for grid-level battery storage systems using the IEEE RTS-GMLC network (Barrows et al. 2020) with random electricity demand and random renewable generation.

The extant literature on choosing the optimal location for electric storage (siting), determining its optimal size, and finding optimal operational decisions is extensive, and we refer to Miletić et al. (2020) for a comprehensive survey.

Most authors use deterministic planning and employ either DC approximations to model power flow (e.g., Wogrin and Gayme 2015) or rely on SDP or SOCP relaxations (e.g., Marley et al. 2017).

Since electricity storage helps to deal with the uncertainty of renewable production, deterministic approaches tend to underinvest in storage and arrive at solutions that perform sub-optimally in practice. Therefore, some authors seek to explicitly incorporate uncertainty into storage planning models.

Most papers in the stochastic optimization literature employ two-stage models where the first stage represents investment decisions while the second stage models operational decisions (e.g., Bucciarelli et al. 2018). Some authors use this setup combined with chance constraints to limit the probability of network failure (e.g., Baker et al. 2017).

There are only a few papers that use multi-stage stochastic programming and explicitly model the uncertainty in storage operation over several time stages when deciding on storage capacity. Pandzic et al. (2015), Qiu et al. (2017) employ a three-stage model using DC power flow while to the best of our knowledge Xiong and Singh (2016) is the only truly multi-stage approach using scenario trees. However, the authors use a DC approximation and a rather crude modeling of randomness using a trinomial scenario tree.

In the following, we propose what we believe is the first stochastic optimization model that combines the decision about storage investment on the first stage with multiple daily stages of stochastic planning in hourly resolution representing the operation of the power system. In Section 3.4.1, we describe the optimization model as an instance of the general model class described in Section 3.3, while Section 3.4.2 is dedicated to the discussion of our numerical results.

3.4.1   Optimization Problem

We use the IEEE RTS-GMLC network (Barrows et al. 2020) that contains 74 buses partitioned in three areas and is one of the few publicly available test cases that, next to technical specifications of the grid and power generation, also contains one year of data on demand as well as renewable generation on the buses for the year

2020.[2] For our numerical experiments, we only use the 24 buses in area 1 of the network.

We consider a stochastic optimization problem with 8 stages $\mathcal{D} = \{0, \ldots, 7\}$: in the first stage $d = 0$, the investment decision on storage capacity is taken and the remaining 7 stages represent one week of operational planning, for which, following Barrows et al. (2020), we choose the 10th to the 16th of July. On each of the days $d \in [7]$, we plan for the hours $\mathcal{H} = \{1, \ldots, 24\}$ in hourly resolution, i.e., we solve 24 AC-OPF problems per stage instead of one as in the models in Section 3.3. The overall problem setup largely follows Barrows et al. (2020) and Helistö et al. (2019) and additionally relaxes unit commitment constraints, enabling a fully convex modeling of conventional dispatchable power plants.

We note that in order to get an accurate picture of the value of storage, one would have to include days from all seasons. Strategies for doing so are, for example, discussed in Qiu et al. (2017) or Xiong and Singh (2016). Since we are mainly interested in the performance of SDDP for AC-OPF problems, we abstain from these complications in the present paper.

We model PV and wind production as well as demand as random and provide a detailed description of the stochastic modeling of these variables in Appendix C. In the model formulation, we are interested in residual demand for active and reactive power P_{dhk}^D and Q_{dhk}^D on the day d, hour h, and on bus k, which we calculate by subtracting the renewable production at bus k from the load. Using the stochastic gradient descent method described in Löhndorf and Wozabal (2021a), we use our stochastic model to simulate scenarios to generate a lattice.

In order to make the investment in electricity storage more attractive, we change the energy mix towards a future partially decarbonized system. To that end, we phase out the coal plants at nodes 101, 102, 115, 116, and 123 with capacities 76MW, 76MW, 155MW, 155MW, and 350MW, respectively, jointly accounting for

---

[2]All case related data is available at `https://github.com/GridMod/RTS-GMLC`.

73% of coal generation capacity. To compensate for the loss of fossil production, we double renewable capacities by multiplying their simulated production by 2.

We denote by $\mathcal{G} = \{1, 2, \ldots, m\}$ the set of all generators and by $\mathcal{G}_k \subseteq \mathcal{G}$ the set of generators at bus k. Furthermore, we let $\mathcal{N}^S \subseteq \mathcal{N}$ be the subset of buses where storage can be built and choose $\mathcal{N}^S$ to be equal to the eight buses with renewable production capacities. We denote the first-stage decision on energy capacity (in MWh) by $\bar{B}_k$ for $k \in \mathcal{N}^S$.

In line with the phase-out of much of fossil fuel capacities and the ramp-up of renewables, we assume a 2030 scenario for storage cost and use the projections of Cole and Frazier (2020) who estimate a cost of \$208/kWh for grid-level battery storage. Due to a lack of detailed cost estimates as functions of energy and power capacity, we follow Cole and Frazier (2020) in assuming that the *duration* of the storages is four hours, i.e., that the storage runs empty latest within four hours if it is discharged at full power capacity. Correspondingly, the maximum real power charge and discharge are $\eta^{-1}\bar{B}_k/4$, $\eta\bar{B}_k/4$, where $\eta \in (0,1)$ is the efficiency of the storage, which is assumed to be symmetric for charging and discharging.

To scale down the cost to one week of planning, we compute annuities based on a lifetime of 20 years and an interest rate of 2% yielding a weekly investment cost of $f^B = \$230$/MWh, where we assume that the year has exactly 52 weeks.

This leads to the following first-stage problem in the l-th iteration of the SDDP algorithm

$$
\bar{C}_{0l}(\xi_0) = \begin{cases} \min & f^B \sum_{k \in \mathcal{N}^S} \overline{B}_k + \theta \\ \text{s.t.} & e_{0i}^0 + \overline{B}^\top e_{0i}^1 \le \theta, \quad \forall i \in [l-1], \end{cases}
$$

where $\overline{B} = (\overline{B}_k)_{k \in \mathcal{N}^S} \in \mathbb{R}^{|\mathcal{N}^S|}$ and e_{0i}^0 and e_{0i}^1 are the intercepts and slopes of the affine functions that approximate $\mathcal{C}^1$.

Next, we describe the nodal problems $\bar{C}_{dl}$ in stages $d \in [7]$, which are solved in the forward and backward pass. The random residual demands are read from the

corresponding lattice node, and we drop the time index d for the day to keep the notation manageable.

To operate the storage, we decide about real injections and withdrawals $O_{hk}^+ \geq 0$, $O_{hk}^- \geq 0$, which are subject to the constraints

$$O_{hk}^+ \leq \overline{B}_k/4\eta, \quad k \in \mathcal{N}^S, \forall h \in \mathcal{H} \quad [\overline{\beta}_{hk}^+] \tag{3.19}$$

$$O_{hk}^- \leq \eta\overline{B}_k/4, \quad k \in \mathcal{N}^S, \forall h \in \mathcal{H} \quad [\overline{\beta}_{hk}^-] \tag{3.20}$$

and the storage balance constraints for the storage level B_{hk}

$$B_{hk} = B_{h-1,k} + \eta O_{hk}^+ - \eta^{-1} O_{hk}^-, \qquad \forall k \in \mathcal{N}^S, \forall h \in \mathcal{H} \quad [\sigma_{hk}] \tag{3.21}$$

$$B_{hk} \leq \overline{B}_k, \qquad \forall k \in \mathcal{N}^S, \forall h \in \mathcal{H} \quad [\overline{\kappa}_{hk}], \tag{3.22}$$

where the initial storage level B_{0k} is the level in hour $h = 24$ on the previous day and together with the storage capacities $\overline{B}_k$ form the environmental state. Note that the Greek letters in the square brackets are the dual variables of the respective constraints.

Since we start planning on a Monday after the weekend, which is characterized by low loads, we assume the storage to be 75% filled in the first hour of stage 1.[3] In order to avoid end-of-horizon effects, we force the storage back to its initial level by imposing the following constraints in the last hour of the problem in $d = 7$,

$$B_{24,k} = 0.75 \times \overline{B}_k, \quad \forall k \in \mathcal{N}^S, \quad [\delta_k]. \tag{3.23}$$

Apart from electricity storage, power can be provided by generators. As specified in the case description, we assume the cost of power generation f^g to be a convex, piecewise linear function of active power generation P_{tg}^G with breakpoints (a_{gi}, b_{gi})

---

[3]Alternatively, one could make the initial storage level a decision variable converting the problem to an infinite horizon logic.

$i = 1, \ldots, r_g$ such that

$$
f^g(P_{hg}^G) =
\begin{cases}
m_{g1}(P_{hg}^G - a_{g1}) + b_{g1}, & a_{g1} < P_{hg}^G \le a_{g2} \\
m_{g2}(P_{hg}^G - a_{g2}) + b_{g2}, & a_{g2} < P_{hg}^G \le a_{g3} \\
\vdots & \vdots \\
m_{g(r_g-1)}(P_{hg}^G - a_{g(r_g-1)}) + b_{g(r_g-1)}, & a_{g(r_g-1)} < P_{hg}^G \le a_{gr_g}.
\end{cases}
$$

To keep the problem convex, we relax the on/off constraints of the power plants, set the lower bound on production $\underline{P}_g = a_{g,1} = 0$, and impose the following linear constraints on active and reactive power generation in hour h

$$P_{hg}^G \le \overline{P}_g, \qquad\qquad \forall g \in \mathcal{G}, \forall h \in \mathcal{H} \quad [\overline{\lambda}_{hg}] \qquad (3.24)$$

$$\underline{Q}_g \le Q_{hg}^G \le \overline{Q}_g, \qquad\qquad \forall g \in \mathcal{G}, \forall h \in \mathcal{H} \quad [\underline{\gamma}_{hg}, \overline{\gamma}_{hg}]. \qquad (3.25)$$

We denote by P_{hk}^D and Q_{hk}^D the active and reactive power demand in hour h at node k, which is the difference of conventional demand and renewable generation, and for all $k \in \mathcal{N}, h \in \mathcal{H}$

$$P_{hk} = \mathbb{Y}_k \bullet W_h = \sum_{g \in \mathcal{G}_k} P_{hg}^G - P_{hk}^D - O_{hk}^+ + O_{hk}^- + D_{hk}^{P+} - D_{hk}^{P-}, \qquad [\lambda_{hk}] \quad (3.26)$$

$$Q_{hk} = \hat{\mathbb{Y}}_k \bullet W_h = \sum_{g \in \mathcal{G}_k} Q_{hg}^G - Q_{hk}^D + D_{hk}^{Q+} - D_{hk}^{Q-}, \qquad [\gamma_{hk}], \quad (3.27)$$

where D_{hk}^+ and D_{hk}^- are curtailment of demand and supply with associated cost f^{D+} and f^{D-}, which we set to \$1000/MWh and \$100/MWh, respectively. This implies that renewable production can be curtailed for a moderate fee, while it is considerably more expensive to curtail load. Note that the possibility of curtailment ensures that the problems at the nodes are always feasible and that Assumption 3.3 is fulfilled.

Furthermore, we impose the following constraints on voltages and powers

$$(\underline{V}_k)^2 \leq |V_{hk}|^2 = M_k \bullet W_h \leq (\overline{V}_k)^2, \qquad\qquad \forall k \in \mathcal{N}, \forall h \in \mathcal{H} \quad [\underline{\mu}_{tk}, \overline{\mu}_{tk}] \quad (3.28)$$

$$|S_{hlm}|^2 = (\mathbb{Y}_{lm} \bullet W_h)^2 + (\hat{\mathbb{Y}}_{lm} \bullet W_h)^2 \leq \overline{S}_{lm}^2, \qquad\qquad \forall (l,m) \in \mathcal{L}, \forall h \in \mathcal{H}, \quad (3.29)$$

where we used the results from Lemma 3.1 to rewrite the constraints in terms of W_h. Note that the dual multipliers for the constraints (3.29), represented in the form of negative semidefiniteness constraints, are positive semidefinite matrices r_{hlm} of the form

$$r = \begin{pmatrix} r^1 & r^2 & r^3 \\ r^2 & r^4 & 0 \\ r^3 & 0 & r^5 \end{pmatrix}.$$

In the stages $d \in [7]$, we thus solve the problems $C_d(\xi_d, \overline{B}, B_{d-1})$

$$\min \quad \sum_{h \in \mathcal{H}} \left[\sum_{g \in \mathcal{G}} f_{hg}^G + \sum_{k \in \mathcal{N}} f^{D+} \left(D_{hk}^{P+} + D_{hk}^{Q+} \right) + f^{D-} \left(D_{hk}^{P-} + D_{hk}^{Q-} \right) \right] + \theta$$

$$\text{s.t.} \quad m_{gi}(P_{hg}^G - a_{gi}) + b_{gi} \leq f_{hg}^G, \qquad\qquad \forall i \in [r_g - 1], g \in \mathcal{G}, h \in \mathcal{H} \quad [\zeta_{hgi}]$$

$$(3.19) - (3.28)$$

$$\begin{bmatrix} -\overline{S}_{lm}^2 & \mathbb{Y}_{lm} \bullet W_h & \hat{\mathbb{Y}}_{lm} \bullet W_h \\ \mathbb{Y}_{lm} \bullet W_h & -1 & 0 \\ \hat{\mathbb{Y}}_{lm} \bullet W_h & 0 & -1 \end{bmatrix} \preceq 0, \qquad\qquad \forall (l,m) \in \mathcal{L}, \forall h \in \mathcal{H} \quad [r_{hlm}]$$

$$e_i^0 + \overline{B}^\top e_i^1 + B_{24}^\top e_i^2 \leq \theta, \qquad\qquad \forall i \in [l-1] \quad [\nu_i]$$

$$P_{hg}^G, Q_{hg}^G \geq 0, \qquad\qquad \forall g \in \mathcal{G}, \forall h \in \mathcal{H}$$

$$B_{hk}, O_{hk}^+, O_{hk}^- \geq 0, \qquad\qquad \forall k \in \mathcal{N}^S, \forall h \in \mathcal{H}$$

$$D_{hk}^{P+}, D_{hk}^{P-}, D_{hk}^{Q+}, D_{hk}^{Q-} \geq 0, \qquad\qquad \forall k \in \mathcal{N}, \forall h \in \mathcal{H}$$

$$W_h \succeq 0, \qquad\qquad \forall h \in \mathcal{H},$$

where the respective dual multipliers are indicated next to the constraints, $\overline{B}$ is the vector of storage capacities, $B_0 = (B_{0,k})_{k \in \mathcal{N}^S}$ are the initial storage levels, and the value function approximation is described by the intercepts e_i^0 and the slopes e_i^1, e_i^2.

We denote by α the collection of Lagrange multipliers in the above problem and collect all terms of the Lagrangian that do not contain primary variables in the function

$$
\begin{aligned}
\Gamma_d(\alpha) = \sum_{h\in\mathcal{H}}\sum_{g\in\mathcal{G}} & \left(\sum_{i=1}^{r_g-1} \zeta_{hgi}(b_{gi} - m_{gi}a_{gi}) - \overline{\lambda}_{hg}\overline{P}_g - \overline{\gamma}_{hg}\overline{Q}_g + \underline{\gamma}_{hg}\underline{Q}_g \right) \\
& + \sum_{h\in\mathcal{H}}\sum_{k\in\mathcal{N}} \left(\underline{\mu}_{hk}\underline{V}_k^2 - \overline{\mu}_{hk}\overline{V}_k^2 + \lambda_{hk}P_{hk}^D + \gamma_{hk}Q_{hk}^D \right) - \sum_{h\in\mathcal{H}}\sum_{(l,m)\in\mathcal{L}} \left(\overline{S}_{lm}^2 r_{hlm}^1 + r_{hlm}^4 + r_{hlm}^5 \right) \\
& - \sum_{k\in\mathcal{N}^S} \left(\sigma_{1k}B_{0,k} + \sum_{h\in\mathcal{H}} \left(\overline{\kappa}_{hk} + \frac{\overline{\beta}_{hk}^+}{4\eta} + \frac{\eta\overline{\beta}_{hk}^-}{4} \right) \overline{B}_k + 0.75\delta_k\overline{B}_k - \overline{B}_k \sum_{i\in[l-1]} \nu_i e_{ik}^1 \right) + \sum_{i\in[l-1]} \nu_i e_i^0
\end{aligned}
$$

$$(3.30)$$

where the terms $0.75\delta_k$ are only required in $d = 7$.

In the next step, we define the matrix that contains all the terms that are multiplied with the primal decision variable W_h

$$
G_h(\alpha) = \sum_{k\in\mathcal{N}} \left(\lambda_{hk}\mathbb{Y}_k + \gamma_{hk}\hat{\mathbb{Y}}_k + (\overline{\mu}_{hk} - \underline{\mu}_{hk})M_k \right) + \sum_{(l,m)\in\mathcal{L}} \left(2r_{hlm}^2\mathbb{Y}_{lm} + 2r_{hlm}^3\hat{\mathbb{Y}}_{lm} \right)
$$

Using this definition, we can define the dual problem in iteration l in a lattice node as

$$\max \quad \Gamma_d(\alpha)$$

$$\text{s.t.} \quad G_h(\alpha) \succeq 0 \qquad\qquad\qquad \forall h \in \mathcal{H} \quad [W_h]$$

$$\sum_{i \in [r_g-1]} \zeta_{hgi} = 1 \qquad\qquad\qquad \forall g \in \mathcal{G}, \forall h \in \mathcal{H} \quad [f_{hg}^G]$$

$$\sum_{i \in [r_g-1]} \zeta_{hgi} m_{gi} + \overline{\lambda}_{hg} - \lambda_{hk} \geq 0 \qquad\qquad \forall k \in \mathcal{N}, \forall g \in \mathcal{G}_k, \forall h \in \mathcal{H} \quad [P_{hg}^G]$$

$$\overline{\gamma}_{hg} - \underline{\gamma}_{hg} - \gamma_{hk} = 0 \qquad\qquad \forall k \in \mathcal{N}, \forall g \in \mathcal{G}_k, \forall h \in \mathcal{H} \quad [Q_{hg}^G]$$

$$\sigma_{hk} - \sigma_{h+1,k} + \overline{\kappa}_{hk} \geq 0 \qquad\qquad \forall k \in \mathcal{N}^S, \forall h \in [23] \quad [B_{hk}]$$

$$\sigma_{24,k} + \overline{\kappa}_{24,k} + \sum_{i \in [l-1]} \nu_i e_{ik}^2 + \delta_k \geq 0 \qquad\qquad \forall k \in \mathcal{N}^S \quad [B_{24,k}]$$

$$\lambda_{hk} - \sigma_{hk}\eta + \overline{\beta}_{hk}^+ \geq 0 \qquad\qquad\qquad \forall k \in \mathcal{N}^S \quad [C_{hk}^+]$$

$$-\lambda_{hk} + \sigma_{hk}\frac{1}{\eta} + \overline{\beta}_{hk}^- \geq 0 \qquad\qquad\qquad \forall k \in \mathcal{N}^S \quad [C_{hk}^-]$$

$$\lambda_{hk} \leq f_{hk}^{D+} \qquad\qquad\qquad \forall k \in \mathcal{N}, \forall h \in \mathcal{H} \quad [D_{hk}^{P+}]$$

$$\lambda_{hk} \geq -f_{hk}^{D-} \qquad\qquad\qquad \forall k \in \mathcal{N}, \forall h \in \mathcal{H} \quad [D_{hk}^{P-}]$$

$$\gamma_{hk} \leq f_{hk}^{D+} \qquad\qquad\qquad \forall k \in \mathcal{N}, \forall h \in \mathcal{H} \quad [D_{hk}^{Q+}]$$

$$\gamma_{hk} \geq -f_{hk}^{D-} \qquad\qquad\qquad \forall k \in \mathcal{N}, \forall h \in \mathcal{H} \quad [D_{hk}^{Q-}]$$

$$\sum_{i \in [l-1]} \nu_i = 1 \qquad\qquad\qquad\qquad [\theta]$$

$$r_{hlm} \succeq 0 \qquad\qquad\qquad\qquad \forall (l,m) \in \mathcal{L}$$

$$\nu_i \geq 0, \qquad\qquad\qquad\qquad \forall i \in [l-1]$$

$$\zeta_{hgi}, \overline{\beta}_{hk}^-, \overline{\beta}_{hk}^+, \overline{\kappa}_{hk}, \overline{\lambda}_{hg}, \overline{\gamma}_{hg}, \underline{\gamma}_{hg}, \overline{\mu}_{hk}, \underline{\mu}_{hk} \geq 0, \quad \forall k \in \mathcal{N}, \forall g \in \mathcal{G}, \forall h \in \mathcal{H},$$

where the variable δ_k is only required on the last stage of the problem and can be removed from Γ_d and the constraint with dual multiplier $B_{24,k}$ in all other stages and $G_h(\alpha)$.

When solving problem $C_d(\xi_d, \overline{B}, B_{d-1})$ with $d \in 2, \ldots, 7$ in a backward pass for a given state $(\overline{B}, B_0)$, it follows from (3.30) that the subgradients of $\overline{B}$ and B_0 are

$$\left(\sum_{i \in [l-1]} \nu_i e_{ik}^1 - \sum_{h \in \mathcal{H}} \left(\overline{\kappa}_{hk} + \frac{\overline{\beta}_{hk}^+}{4\eta} + \frac{\eta \overline{\beta}_{hk}^-}{4} \right) - 0.75 \delta_k \right)_{k \in \mathcal{N}^S}$$

and $(-\sigma_{1k})_{k \in \mathcal{N}^S}$, respectively, where again the last term $0.75 \delta_k$ is only present in the last stage of the problem. For $d = 1$, the environmental state space only consists of $\overline{B}$ and the subgradient of $\overline{C}_{1l}$ with respect to storage capacity is

$$\left(\sum_{i \in [l-1]} \nu_i e_{ik}^1 - \sum_{h \in \mathcal{H}} \left(\overline{\kappa}_{hk} + \frac{\overline{\beta}_{hk}^+}{4\eta} + \frac{\eta \overline{\beta}_{hk}^-}{4} \right) + 0.75(-\sigma_{1k}) \right)_{k \in \mathcal{N}^S}$$

as the initial storage level is 75% of storage capacity.

We conclude this section by showing that the Slater condition holds for the problems on the nodes, implying no duality gap between the primal and dual problem.

Proposition 3.4. *Strong duality holds between the primal and dual of $C_d(\xi_d, \bar{B}, B_{d-1})$.*

3.4.2   Numerical Results

We implement the algorithm in MATLAB 2021b and use MOSEK 9.3.10 to solve the optimization problems on the nodes. We approximate ξ using a scenario lattice with 100 nodes per stage. Furthermore, we use YALMIP (Löfberg 2004) to formulate optimization problems and solve problems on nodes in the same stage in the backward pass as well as multiple forward passes for convergence checks in parallel.

In our experiment, we run the algorithm for 100 iterations, where in every fifth iteration, we increase the number of scenarios in the forward pass to 150 to generate upper bounds on the cost generated by the current policy. All calculations are performed on an Amazon virtual machine of the type *c5a.16xlarge* (256 GB, 64 AMD CPU@3.3 GHz) on which the computations took 17.94 hours. Looking at the convergence plot in the left panel of Figure 3.4, we can observe that the algorithm
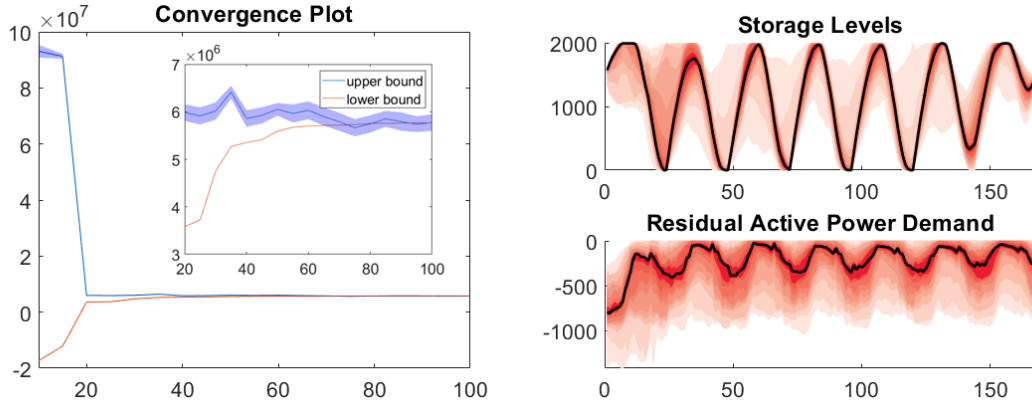
Figure 3.4: The panel on the left shows the convergence of SDDP upper and lower bound and a 95% confidence interval for the upper bound. The right panel shows fan plots of the distributions of storage level as well as the residual load on node 122 from 500 scenarios.

converges roughly after 60 iterations.

In order to assess the performance of the approach, we generate 500 scenarios and solve the relaxed OPF problem using the approximations of the cost-to-go functions obtained in the last SDDP iteration. We obtain that the optimal storage capacity is equal to 3732 MWh, where storage at buses 122 and 119 account for 53% and 28% of the capacity, respectively. As the storage capacity at bus 122 plays a crucial role and the only wind power plant is placed at this bus, we present the operation of this storage on the right panel of Figure 3.4, where it can be observed that the storage level fluctuates around a regular daily pattern and that the deviations from this pattern are frequent and occasionally substantial.

As the presented approach relies on a convex relaxation of the OPF problem, in some situations optimal decisions W_h do not correspond to physically feasible solutions. To obtain a physically feasible policy for these cases, we solve (3.18) using the MATLAB function *fmincon* using the *sqp* algorithm and $\delta = 1.25$ to find voltages $\hat{V}_h$ for the 500 forward passes and re-solve the primal nodal problems fixing these voltages as discussed in Section 3.3.3. We find that the cost for this modified primal problem is only 1.8% (standard deviation 0.0013) higher than the

cost when the convex approximation is used, which implies that the dual relaxation
of the AC-OPF problem is relatively tight and physically feasible voltages that do
not significantly increase cost, can be found using (3.18). After this operation,
we obtain a new upper bound of 5.95 mio. (standard deviation $50,982$) and thus
an optimality gap of 0.19 millions representing 3% of the SDDP lower bound as
computed after 100 iterations.

To compute the value of the stochastic solution, we calculate the value of a
rolling horizon deterministic policy, which uses conditional means of the stochastic
process to re-optimize decisions in every stage of the problem (see Powell 2019,
Schildbach and Morari 2016, Sethi and Sorger 1991, for similar approaches). More
specifically, we first solve one large deterministic problem over seven days, replacing
all stochastic variables by their unconditional means and using the resulting storage
investment cost as the cost of the policy in stage 0. We then simulate a random
state transition to a lattice node $\hat{\xi}_{1j}$ in stage 1, update the expected realizations of
ξ_d for $d \geq 2$ conditional on $\hat{\xi}_{1j}$, re-solve the problem for the 7 days of operation, and
use the cost incurred on day $d = 1$ as the cost of the deterministic policy for that
day. We proceed in this manner until the last stage to simulate the overall cost of
deterministic planning for the sampled scenario. We repeat this procedure for the
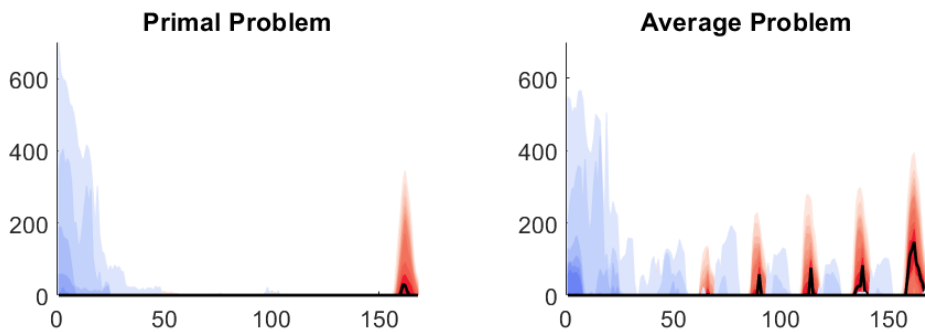500 scenarios and we used above to test the SDDP policy.

Figure 3.5: Comparison of curtailment values for the primal problem and the rolling
deterministic approach. Blue and red indicate curtailment of supply and demand
respectively.

The deterministic benchmark policy invests in 1402 MWh of storage, which is only 37% of the storage capacity bought by the SDDP policy. Comparing curtailed power Figure 3.5 shows that this reduced storage capacity leads to substantially increased curtailment and is therefore suboptimal. This results in an average cost of 7.56 mio (standard deviation $8,362$), which is 27% higher than the optimal cost incurred by the SDDP policy, which equals 5.96 (standard deviation $50,982$) million dollars. We can thus conclude that stochastic planning has a substantial added value over state-of-the-art deterministic planning approaches.

3.5   Conclusions

We propose the first framework to solve multi-stage stochastic AC-OPF problems. To find solutions to these NP-hard problems, we combine SDDP, which allows to efficiently solve Markovian stochastic programming problems with many stages, with a convex SDP relaxation for AC-OPF problems, which has proven to be of a high quality in deterministic optimization.

We investigate the convergence properties of the resulting algorithmic framework and describe how a physically feasible policy that yields a valid upper bound on the original non-convex problem can be obtained. Together with the SDDP lower bound, which is valid for the non-convex stochastic AC-OPF problem, an optimality gap can be computed.

In a numerical example on storage siting, sizing, and operations, we show that the proposed approach is computationally tractable for medium-sized problems and allows to learn policies that have a small optimality gap.

Our numerical results show that the value of the stochastic solution is substantial, and therefore, stochastic optimization is able to dramatically reduce expected costs in systems with a high share of unpredictable renewable generation.

This paper opens several avenues for further research. Firstly, it would be inter-

esting to extend the problem class to include binary variables in the non-electrical part of the problem, which would enable $(N-1)$ security-constrained dispatch and more accurate modeling of technical characteristics of power plants.

Secondly, a speed-up in solving the AC-OPF problems in the nodes could be achieved by partitioning the admittance matrix for larger networks as in Andersen et al. (2014), Molzahn et al. (2013) or the switch to looser but faster relaxations of the AC-OPF power flow problems in the backward passes, for example, by reformulation as SOCP as in Coffrin et al. (2016), Marley et al. (2017).

Thirdly, a more efficient implementation of SDDP in a low-level programming language would help leverage speed-ups from parallelization in the backward pass as well as from quicker setup of optimization problems. Furthermore, an asynchronous version of SDDP would facilitate the distribution of a problem instance amongst several machines in a cluster.

Chapter 4

Optimal Renewable Expansion and Storage Integration Planning under Uncertainty

This paper proposes a multi-stage stochastic formulation for renewable and storage expansion planning, accounting for uncertainties in both demand and renewable generation as well as the physical laws of alternating current (AC) power flows. The optimization problem comprises an initial stage involving investment decisions and subsequent stages representing daily network operations at an hourly resolution. The objective is to minimize costs over the specified time horizon and identify the optimal location and capacity of storage units and renewable generation sources necessary to achieve a targeted share of renewable generation.

To address the computational challenges posed by this large-scale problem, we apply the solution strategy proposed in Kiszka and Wozabal (2024) and provide a detailed explanation and reformulations of the optimization problem required to implement the algorithm.

To illustrate the computational tractability of the problem, the for-

mulated model and algorithm are implemented in an extensive case study focusing on renewable expansion and storage integration within the part of the IEEE RTS-GMLC network. The results demonstrate the evolution of the generation infrastructure needed to achieve future renewable generation targets.

4.1   Introduction

The world is facing a critical challenge of reducing greenhouse gas emissions to mitigate the impacts of climate change. According to the Intergovernmental Panel on Climate Change (2018), emissions from fossil fuels and industry are the primary driver of global warming, which accounted for 89% of global CO_2 emissions in 2018. Consequently, there is a growing consensus to eliminate fossil fuels and shift towards cleaner, renewable energy sources. As a consequence, the profound transformation of the power system is necessary to address climate change, ensure energy security, and promote sustainable economic growth.

The transition to a low-carbon energy future requires the crucial participation of both governments and communities, and many nations are taking active measures by employing policy targets that aim to expand the use of renewable energy sources. For example, the European Climate Law sets the goal to become climate neutral by 2050 and the intermediate target of reducing net greenhouse gas emissions by at least 55% by 2030 compared to 1990 levels. The -55% target implies that coal power plants in Europe will be phased out almost completely by 2030 as coal is the dirtiest of the fossil fuels and responsible for over 30% of the global average temperature increase.

According to International Renewable Energy Agency (2021b), replacing 800 GW of coal-fired capacity with new renewable capacity could significantly reduce emissions by 2030, as it would avoid around 3 giga tonnes of CO_2 per year, which

correspond to 9% of global energy-related CO_2 emissions in 2020. Additionally, retiring these power plants would bring financial benefits up to \$32.3 billion annually by reducing power generation costs.

To determine the optimal direction of changes needed in the specific power network infrastructure to meet given targets, a generation expansion planning problem can be formulated and solved to support decision-makers.

There is a rich literature on optimization techniques used to solve generation expansion planning problems. The most common include linear programming in Diewvilai and Audomvongseree (2021), Massé and Gibrat (1957), integer programming in Heuberger et al. (2017), Koltsaklis et al. (2014), Quiroga et al. (2019), non-linear programming in Hemmati et al. (2016), Zhang et al. (2017), dynamic programming in Booth (1972), Oree et al. (2017) and metaheurstic methods in Gupta et al. (2014), Neshat and Amin-Naseri (2015). Due to the computational complexity of non-linear models, simplified mixed-integer linear programming models (MILP), especially multi-period MILP, gained significant attention in the expansion planning area. Among these models, we can find a multi-period MILP model with area discretization and integrated energy resource management in Koltsaklis et al. (2014), a multi-period stochastic MILP with budget constraints in Afful-Dadzie et al. (2017), a multi-period MILP model for generation and transmission expansion planning in Guerra et al. (2016) or a multi-period MILP model with operation constraints in Koltsaklis and Georgiadis (2015).

As renewable production is highly variable and largely unpredictable, a number of flexibility sources need to be exploited and planned ahead of time. An effective tool to mitigate the impact of variable renewable energy on power system planning and operation is energy storage. For example, Opathella et al. (2020) presents a MILP formulation for generation and storage expansion planning with power balance constraints, Hemmati et al. (2017) proposes a two-level microgrid planning tool considering distributed generation resources and energy storage, Xiong and Singh

(2016) propose an approach for determining the optimal location and size of energy storage in power system with wind power generation in which economic dispatch and power flow need to be solved.

In the generation expansion planning problem, a trade-off between investment and operating decisions can be critically assessed only if we include hourly or sub-hourly operational decisions as an evaluation of the flexibility of the system. As solving the alternating current optimal power flow (AC OPF) problem is NP-hard (see Bienstock and Verma 2019), planners usually use linearized direct current (DC) approximation models of power flow in expansion planning, e.g. Bussar et al. (2014), Khodaei and Shahidehpour (2012), Lara et al. (2018), López-Ramos et al. (2020), Pineda et al. (2016). In practice, the approximations are attractive from the computational perspective and sufficient for the needs of operational planners. However, the DC OPF problem doesn't faithfully model physical variables of AC power system in expansion and integration planning. For example, a comparison of DC OPF and AC OPF deterministic model for the RTS GMLC network can be found in Bent et al. (2011), where it is shown that a plan based upon DC power flow must be significantly modified to meet requirements of the AC power flow model.

Another significant complication in expansion planning models is accounting for uncertainty. In literature, many authors use deterministic approaches (e.g. Bussar et al. 2014, Lara et al. 2018) and conduct analysis of certain scenarios (e.g. Hirth 2015, Peter and Wagner 2021). Nevertheless, there also exist stochastic approaches: Pineda et al. (2016) presents a market-focused approach with uncertainty in demand and renewable generation, Dehghan et al. (2016) propose tri-stage reliability-constrained model allowing for randomness in demand, wind generation and availability of generation and transmission, Moreira et al. (2021) adopts robust optimization model to schedule operating of the network. However, they mostly don't include operational decisions in problem setting or use DC approximation, which significantly simplifies the problem.

As we can observe, generation expansion planning models can vary widely in scope and components as well as in the resolution of time and space, which drive the complexity of optimization problems. Therefore, planners usually focus on one aspect while relaxing other assumptions or using approximations of the original problem. We refer to Skolfield and Escobedo (2021) for an extensive guide to recent methodologies and applications of optimal power flow problems.

In this paper, a multi-stage stochastic optimization model is proposed to evaluate the expansion of the grid infrastructure required to phase out fossil fuels while taking into account operating constraints and the variability of the demand and renewable generation sources. The model aims to identify the location and capacity of storage units and new renewable generation sources that ensure the stability and flexibility of the network while minimizing investment and operating costs over the given time horizon. The optimization problem is divided into two parts: the first stage with investment decisions and the consecutive stages representing days of operation with hourly resolution using AC OPF.

As already mentioned, AC OPF itself is an NP-hard nonconvex optimization problem, and considering an extension to a multi-stage optimization problem significantly increases the complexity of the problem. We use the method proposed in Kiszka and Wozabal (2024), which constitutes an innovative approach capturing the complexities of this optimization model.

Next, the model and the algorithm are implemented in the case study considering part of the IEEE RTS GMLC network. The optimal storage and renewable energy capacities are compared for different seasons and analyzed with respect to changes in the required share of renewable energy generation.

To the best of our knowledge, the presented generation expansion planning formulation is the first one covering multi-stage planning, AC OPF, and uncertainty simultaneously, and the applied methodology ensures the computational tractability of the problem.

The contribution of this paper can be summarized as follows:

1. We propose a generation expansion planning problem including multi-stage formulation, alternating current nature of power flows, and uncertainty of demand and renewable generation simultaneously. The optimization problem can be divided into the first stage, representing investment decisions, and subsequent stages, reflecting operational planning of the network over a given time horizon.

2. We model the reactive power limits of wind power generation as a function of random generation leading to randomness in inequality constraints.

3. We introduce the constraint ensuring the minimum daily renewable generation requirement expressed as a percentage of daily demand.

4. We apply the solution strategy proposed in Kiszka and Wozabal (2024), providing a detailed explanation of the reformulations and adaptation of the algorithm.

5. We implement the model using the part of the IEEE RTS GMLC network. The resulting expansion strategies are compared for different seasons and minimum renewable generation targets.

Section 4.2 presents the multi-stage problem formulation with an explanation of all variables and constraints. The applied solution strategy is described in section 4.3 with a detailed explanation of the problem evaluation. Section 4.4 describes the case study on the real data, providing all optimization parameters and analyzing numerical results. Section 4.5 concludes the paper.

Notation: $\mathfrak{Re}(\cdot)$ and $\mathfrak{Im}(\cdot)$ denote real and imaginary parts of their arguments. * denotes complex conjugation.

4.2 Problem Description

This section proposes a generation expansion planning problem to provide the optimal investment strategy required to accomplish a given share of renewable energy and guarantee stable power network operation over a defined time horizon while minimizing the expected costs. In order to include uncertainty of renewable generation and load, Markov process in the form of scenario lattice is used in the proposed multi-stage stochastic optimization model.

The generation expansion planning model is assumed to consist of $T + 1$ stages. The first stage is denoted by 0 and comprises the investment decisions on storage and new renewable capacity at predefined units. As solar and wind energy continue to lead renewable generation expansion in the last few years, we focus only on those technologies in the proposed model. The following stages $\mathcal{T} = \{1, \ldots, T\}$ represent T days of operational planning where every day includes planning for every hour $\mathcal{H} = \{1, \ldots, 24\}$.

In order to address the uncertainty of load and renewable generation, we introduce a random process $\xi = (\xi_0, \xi_1, \ldots, \xi_T), \xi_t : \Omega_t \to \mathbb{R}^{4 \times 24}$ with $\xi_t = (\xi_{ht})_{h \in \mathcal{H}}$ and $\xi_{ht} = (\xi_{ht}^L, \xi_{ht}^S, \xi_{ht}^W, \xi_{ht}^H)$ representing random load of the area, solar, wind and hydro generation per unit of capacity respectively. It means that $\xi_{ht}^S, \xi_{ht}^W, \xi_{ht}^H \in [0, 1]$ for every $h \in \mathcal{H}, t \in \mathcal{T}$. ξ is assumed to be a finitely supported Markov process, implying that the set Ω_t is finite and conditional distribution of ξ_{t+1} depends only on ξ_t for every $t \in \{0, 1, \ldots, T - 1\}$. Let assume that $\Pi_t(\omega_t, \omega_{t+1})$ represents the conditional probability $\mathbb{P}(\xi_{t+1} = \xi_{t+1}(\omega_{t+1}) | \xi_t = \xi_t(\omega_t))$ establishing the transition matrix Π_t.

The power network is represented by n buses $\mathcal{N} = \{1, \ldots, n\}$ which are interconnected by lines $\mathcal{L} \subseteq \mathcal{N} \times \mathcal{N}$. The generation units are divided into two categories: conventional generators and renewable energy sources. The conventional generators include coal, gas, oil, and nuclear power plants and are designated as $\mathcal{G} = \{1, \ldots, m\}$. Renewable energy sources, on the other hand, are comprised of solar, wind, and hydropower plants and are denoted as $\tilde{\mathcal{G}} = \{1, \ldots, \tilde{m}\} = \tilde{\mathcal{G}}^S \cup \tilde{\mathcal{G}}^W \cup \tilde{\mathcal{G}}^H$, where $\tilde{\mathcal{G}}^S$,

$\tilde{\mathcal{G}}^W$, and $\tilde{\mathcal{G}}^H$ represent solar, wind and hydropower plants, respectively. The set $\tilde{\mathcal{G}}$ encompasses not only existing units but also the potential solar and wind power plants represented by subsets $\tilde{\mathcal{G}}^{S,new} \subseteq \tilde{\mathcal{G}}^S$ and $\tilde{\mathcal{G}}^{W,new} \subseteq \tilde{\mathcal{G}}^W$, respectively, and the sum of which forms $\tilde{\mathcal{G}}^{new} \subseteq \tilde{\mathcal{G}}$. To identify the set of generators at a specific bus, we use the subscript k, i.e. $\mathcal{G}_k$, and define the functions $k : \mathcal{G} \to \mathcal{N}$ and $\tilde{k} : \tilde{\mathcal{G}} \to \mathcal{N}$ to associate a generator with its corresponding bus number.

To ensure the stability and reliability of the energy system, we also consider energy storage solutions and $\mathcal{N}^S \subseteq \mathcal{N}$ denotes the subset of buses where storage capacity can be built.

The network topology is defined by the admittance matrix $Y \in C^{n \times n}$, which is based on the provided impedance and shunt admittance values of each line and bus in the power system. For more information on obtaining the admittance matrix and its transformations, refer to Frank and Rebennack (2016) and Kiszka and Wozabal (2024).

The first stage in the proposed optimization model corresponds to the investment planning for renewable energy and storage capacity. Three vectors represent the decision variables:

$$\overline{B} = (\overline{B}_k)_{k \in \mathcal{N}^S} \in \mathbb{R}^{|\mathcal{N}^S|},$$

$$P^{S,max} = (P_j^{\tilde{G},max})_{j \in \tilde{\mathcal{G}}^{S,new}} \in \mathbb{R}^{|\tilde{\mathcal{G}}^{S,new}|},$$

$$P^{W,max} = (P_j^{\tilde{G},max})_{j \in \tilde{\mathcal{G}}^{W,new}} \in \mathbb{R}^{|\tilde{\mathcal{G}}^{W,new}|}$$

which define the storage capacity, new solar, and new wind power capacity at selected locations respectively. These decisions are assumed to be nonnegative and have investment costs $f^B, f^S, f^W \geq 0$, denoting the cost per MW of storage, solar, and wind capacity, respectively, that add up to the value of

$$c_0(\overline{B}, P^{S,max}, P^{W,max}) = f^B \sum_{k \in \mathcal{N}^S} \overline{B}_k + f^S \sum_{j \in \tilde{\mathcal{G}}^{S,new}} P_j^{\tilde{G},max} + f^W \sum_{j \in \tilde{\mathcal{G}}^{W,new}} P_j^{\tilde{G},max}. \quad (4.1)$$

The following stages $t \in \{1, \ldots, T\}$ focus on the operational planning of the power system, aiming to ensure optimal power flow while minimizing costs. Decisions on power generation, storage operation, and curtailment have to be made at every stage based on the realization of the random process.

The random variable ξ^L, which represents the random demand for the entire area, must be scaled to calculate the load for individual buses, taking into account both active and reactive power. Therefore, we assume that

$$P_{k,ht}^D = \xi_{ht}^L \rho_k^P \quad \forall k \in \mathcal{N}, \forall h \in \mathcal{H}, \tag{4.2}$$

$$Q_{k,ht}^D = \xi_{ht}^L \rho_k^Q \quad \forall k \in \mathcal{N}, \forall h \in \mathcal{H} \tag{4.3}$$

where $\rho_k^P, \rho_k^Q \geq 0$ are predefined coefficients for every $k \in \mathcal{N}$, representing the distribution of the total demand among buses.

To calculate the production from renewable sources, we need to multiply the capacity of each generator by the generation per capacity unit represented by random variables ξ^S, ξ^W, and ξ^H. Using capacities for existing generators $j \in \tilde{\mathcal{G}} \backslash \tilde{\mathcal{G}}^{new}$ and the optimal decisions from the first stage optimization for potential generators $j \in \tilde{\mathcal{G}}^{new}$ the output of the renewable energy sources is given as follows:

$$P_{j,ht}^{\tilde{G}} = \xi_{ht}^R P_j^{\tilde{G},max} \quad \forall R \in \{S, W, H\}, \forall j \in \tilde{\mathcal{G}}^R, \forall h \in \mathcal{H}. \tag{4.4}$$

The reactive power of renewable generators $Q_{j,ht}^{\tilde{G}}$ is considered a decision variable that must comply with the provided limits. For wind power plants, we use the approach introduced in Gil-González et al. (2020), stating that

$$|Q_{j,ht}^{\tilde{G}}| \leq \frac{P_j^{\tilde{G},max}}{\kappa} \sqrt{1 - \kappa^2 (\xi_{ht}^W)^2} \quad \forall j \in \tilde{\mathcal{G}}^W, \forall h \in \mathcal{H} \tag{4.5}$$

where $0 < \kappa \leq 1$ is a chargeability factor of the paired wind turbine-power converter, representing that when the maximum active power is obtained from the wind power system, the power conversion system works at level κ. It enables the use of the wind

power system as a variable energy compensator which can operate with lagging or leading power factor depending on the grid requirements, as the reactive power can be positive or negative.

Whereas solar power plants do not produce reactive power, they are considered DC generators, implying that

$$Q_{j,ht}^{\tilde{G}} = 0 \quad \forall j \in \tilde{\mathcal{G}}^S, \forall h \in \mathcal{H}.$$

For hydropower plants, the reactive power is restricted by the network limits:

$$Q_j^{\tilde{G},min} \leq Q_{j,ht}^{\tilde{G}} \leq Q_j^{\tilde{G},max} \quad \forall j \in \tilde{\mathcal{G}}^H, \forall h \in \mathcal{H}. \tag{4.6}$$

The active power $P_{g,ht}^G$ and reactive power $Q_{g,ht}^G$ for conventional generators $g \in \mathcal{G}$ are decision variables constrained as follows:

$$P_g^{G,min} \leq P_{g,ht}^G \leq P_g^{G,max} \qquad\qquad \forall g \in \mathcal{G}, \forall h \in \mathcal{H} \tag{4.7}$$

$$Q_g^{G,min} \leq Q_{g,ht}^G \leq Q_g^{G,max} \qquad\qquad \forall g \in \mathcal{G}, \forall h \in \mathcal{H} \tag{4.8}$$

where $P_g^{G,min}, P_g^{G,max}$ and $Q_g^{G,min}, Q_g^{G,max}$ are the network limits. Contrary to renewable energy sources, conventional power generation has a cost that is assumed to be a convex, piecewise linear function of active power generation $P_{g,ht}^G$ with breakpoints (a_{gi}, b_{gi}), $i = 1, \ldots, r_g$ such that

$$f^g(P_{g,ht}^G) = \begin{cases} m_{g1}(P_{g,ht}^G - a_{g1}) + b_{g1}, & a_{g1} < P_{g,ht}^G \leq a_{g2} \\ m_{g2}(P_{g,ht}^G - a_{g2}) + b_{g2}, & a_{g2} < P_{g,ht}^G \leq a_{g3} \\ \vdots & \vdots \\ m_{g(r_g-1)}(P_{g,ht}^G - a_{g(r_g-1)}) + b_{g(r_g-1)}, & a_{g(r_g-1)} < P_{g,ht}^G \leq a_{gr_g}. \end{cases}$$

Due to its convexity, the cost function can be reformulated in an equivalent form:

$$f^g(P^G_{g,ht}) = \max_{i=1,\dots,r_g-1}(m_{gi}(P^G_{g,ht} - a_{gi}) + b_{gi})$$

$$= \begin{cases} \min & \alpha_{g,ht} \\ \text{s.t.} & m_{gi}(P^G_{g,ht} - a_{gi}) + b_{gi} \leq \alpha_{g,ht} \quad \forall i \in [r_g - 1] \end{cases} \tag{4.9}$$

This simplifies the optimization problem's solving procedure, particularly the dualization step.

Remark 4.1. *In the presented generation expansion model, once the first stage optimization problem is resolved, the renewable generation becomes a random variable while the conventional generation is treated as a decision variable.*

To ensure the flexibility of the power system, energy storage is considered in the first stage of investment planning. As proposed by Cole and Frazier (2020), we assume that the duration of the storage is four hours, meaning that the storage runs empty within four hours if it is fully charged. It implies that real injections $O^+_{k,ht} \geq 0$ and withdrawals $O^-_{k,ht} \geq 0$, which represent the operation of energy storage, are restricted in the following way:

$$0 \leq O^+_{k,ht} \leq \frac{\overline{B}_k}{4\eta} \quad \forall k \in \mathcal{N}^S, \forall h \in \mathcal{H},$$

$$0 \leq O^-_{k,ht} \leq \frac{\eta \overline{B}_k}{4} \quad \forall k \in \mathcal{N}^S, \forall h \in \mathcal{H} \tag{4.10}$$

where $\eta \in (0,1)$ is the efficiency assumed to be symmetric for charging and discharging decisions. The balancing equation for the storage level $B_{k,ht}$ is determined by the operational decisions and the storage level at the previous step:

$$B_{k,ht} = B_{k,(h-1)t} + \eta O^+_{k,ht} - \eta^{-1} O^-_{k,ht} \quad \forall k \in \mathcal{N}^S, \forall h \in \mathcal{H} \tag{4.11}$$

and it has to satisfy the technical restrictions:

$$0 \leq B_{k,ht} \leq \overline{B}_k \quad \forall k \in \mathcal{N}^S, \forall h \in \mathcal{H}. \tag{4.12}$$

The initial storage level of the planning period is defined as a proportion B_0 of the storage capacity, meaning that $B_{k,01} = B_0 \overline{B}_k$. For the consecutive days, the initial storage level is equal to the level in the last hour $h = 24$ on the previous day $B_{k,0t} = B_{k,24(t-1)}$. In order to obtain an objective assessment of the model, the storage level at the end of the operational period is forced back to the initial one by the constraint:

$$B_{k,24T} = B_0 \overline{B}_k \quad \forall k \in \mathcal{N}^S. \tag{4.13}$$

Taking into account all described components, the active and reactive injections can be determined for every bus $k \in \mathcal{N}$ and time step $h \in \mathcal{H}$ by equations:

$$P_{k,ht} = \sum_{g \in \mathcal{G}_k} P_{g,ht}^G + \sum_{j \in \tilde{\mathcal{G}}_k} P_{j,ht}^{\tilde{G}} - P_{k,ht}^D - O_{k,ht}^+ + O_{k,ht}^- + D_{k,ht}^{P+} - D_{k,ht}^{P-} \tag{4.14}$$

$$Q_{k,ht} = \sum_{g \in \mathcal{G}_k} Q_{g,ht}^G + \sum_{j \in \tilde{\mathcal{G}}_k} Q_{j,ht}^{\tilde{G}} - Q_{k,ht}^D + D_{k,ht}^{Q+} - D_{k,ht}^{Q-} \tag{4.15}$$

where

$$D_{k,ht}^{P+}, D_{k,ht}^{P-}, D_{k,ht}^{Q+}, D_{k,ht}^{Q-} \geq 0 \tag{4.16}$$

and $D_{k,ht}^+ = D_{k,ht}^{P+} + D_{k,ht}^{Q+}$, $D_{k,ht}^- = D_{k,ht}^{P-} + D_{k,ht}^{Q-}$ denote curtailment of demand and supply with associated cost f^{D+} and f^{D-} respectively.

Remark 4.2. *Introducing curtailment decisions ensures that the problems are always feasible and have relatively complete recourse, which is required to apply the solution strategy proposed in Kiszka and Wozabal (2024).*

On the other hand, the power, voltages, and admittance matrix are strictly related to the generalization of Ohm's law to AC networks. It implies that

$$P_{k,ht} = \mathfrak{Re}(V_{k,ht} e_k^T Y^* V_{ht}^*) \quad \forall k \in \mathcal{N}, \forall h \in \mathcal{H}$$

$$Q_{k,ht} = \mathfrak{Im}(V_{k,ht} e_k^T Y^* V_{ht}^*) \quad \forall k \in \mathcal{N}, \forall h \in \mathcal{H} \tag{4.17}$$

$$S_{lm,ht} = V_{ht}^T Y_{lm}^* V_{ht}^* \quad \forall (l,m) \in \mathcal{L}, \forall h \in \mathcal{H}$$

where $V_{ht} = (V_{1,ht}, \ldots, V_{n,ht})^T$ is a vector of voltages for all buses. As the network

infrastructure imposes limitations on the power flow, additional constraints are required to ensure the reliability of the power system. Therefore the voltages at buses are bounded according to the following inequality:

$$V_k^{min} \leq |V_{k,ht}| \leq V_k^{max}, \quad \forall k \in \mathcal{N}, \forall h \in \mathcal{H}. \tag{4.18}$$

Additionally, the power flow through the lines, expressed by the apparent power, is limited as follows:

$$|S_{lm,ht}|^2 \leq \overline{S}_{lm}^2, \quad \forall (l,m) \in \mathcal{L}, \forall h \in \mathcal{H}. \tag{4.19}$$

These constraints ensure the power system operates within safe parameters and avoids potential failures or disruptions.

Investing in renewable energy infrastructure entails high initial costs and uncertain output due to weather conditions. To promote the expansion of renewable energy sources, we propose introducing an additional constraint that guarantees a specific percentage $\Delta \in (0,1)$ of renewable generation in the daily power demand:

$$\sum_{h \in \mathcal{H}} \sum_{j \in \tilde{\mathcal{G}}} P_{j,ht}^{\tilde{G}} + TR_t \geq \Delta \sum_{h \in \mathcal{H}} \sum_{k \in \mathcal{N}} P_{k,ht}^D. \tag{4.20}$$

We penalize any deviation from this target using the cost $f^{TR} \geq 0$ per MWh, which accounts for the missing generation TR_t that results from not meeting the goal.

As all required components of the model are already defined, the generation expansion planning problem can be formulated to provide the optimal investment strategy and optimal power flow decisions for the given period. The optimization problem can be written in the form:

$$\begin{aligned} \min \quad & c_0(\overline{B}, P^{S,max}, P^{W,max}) + \mathbb{E}\left(\sum_{t \in \mathcal{T}} c_t(\xi_t, \overline{B}, P^{S,max}, P^{W,max}, B_{0t})\right) \\ \text{s.t.} \quad & (4.4) - (4.20) \quad \forall t \in \mathcal{T} \end{aligned} \tag{4.21}$$

where the cost for particular stage $t \in \mathcal{T}$ is defined as

$$c_t = \sum_{h \in \mathcal{H}} \sum_{k \in \mathcal{N}} \left(\sum_{g \in \mathcal{G}_k} \alpha_{g,ht} + f^{D+} D^+_{k,ht} + f^{D-} D^-_{k,ht} \right) + f^{TR} TR_t. \qquad (4.22)$$

In the problem formulation, all decisions depend on the realization of random variables, but we omit the subscript to simplify the notation.

Remark 4.3. *Dependence between subsequent stages of the optimization model is hidden in the balancing constraint of the storage. Additionally, operational stages depend on the capacities obtained in the first stage.*

4.3   Solution Strategy

In this section, we present the applicability of the solution strategy proposed in Kiszka and Wozabal (2024) to the formulated generation expansion planning problem. The primary description of the method will be complemented with detailed reformulations and instructions for the considered class of problems.

Before applying the proposed algorithm, the required assumptions have to be verified. The stochastic process ξ should be finitely supported and Markovian in order to obtain numerical results, as imposed by the definition of the process ξ in Section 4.2. Additionally, the feasible decisions at stage t should depend only on decisions at stage $t-1$, not the whole history of decisions. This condition is ensured by the formulation of the problem, where the storage level and capacity decisions connect consecutive stages. Furthermore, the curtailment decisions introduced in the problem description ensure the assumption of relatively complete recourse. Once we have verified that all assumptions are met, we can proceed with reformulating the problem and applying the algorithm.

In Section 4.3.1, we implement the recommended reformulation and relaxation of the problem. Subsequently, in section 4.3.2, we present the dynamic formulation of the problem, and in section 4.3.3, we perform dualization of the problem required

to apply the SDDP algorithm and find a solution. In the section 4.3.4, details of the SDDP algorithm are provided, and in the last section 4.3.5, a simplified model is explored to facilitate the straightforward application of the procedure to the slightly modified expansion problems.

4.3.1   Reformulation and Relaxation

The formulation of the problem (4.21) requires operations on the complex numbers, which significantly increase the difficulty of the problem. To overcome this obstacle Lavaei and Low (2012) propose Lemma 1 with an equivalent form of equations (4.17) where the real and imaginary part of voltage values are separated. In consequence equations (4.14)-(4.15) can be reformulated as follows:

$$tr(\mathbb{Y}_k W_{ht}) = \sum_{g \in \mathcal{G}_k} P_{g,ht}^G + \sum_{j \in \tilde{\mathcal{G}}_k} P_{j,ht}^{\tilde{G}} - P_{k,ht}^D - O_{k,ht}^+ + O_{k,ht}^- + D_{k,ht}^{P+} - D_{k,ht}^{P-} \quad (4.23)$$

$$tr(\hat{\mathbb{Y}}_k W_{ht}) = \sum_{g \in \mathcal{G}_k} Q_{g,ht}^G + \sum_{j \in \tilde{\mathcal{G}}_k} Q_{j,ht}^{\tilde{G}} - Q_{k,ht}^D + D_{k,ht}^{Q+} - D_{k,ht}^{Q-} \quad (4.24)$$

where

$$W_{ht} = \tilde{V}_{ht} \tilde{V}_{ht}^T \quad \text{for} \quad \tilde{V}_{ht} = \begin{bmatrix} \mathfrak{Re}(V_{ht}) \\ \mathfrak{Im}(V_{ht}) \end{bmatrix}$$

and $\mathbb{Y}_k, \hat{\mathbb{Y}}_k$ represent adaptations of the admittance matrix Y, as defined in Lavaei and Low (2012) and thoroughly elaborated upon in Kiszka and Wozabal (2024).

Furthermore, the combination of Lemma 1 and Schur's complement formula enables the transformation of the quadratic constraint (4.19) into a semidefinite inequality:

$$\begin{bmatrix} -\overline{S}_{lm}^2 & \mathbb{Y}_{lm} \bullet W_{ht} & \hat{\mathbb{Y}}_{lm} \bullet W_{ht} \\ \mathbb{Y}_{lm} \bullet W_{ht} & -1 & 0 \\ \hat{\mathbb{Y}}_{lm} \bullet W_{ht} & 0 & -1 \end{bmatrix} \preceq 0. \quad (4.25)$$

As the constraint (4.18) can also be reformulated using the matrix W_{ht} to the

form of:

$$(V_k^{min})^2 \leq tr(M_k W_{ht}) \leq (V_k^{max})^2, \tag{4.26}$$

the variable $\tilde{V}_{ht}$ can be eliminated from the problem. To ensure the equivalence of the problems, it is necessary to leverage the fact that a given matrix W_{ht} can be expressed as $\tilde{V}_{ht}\tilde{V}_{ht}^T$ for some nonzero vector $\tilde{V}_{ht}$ if and only if W_{ht} is both positive semidefinite and of rank 1. Consequently, the following constraints must be imposed:

$$W_{ht} \succeq 0 \tag{4.27}$$

$$\text{rank}(W_{ht}) = 1 \tag{4.28}$$

to eliminate the decision variable $\tilde{V}_{ht}$ and maintain the equivalence of the problems.

Given that the reformulated problem is a non-convex optimization problem, with non-convexity arising from the rank constraint, we alleviate this by eliminating the rank constraint. This transformation yields a convex optimization problem that serves as a lower-bound approximation to the original problem.

4.3.2   Dynamic Formulation

In this section, we present the dynamic formulation of the problem, enabling the application of the SDDP algorithm. As mentioned before, the existence of storage introduces dependence on the storage level between consecutive stages. Additionally, the feasible set at a given stage depends on the storage and renewable capacity, which are the first-stage decisions. This enables writing the problem using the value functions, as suggested in Kiszka and Wozabal (2024), assuming that the random parameter is an *environmental state*, and storage and renewable capacity with the initial storage level of the stage compose a *resource state*. The dynamic programming

equations of the problem take the following form:

$$C_0(\xi_0, B_0) = \begin{cases} \min & c_0(\overline{B}, P^{S,max}, P^{W,max}) + \mathcal{C}_1(\xi_0, \overline{B}, P^{S,max}, P^{W,max}, B_{01}) \\ \text{s.t.} & \overline{B}, P^{S,max}, P^{W,max} \geq 0 \\ & B_{01} = B_0 \overline{B} \end{cases}$$

and

$$C_t(\xi_t, \overline{B}, P^{S,max}, P^{W,max}, B_{0t}) =$$

$$\begin{cases} \min & c_t(\xi_t, \overline{B}, P^{S,max}, P^{W,max}, B_{0t}) + \mathcal{C}_{t+1}(\xi_t, \overline{B}, P^{S,max}, P^{W,max}, B_{24t}) \\ \text{s.t.} & (4.4) - (4.13), (4.16), (4.20), (4.23) - (4.27) \end{cases}$$

for operational stages $t \in \mathcal{T}$, where the recourse functions are defined as:

$$\mathcal{C}_{t+1}(\xi_t, \overline{B}, P^{S,max}, P^{W,max}, B_{24t}) = \mathbb{E}(C_{t+1}(\xi_{t+1}, \overline{B}, P^{S,max}, P^{W,max}, B_{24t})|\xi_t). \quad (4.29)$$

Given that the functions C_t are convex, the recourse functions can be effectively approximated from below by the maximum of affine functions, converging to the actual function. Therefore the approximation of the recourse function based on l affine functions is introduced as $\bar{\mathcal{C}}_{t+1,l}$ and can be written as

$$\bar{\mathcal{C}}_{t+1,l}(\xi_t, \overline{B}, P^{S,max}, P^{W,max}, B_{24t}) =$$

$$\begin{cases} \min & \theta \\ \text{s.t.} & e_{i,t}^0 + e_{i,t}^1 \overline{B} + e_{i,t}^2 P^{S,max} + e_{i,t}^3 P^{W,max} + e_{i,t}^4 B_{24t} \leq \theta \quad \forall i \in [l] \end{cases}$$

where $e_{i,t}^0 \in \mathbb{R}, e_{i,t}^1, e_{i,t}^4 \in \mathbb{R}^{|\mathcal{N}^S|}$ and $e_{i,t}^2 \in \mathbb{R}^{|\tilde{\mathcal{G}}^{S,new}|}, e_{i,t}^3 \in \mathbb{R}^{|\tilde{\mathcal{G}}^{W,new}|}$ for all $i \in [l], t \in \mathcal{T}$. It implies that the approximation of the value function at stage t has the following form with the dual multipliers indicated in the square brackets:

$$\bar{C}_{tl}(\xi_t, \overline{B}, P^{S,max}, P^{W,max}, B_{0t}) =$$

$$
\begin{cases}
\min \quad c_t(\xi_t, \overline{B}, P^{S,max}, P^{W,max}, B_{0t}) + \theta \\[4pt]
\text{s.t.} \quad tr(\mathbb{Y}_k W_{ht}) = \sum_{g \in \mathcal{G}_k} P^G_{g,ht} + \sum_{j \in \tilde{\mathcal{G}}_k} P^{\tilde{G}}_{j,ht} - P^D_{k,ht} \\[4pt]
\qquad\qquad -O^+_{k,ht} + O^-_{k,ht} + D^{P+}_{k,ht} - D^{P-}_{k,ht} \qquad\qquad \forall k \in \mathcal{N}, h \in \mathcal{H} \qquad\qquad [\lambda_{k,ht}] \\[4pt]
\qquad tr(\hat{\mathbb{Y}}_k W_{ht}) = \sum_{g \in \mathcal{G}_k} Q^G_{g,ht} + \sum_{j \in \tilde{\mathcal{G}}_k} Q^{\tilde{G}}_{j,ht} - Q^D_{k,ht} \\[4pt]
\qquad\qquad +D^{Q+}_{k,ht} - D^{Q-}_{k,ht} \qquad\qquad\qquad \forall k \in \mathcal{N}, h \in \mathcal{H} \qquad\qquad [\gamma_{k,ht}] \\[4pt]
\qquad (V^{min}_k)^2 \le tr(M_k W_{ht}) \le (V^{max}_k)^2 \qquad \forall k \in \mathcal{N}, h \in \mathcal{H} \qquad\qquad [\underline{\mu}_{k,ht}, \overline{\mu}_{k,ht}] \\[4pt]
\qquad \begin{bmatrix} -\overline{S}^2_{lm} & \mathbb{Y}_{lm} \bullet W_{ht} & \hat{\mathbb{Y}}_{lm} \bullet W_{ht} \\[4pt] \mathbb{Y}_{lm} \bullet W_{ht} & -1 & 0 \\[4pt] \hat{\mathbb{Y}}_{lm} \bullet W_{ht} & 0 & -1 \end{bmatrix} \preceq 0 \qquad \forall(l,m) \in \mathcal{L}, h \in \mathcal{H} \qquad [r_{lm,ht}] \\[8pt]
\qquad P^{G,min}_g \le P^G_{g,ht} \le P^{G,max}_g \qquad\qquad \forall g \in \mathcal{G}, h \in \mathcal{H} \qquad\qquad [\underline{\lambda}_{g,ht}, \overline{\lambda}_{g,ht}] \\[4pt]
\qquad Q^{G,min}_g \le Q^G_{g,ht} \le Q^{G,max}_g \qquad\qquad \forall g \in \mathcal{G}, h \in \mathcal{H} \qquad\qquad [\underline{\gamma}_{g,ht}, \overline{\gamma}_{g,ht}] \\[4pt]
\qquad m_{gi}(P^G_{g,ht} - a_{gi}) + b_{gi} \le \alpha_g \qquad \forall g \in \mathcal{G}, i \in [r_g - 1], h \in \mathcal{H} \quad [\zeta_{gi,ht}] \\[4pt]
\qquad |Q^{\tilde{G}}_{j,ht}| \le \frac{P^{\tilde{G},max}_j}{\kappa}\sqrt{1 - \kappa^2(\xi^W_{ht})^2} \qquad \forall j \in \tilde{\mathcal{G}}^W, h \in \mathcal{H} \qquad [\underline{\gamma}^W_{j,ht}, \overline{\gamma}^W_{j,ht}] \\[4pt]
\qquad Q^{\tilde{G},min}_j \le Q^{\tilde{G}}_{j,ht} \le Q^{\tilde{G},max}_j \qquad\qquad \forall j \in \tilde{\mathcal{G}}^H, h \in \mathcal{H} \qquad [\underline{\gamma}^H_{j,ht}, \overline{\gamma}^H_{j,ht}] \\[4pt]
\qquad \sum_{h \in \mathcal{H}} \sum_{j \in \tilde{\mathcal{G}}} P^{\tilde{G}}_{j,ht} + TR_t \ge \Delta \sum_{h \in \mathcal{H}} \sum_{k \in \mathcal{N}} P^D_{k,ht} \qquad\qquad\qquad\qquad [\tau_t] \\[4pt]
\qquad O^+_{k,ht} \le \frac{\overline{B}_k}{4\eta} \qquad\qquad\qquad\qquad \forall k \in \mathcal{N}^S, h \in \mathcal{H} \qquad\qquad [\overline{\beta}^+_{k,ht}] \\[4pt]
\qquad O^-_{k,ht} \le \frac{\eta \overline{B}_k}{4} \qquad\qquad\qquad\qquad \forall k \in \mathcal{N}^S, h \in \mathcal{H} \qquad\qquad [\overline{\beta}^-_{k,ht}] \\[4pt]
\qquad B_{k,ht} = B_{k,(h-1)t} + \eta O^+_{k,ht} - \eta^{-1} O^-_{k,ht} \qquad \forall k \in \mathcal{N}^S, h \in \mathcal{H} \qquad [\sigma_{k,ht}] \\[4pt]
\qquad B_{k,ht} \le \overline{B}_k \qquad\qquad\qquad\qquad \forall k \in \mathcal{N}^S, h \in \mathcal{H} \qquad\qquad [\overline{\kappa}_{k,ht}] \\[4pt]
\qquad B_{k,24T} = B_0 \overline{B}_k \qquad\qquad\qquad\qquad \forall k \in \mathcal{N}^S, h \in \mathcal{H} \qquad\qquad [\delta_k] \\[4pt]
\qquad e^0_{i,t} + e^1_{i,t}\overline{B} + e^2_{i,t}P^{S,max} + e^3_{i,t}P^{W,max} + e^4_{i,t}B_{24t} \le \theta \quad \forall i \in [l], h \in \mathcal{H} \quad [\nu_{i,t}] \\[4pt]
\qquad B_{k,ht} \ge 0 \qquad\qquad\qquad\qquad\qquad \forall k \in \mathcal{N}^S, h \in \mathcal{H} \\[4pt]
\qquad D^{P+}_{k,ht}, D^{P-}_{k,ht}, D^{Q+}_{k,ht}, D^{Q-}_{k,ht} \ge 0 \qquad \forall k \in \mathcal{N}, h \in \mathcal{H} \\[4pt]
\qquad TR_t \ge 0, W_{ht} \succeq 0
\end{cases}
$$

$$(4.30)$$

Distinguished from the others, the dual multiplier for the semidefinite inequality has the matrix form:

$$
r_{lm,ht} = \begin{pmatrix} r^1_{lm,ht} & r^2_{lm,ht} & r^3_{lm,ht} \\ r^2_{lm,ht} & r^4_{lm,ht} & 0 \\ r^3_{lm,ht} & 0 & r^5_{lm,ht} \end{pmatrix}
$$

Remark 4.4. *As $C_{T+1} = 0$, it means that $e^0_{i,T}, \ldots, e^4_{i,T}$ for every $i \in [l]$ are also equal to zero.*

Remark 4.5. *Note that parameters of affine functions in the problem (4.30) depend on the value of an environmental state ξ_t. However, for the sake of notational simplicity, we omit this dependence.*

4.3.3   Dualization

Following the approach proposed in Lavaei and Low (2012) and subsequently reiterated in Kiszka and Wozabal (2024), in the next step, the dual of (4.30) is defined and has the following form:

$\tilde{C}_{tl}(\xi_t, \overline{B}, P^{S,max}, P^{W,max}, B_{0t}) =$

$$
\begin{cases}
\max \quad h_t \\[4pt]
\text{s.t.} \quad A_{ht} \succeq 0 & & [W_{ht}] \\[6pt]
\qquad \sum_{i \in [r_g - 1]} \zeta_{gi,ht} = 1 & \forall g \in \mathcal{G}, h \in \mathcal{H} & [\alpha^G_{g,ht}] \\[6pt]
\overline{\lambda}_{g,ht} - \underline{\lambda}_{g,ht} + \sum_{i \in [r_g-1]} \zeta_{gi,ht} m_{gi} - \lambda_{k(g)} = 0 & \forall g \in \mathcal{G}, h \in \mathcal{H} & [P^G_{g,ht}] \\[6pt]
\overline{\gamma}_{g,ht} - \underline{\gamma}_{g,ht} - \gamma_{k(g)} = 0 & \forall g \in \mathcal{G}, h \in \mathcal{H} & [Q^G_{g,ht}] \\[6pt]
\overline{\gamma}^R_{j,ht} - \underline{\gamma}^R_{j,ht} - \gamma_{\tilde{k}(j)} = 0 & \forall R \in \{W, H\}, j \in \tilde{\mathcal{G}}^R, h \in \mathcal{H} & [Q^{\tilde{G}}_{j,ht}] \\[6pt]
\beta^+_{k,ht} + \lambda_{k,ht} - \eta \sigma_{k,ht} \geq 0 & \forall k \in \mathcal{N}^S, h \in \mathcal{H} & [O^+_{k,ht}] \\[6pt]
\beta^-_{k,ht} - \lambda_{k,ht} + \frac{1}{\eta} \sigma_{k,ht} \geq 0 & \forall k \in \mathcal{N}^S, h \in \mathcal{H} & [O^-_{k,ht}] \\[6pt]
\sigma_{k,ht} - \sigma_{k,(h+1)t} + \overline{\kappa}_{k,ht} \geq 0 & \forall k \in \mathcal{N}^S, h \in \mathcal{H} & [B_{k,ht}] \\[6pt]
\sigma_{k,24t} + \overline{\kappa}_{k,24t} + \sum_{i \in [l]} \nu_{i,t} e^4_{ki,t} + \delta_k \mathbb{1}(t = T) \geq 0 & \forall k \in \mathcal{N}^S, h \in \mathcal{H} & [B_{k,24t}] \\[6pt]
f^{D+} - \lambda_{k,ht} \geq 0 & \forall k \in \mathcal{N}, h \in \mathcal{H} & [D^{P+}_{k,ht}] \\[6pt]
f^{D-} + \lambda_{k,ht} \geq 0 & \forall k \in \mathcal{N}, h \in \mathcal{H} & [D^{P-}_{k,ht}] \\[6pt]
f^{D+} - \gamma_{k,ht} \geq 0 & \forall k \in \mathcal{N}, h \in \mathcal{H} & [D^{Q+}_{k,ht}] \\[6pt]
f^{D-} + \gamma_{k,ht} \geq 0 & \forall k \in \mathcal{N}, h \in \mathcal{H} & [D^{Q-}_{k,ht}] \\[6pt]
\sum_{i \in [l]} \nu_{i,t} = 1 & & [\theta] \\[6pt]
f^{TR} - \tau_t \geq 0 & & [TR_t] \\[6pt]
r_{lm,ht} \succeq 0 & \forall (l, m) \in \mathcal{L}, h \in \mathcal{H} \\[6pt]
\nu_{i,t} \geq 0 & \forall i \in [l] \\[6pt]
\overline{\mu}_{k,ht}, \underline{\mu}_{k,ht}, , \overline{\beta}^-_{k,ht}, \overline{\beta}^+_{k,ht}, \overline{\kappa}_{k,ht}, \geq 0 & \forall k \in \mathcal{N}, h \in \mathcal{H} \\[6pt]
\overline{\lambda}_{g,ht}, \underline{\lambda}_{g,ht}, \overline{\gamma}_{g,ht}, \underline{\gamma}_{g,ht}, \zeta_{gi,ht} \geq 0 & \forall g \in \mathcal{G}, h \in \mathcal{H} \\[6pt]
\overline{\gamma}^R_{j,ht}, \underline{\gamma}^R_{j,ht} \geq 0 & \forall R \in \{W, H\}, j \in \tilde{\mathcal{G}}^R, h \in \mathcal{H} \\[6pt]
\tau_t \geq 0
\end{cases}
$$

$$(4.31)$$

where

$$h_t = \sum_{h \in \mathcal{H}} \sum_{k \in \mathcal{N}} \lambda_{k,ht} \left(P^D_{k,ht} - \sum_{j \in \tilde{\mathcal{G}}_k} P^{\tilde{G}}_{j,ht} \right) + \gamma_{k,ht} Q^D_{k,ht} + \underline{\mu}_{k,ht}(V^{min}_k)^2 - \overline{\mu}_{k,ht}(V^{max}_k)^2$$

$$- \sum_{h \in \mathcal{H}} \sum_{(l,m) \in \mathcal{L}} \left(\overline{S}^2_{lm} + r^4_{lm,ht} + r^5_{lm,ht} \right) + \tau_t \left(\Delta \sum_{h \in \mathcal{H}} \sum_{k \in \mathcal{N}} P^D_{k,ht} - \sum_{h \in \mathcal{H}} \sum_{j \in \tilde{\mathcal{G}}} P^{\tilde{G}}_{j,ht} \right)$$

$$+ \sum_{h \in \mathcal{H}} \sum_{k \in \mathcal{N}} \sum_{g \in \mathcal{G}_k} \left(\underline{\lambda}_{g,ht} P^{G,min}_g - \overline{\lambda}_{g,ht} P^{G,max}_g + \underline{\gamma}_{g,ht} Q^{G,min}_g - \overline{\gamma}_{g,ht} Q^{G,max}_g + \sum_{i=1}^{r_g-1} \zeta_{gi,ht}(b_{gi} - m_{gi}a_{gi}) \right)$$

$$- \sum_{h \in \mathcal{H}} \sum_{j \in \tilde{\mathcal{G}}^W} \frac{P^{\tilde{G},max}_j}{\kappa} \sqrt{1 - \kappa^2(\xi^W_{ht})^2}(\underline{\gamma}^W_{j,ht} + \overline{\gamma}^W_{j,ht}) + \sum_{h \in \mathcal{H}} \sum_{j \in \tilde{\mathcal{G}}^H} \left(\underline{\gamma}^h_{j,ht} Q^{\tilde{G},min}_j - \overline{\gamma}^H_{j,ht} Q^{\tilde{G},max}_j \right)$$

$$- \sum_{k \in \mathcal{N}^S} \left(\sigma_{k,1t} B_{k,0t} + \sum_{h \in \mathcal{H}} \left(\overline{\kappa}_{k,ht} + \frac{\overline{\beta}^+_{k,ht}}{4\eta} + \frac{\eta\overline{\beta}^-_{k,ht}}{4} \right) \overline{B}_k + \delta_k \mathbb{1}(t = T)B_0\overline{B}_k \right)$$

$$+ \sum_{i \in [l]} \nu_{i,t}e^0_{i,t} + \sum_{k \in \mathcal{N}^S} \overline{B}_k \sum_{i \in [l]} \nu_{i,t}e^1_{ki,t} + \sum_{j \in \tilde{\mathcal{G}}^{S,new}} P^{\tilde{G},max}_j \sum_{i \in [l]} \nu_{i,t}e^2_{ji,t} + \sum_{j \in \tilde{\mathcal{G}}^{W,new}} P^{\tilde{G},max}_j \sum_{i \in [l]} \nu_{i,t}e^3_{ji,t}$$

and

$$A_{ht} = \sum_{k \in \mathcal{N}} \left(\lambda_{k,ht} \mathbb{Y}_k + \gamma_{k,ht} \hat{\mathbb{Y}}_k + (\overline{\mu}_{k,ht} - \underline{\mu}_{k,ht})M_k \right) + \sum_{(l,m) \in \mathcal{L}} \left(2r^2_{lm,ht} \mathbb{Y}_{lm} + 2r^3_{lm,ht} \hat{\mathbb{Y}}_{lm} \right).$$

To ensure strong duality between (4.30) and (4.31), the satisfaction of the Slater condition is imperative. Demonstrating this condition involves proving that the primal problem attains a finite optimal value and that the dual problem possesses a feasible solution within the interior of the feasible set. The first condition is evidently satisfied based on the problem formulation and the feasible set of the dual problem

has an interior point defined by:

$$\lambda_{k,ht} = 0, \quad \gamma_{k,ht} = 0, \quad \overline{\mu}_{k,ht} = 2, \quad \underline{\mu}_{k,ht} = 1 \quad \forall k \in \mathcal{N}$$

$$\overline{\lambda}_{g,ht} = \left| \frac{1}{r_g - 1} \sum_{i \in [r_g - 1]} m_{gi} - \frac{1}{r_g - 1} \sum_{i \in [r_g - 1]} m_{gi} + 1 \right|, \quad \underline{\lambda}_{g,ht} = \left| \frac{1}{r_g - 1} \sum_{i \in [r_g - 1]} m_{gi} \right| + 1 \quad \forall g \in \mathcal{G}$$

$$\zeta_{gi,ht} = \frac{1}{r_g - 1} \quad \forall i \in [r_g - 1]$$

$$\overline{\gamma}_{g,ht} = \underline{\gamma}_{g,ht} = 1, \quad \overline{\gamma}_{j,ht}^R = \underline{\gamma}_{j,ht}^R = 1 \quad \forall g \in \mathcal{G}, R \in \{W, H\}, j \in \tilde{\mathcal{G}}^R$$

$$\sigma_{k,ht} = 25 - h, \quad \overline{\kappa}_{k,ht} = 1, \quad \delta_k = 1, \quad \overline{\beta}_{k,ht}^+ = (25 - h)\eta + 1, \quad \overline{\beta}_{k,ht}^- = 1 \quad \forall k \in \mathcal{N}^S$$

$$\tau_t = \frac{1}{2} f^{TR}, \quad \nu_{i,t} = \frac{1}{l} \quad \forall i \in [l]$$

$$r_{lm,ht}^1 = r_{lm,ht}^4 = r_{lm,ht}^5 = 1, \quad r_{lm,ht}^2 = r_{lm,ht}^3 = 0 \quad \forall (l, m) \in \mathcal{L}$$

for $h \in \mathcal{H}$. All variables in the presented feasible solution are strictly positive, except for $\lambda_{k,ht}$ and $\gamma_{k,ht}$, indicating an interior point.

4.3.4   Details of SDDP Algorithm

After reformulation, relaxation, and dualization of the formulated problem, the SDDP algorithm can be applied. The procedure consists of two main parts: forward and backward passes, which are described in Kiszka and Wozabal (2024).

First, we address the problem consecutively across stages for generated scenarios during the forward pass, determining the resource state values. In the backward pass, we solve the problem 4.31 starting from the last stage, assuming the resource state values obtained in the forward pass and considering all possible environmental states on the stage. Slopes of a new cut approximating the recourse function $\mathcal{C}_t(\xi_{t-1}, \overline{B}, P^{S,max}, P^{W,max}, B_{24,t-1})$ for state ω_{t-1} are calculated as the conditional expectation of slopes of $\tilde{\mathcal{C}}_{tl}(\xi_t, \overline{B}, P^{S,max}, P^{W,max}, B_{0t})$ with respect to $\overline{B}, P^{S,max}, P^{W,max}$ and B_{0t} over all environmental states ω_t. The particular slopes of $\tilde{\mathcal{C}}_{tl}$ are obtained as derivatives with respect to the given parameters and can be

easily extracted from the objective function h_t of the dual problem for the optimal solution. Thereby, with every consecutive iteration, we gain a new cut to the recourse function where slopes with respect to storage capacity, solar capacity, wind capacity, and storage level are calculated using the following formulas:

$\forall k \in \mathcal{N}^S :$

$$e^1_{k(l+1),t-1} = \sum_{\omega_t \in \Omega_t} \Pi_{t-1}(\omega_{t-1}, \omega_t) \left(\sum_{i \in [l]} \nu_{i,t} e^1_{ki,t} - \sum_{h \in \mathcal{H}} \left(\overline{\kappa}_{k,ht} + \frac{\overline{\beta}^+_{k,ht}}{4\eta} + \frac{\eta \overline{\beta}^-_{k,ht}}{4} \right) - B_0 \delta_k \mathbb{1}(t = T) \right)$$

$$e^4_{k(l+1),t-1} = - \sum_{\omega_t \in \Omega_t} \Pi_{t-1}(\omega_{t-1}, \omega_t) \sigma_{k,1t}$$

$\forall j \in \tilde{\mathcal{G}}^{S,new} :$

$$e^2_{j(l+1),t-1} = \sum_{\omega_t \in \Omega_t} \Pi_{t-1}(\omega_{t-1}, \omega_t) \left(\sum_{i \in [l]} \nu_{i,t} e^2_{ji,t} - \sum_{h \in \mathcal{H}} (\lambda_{\tilde{k}(j),ht} + \tau_t) \xi^S_{ht} \right)$$

$\forall j \in \tilde{\mathcal{G}}^{W,new} :$

$$e^3_{j(l+1),t-1} =$$

$$= \sum_{\omega_t \in \Omega_t} \Pi_{t-1}(\omega_{t-1}, \omega_t) \left(\sum_{i \in [l]} \nu_{i,t} e^3_{ji,t} - \sum_{h \in \mathcal{H}} \frac{1}{\kappa} \sqrt{1 - \kappa^2(\xi^W_{ht})^2}(\underline{\gamma}^W_{j,ht} + \overline{\gamma}^W_{j,ht}) - \sum_{h \in \mathcal{H}} (\lambda_{\tilde{k}(j),ht} + \tau_t) \xi^W_{ht} \right)$$

for the environmental state ω_{t-1}. As the initial storage level of the operational period is represented as the share of storage capacity $B_{k,01} = B_0 \bar{B}_k$, the affine function approximating the recourse function at the first stage depends on three, not four, variables having the form

$$e^0_{l+1,0} + (e^1_{l+1,0} + B_0 e^4_{l+1,0})\overline{B} + e^2_{l+1,0} P^{S,max} + e^3_{l+1,0} P^{W,max}.$$

4.3.5   Simplified Expansion Model

Due to the curse of dimensionality, a problem featuring only a few candidate locations for new renewable power plants may become computationally intractable. Consequently, we present a simplified model with a reduced number of first-stage

decisions, where the determination of the total new solar and wind capacity, along with its distribution among predefined locations according to the given ratios, is consolidated into single decisions denoted as $P^{S,max} \in \mathbb{R}$ and $P^{W,max} \in \mathbb{R}$. The first-stage cost function is then slightly modified to the following form:

$$c_0(\overline{B}, P^{S,max}, P^{W,max}) = f^B \sum_{k \in \mathcal{N}^S} \overline{B}_k + f^S P^{S,max} + f^W P^{W,max}. \tag{4.32}$$

Capacity for a single newly built renewable generator can be calculated using the formula

$$
\begin{aligned}
P_j^{\tilde{G},max} &= \rho_j^S P^{S,max} \quad \forall j \in \tilde{\mathcal{G}}^{S,new}, \\
P_j^{\tilde{G},max} &= \rho_j^W P^{W,max} \quad \forall j \in \tilde{\mathcal{G}}^{W,new},
\end{aligned}
\tag{4.33}
$$

where all coefficients $\rho_j^S \geq 0, \rho_j^W \geq 0$ are predefined and represent a distribution of the total source capacity with

$$\sum_{j \in \tilde{\mathcal{G}}^{S,new}} \rho_j^S = 1 \quad \text{and} \quad \sum_{j \in \tilde{\mathcal{G}}^{W,new}} \rho_j^W = 1.$$

It also requires two additional updates in equations (4.4),(4.5) where we have to replace decisions $P_j^{\tilde{G},max}$ with values from equation (4.33).

Furthermore, the coefficients $e_{l+1,t}^2$ and $e_{l+1,t}^3$ in the linear approximation of the recourse function undergo a change in both dimension and value. Consequently, the slope of the total new capacity for a given renewable source equals the weighted average of the slopes of individual capacities, with respective weights ρ^S and ρ^W:

$$e_{(l+1),t-1}^2 = \sum_{\omega_t \in \Omega_t} \Pi_{t-1}(\omega_{t-1}, \omega_t) \left(\sum_{i \in [l]} \nu_{i,t} e_{i,t}^2 - \sum_{j \in \tilde{\mathcal{G}}^{S,new}} \rho_j^S \sum_{h \in \mathcal{H}} (\lambda_{\tilde{k}(j),ht} + \tau_t) \xi_{ht}^S \right)$$

$$e_{(l+1),t-1}^3 = \sum_{\omega_t \in \Omega_t} \Pi_{t-1}(\omega_{t-1}, \omega_t) \left(\sum_{i \in [l]} \nu_{i,t} e_{i,t}^3 \right.$$

$$\left. - \sum_{j \in \tilde{\mathcal{G}}^{W,new}} \rho_j^W \left(\sum_{h \in \mathcal{H}} \frac{1}{\kappa} \sqrt{1 - \kappa^2(\xi_{ht}^W)^2} (\underline{\gamma}_{j,ht}^W + \overline{\gamma}_{j,ht}^W) + \sum_{h \in \mathcal{H}} (\lambda_{\tilde{k}(j),ht} + \tau_t) \xi_{ht}^W \right) \right)$$

Remark 4.6. *The utilization of the simplified model significantly diminishes the dimension of the resource state while still yielding satisfactory results when the weights are appropriately chosen.*

4.4   Case Study

In this section, we present numerical results for the formulated generation expansion planning problem defined for part of the IEEE RTS-GMLC network (Barrows et al. 2020), incorporating random electricity demand and renewable generation. This case study aims to determine the optimal wind, solar, and storage capacities to achieve a targeted share of renewable generation and enable the phase-out of fossil fuels.
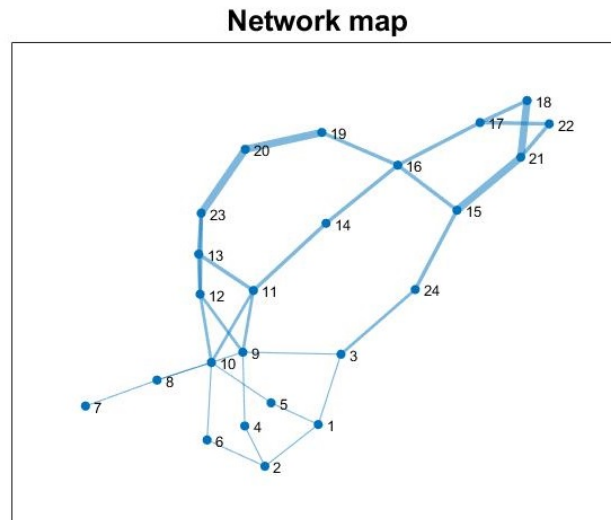

Figure 4.1: Map of connections between buses for the area 1.

The IEEE RTS-GMLC network serves as a comprehensive test case, providing technical parameters of the grid along with one year of demand and renewable generation data for 2020 at an hourly resolution. The network includes 74 buses distributed across three areas. For this numerical experiment, we focus on 24 buses

within area 1 presented in Figure 4.1 where the width of a line connecting buses denotes the flow limit of a line. The existing generation capacities for the area and their distribution across individual buses are depicted and compared to the base load in Figure 4.2. The ratio of the base load of the bus to the total base load of the area is used to distribute the random demand of the area among individual buses. Considering the environmental impact, particularly the high emissions associated with coal power plants, and our commitment to phasing out fossil fuels through the proposed strategy, we exclude them from the network in the calculations.

To model random demand and renewable generation per capacity unit, denoted by ξ, we adopt the approach outlined in Kiszka and Wozabal (2024). This involves identifying seasonal effects by estimation of a LASSO regression model with 10-fold cross-validation and applying Principal Component Analysis (PCA) to the transformed residuals. Subsequently, scenarios for the random process are generated using the resampling method and reverse procedure. Employing these scenarios, we construct a scenario lattice with 50 nodes per stage using the stochastic gradient descent method described in Löhndorf and Wozabal (2021b), which is provided in the library Quasar.

4.4.1   Optimization Parameters

In the presented case study, we examine the simplified model of the formulated expansion problem where the investment decisions in the first stage involve the storage capacity at predefined buses and the total renewable capacity built for wind and solar power generation. Subsequent stages address operational planning for the network over a one-week horizon, with $t \in \mathcal{T} = \{1, 2, \ldots, 7\}$ representing individual days and $h \in \mathcal{H} = \{1, 2, \ldots, 24\}$ denoting each hour within a day.

The investment decisions require selecting specific buses where both storage and renewable capacity will be installed in addition to the existing generation capacities. Based on the network map presented in Figure 4.1 and existing generation capacities

compared in Figure 4.2, we choose the buses $1, 13, 21$ as candidates to build the storage capacity. We additionally assume that the storage efficiency, denoted by η, is set at 0.9 and that the storage is initially filled to 50% capacity, with the requirement to maintain this level by the end of the period.
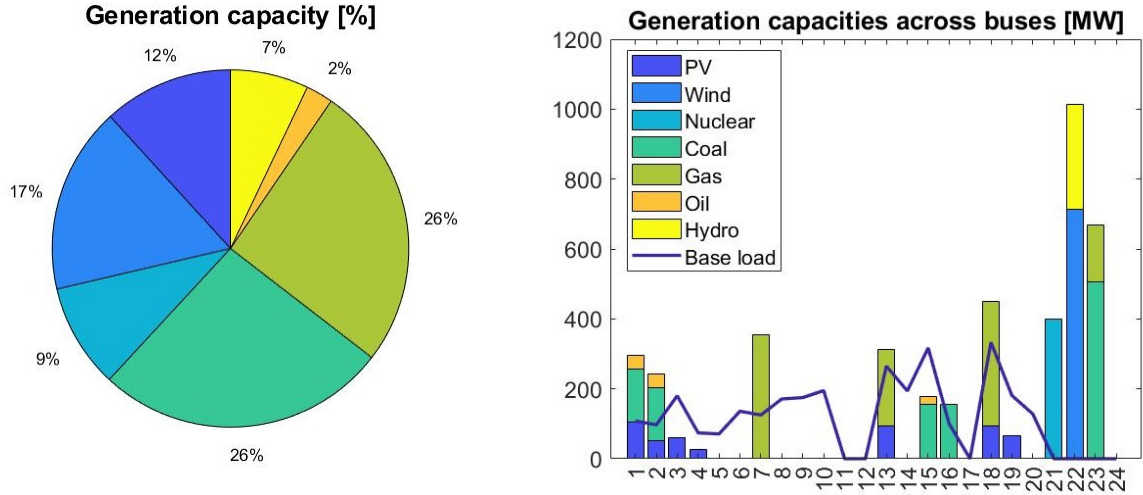

Figure 4.2: The left graph presents the original generation capacities in the network for area 1, and the right plot shows the distribution of generation capacities across individual buses in comparison to the base load.

In the renewable generation expansion, our primary focus lies on extending the existing capacities of solar and wind power plants depicted in Figure 4.2. We consider buses $1, 2, 4, 13$ as potential candidates for solar capacity installation, as they exhibit the highest ratio of generated power to the existing capacity based on the historical data. As the simplified model provides the total new solar capacity as the investment decision, we assume it will be distributed among selected candidates in proportion to the existing solar capacity at those buses.

Given that only one wind power plant is in this network, the investment decision determines the new capacity installed at bus 22. Additionally, we assume the charge-ability factor denoted by κ to be equal to 0.9.

Running the case study requires the configuration of the specific parameters ap-

Table 4.1: Parameters of investment decisions

Source	Cost ($/MW)	Candidate buses	Existing capacity (MW)
Storage	230	1,13,21	0
PV	2149	1,2,4,13	498.1
Wind	2182	22	713.5

pearing in the optimization problem, such as the costs associated with the respective decisions. To estimate the cost of storage capacity, we rely on projections from Cole and Frazier (2020), forecasting a cost of $208/kW for grid-level battery storage. Considering our one-week planning horizon, we scale the cost by calculating annuities based on a $20-$year lifetime and a 2% interest rate. Consequently, we arrive at a weekly investment cost of $230/MW, assuming a year consists of 52 weeks.

Similarly, we estimate the costs of wind and solar capacity by referencing data from the U.S. Energy Information Administration. Accounting for both capacity investment costs and operational and maintenance costs, we scale them by calculating annuities based on the life expectancy of 25 and 30 years for wind and solar, respectively, along with a 2% interest rate. Dividing the results by 52, we obtain a weekly cost of $2182/MW and $2149/MW for wind and solar capacity, respectively.

We introduce the penalty for the curtailment of demand and generation with the cost of $f^{D+} = \$5000$/MWh and $f^{D-} = \$500$/MWh, respectively, indicating that it is more expensive to curtail load than supply. Additionally, our aim is to convince the decision-maker to invest in renewable energy sources and storage capacities instead of using fossil fuels to achieve a specified share of renewable generation covering daily demand. We integrate this objective in the problem formulation by assuming that any shortfall in meeting the target incurs a penalty, with the cost of $f^{TR} = \$50$ for each MWh.

4.4.2   Numerical Results

In order to solve the case study, we implemented the SDDP algorithm in MAT-LAB 2021b using YALMIP (Löfberg 2004) to formulate the presented optimization problem and the solver MOSEK 9.3.11 for execution. The algorithm was run with the increased number of scenarios in forward passes to 100 every fifth iteration. The number of iterations was established based on the convergence check, ensuring that the difference between the upper and lower bound constitutes less than 5% of the lower bound. The experiment was run on a private computer, DELL Precision 5520, with the Intel(R) Core(TM) i7-7820HQ CPU@2.90GHz processor, and installed RAM memory of 32GB.
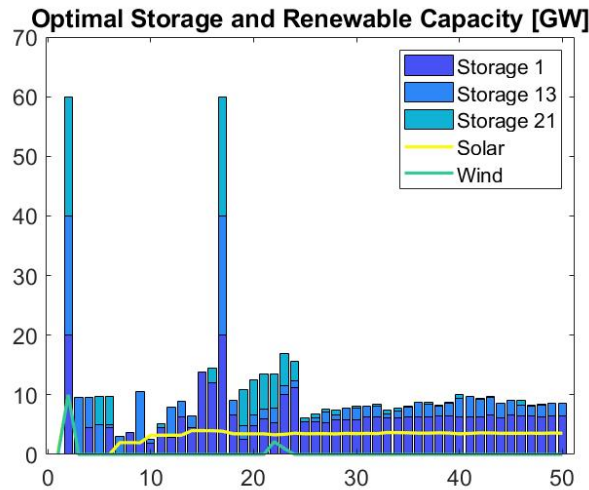

Figure 4.3: Evolution of optimal renewable and storage capacities for the 29th week of the year and renewable target of 55% over the algorithm iterations.

At the beginning, we assess the performance of the algorithm for the defined generation expansion planning problem. Figure 4.3 illustrates the evolution of the optimal renewable and storage capacities for the 29th week of the year alongside a renewable target of 55%, enabling a comparison of solution change over iterations. Notably, we observe the stabilization of the optimal solution after 30 iterations, which is remarkable given the complexity of the problem. It demonstrates that

the applied solution strategy is appropriate for the specified problem and exhibits strong convergence properties. In this case, the optimal solution recommends no investment in the extension of the wind power capacity, and the reason for this can include the price difference between wind and solar capacity as well as the lack of demand at the candidate bus and its neighboring buses.

We observed distinct seasonal patterns by analyzing the network's historical data on demand and renewable generation. Therefore, we have decided to assess the influence of seasons on investment decisions, selecting two weeks for analysis: the 7th and 29th week of the year representing diverse weather conditions. Furthermore, we explore the impact of the minimum daily renewable generation requirement on optimal renewable and storage capacity, considering targets from 40% to 90% every 5%.
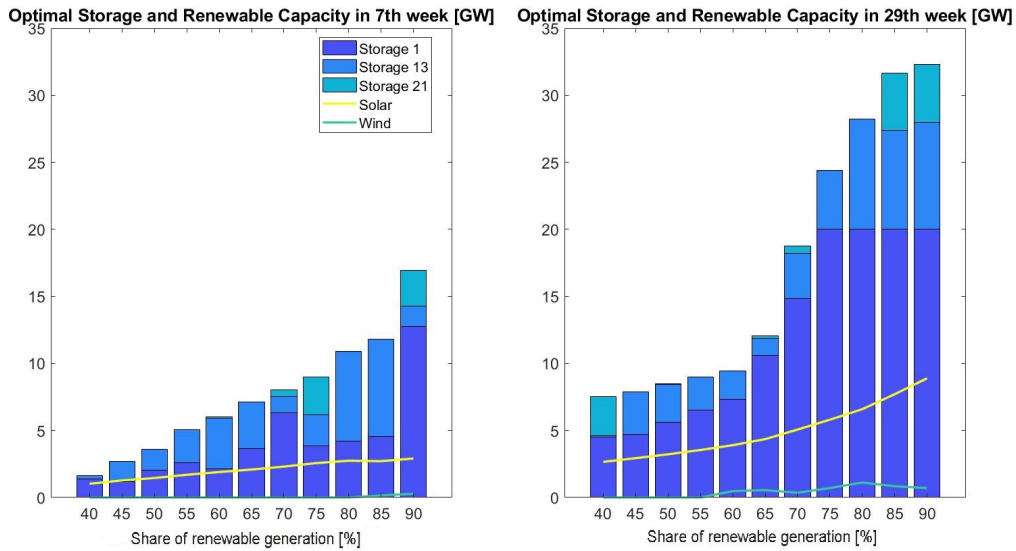
Figure 4.4: Comparison of optimal renewable and storage capacities for the 7th and the 29th week of the year.

The comparison of optimal capacities for the considered settings is illustrated in Figure 4.4. A noticeable disparity in investment decisions between the 7th and 29th week of the year highlights the significant impact of varying weather conditions on the outcomes. The approach to addressing this divergence could involve using the

solution for the 29th week, which is the maximum of both solutions or averaging the optimal solutions based on the probabilities of each week's pattern occurring.

In addition, the preference for solar over wind power plants can be observed mainly due to slightly lower costs. However, the number of investigated locations and the base load values of candidate buses can also influence those decisions. Furthermore, a strong dependence between investment decisions on storage and renewable capacity can be noticed, as the storage candidate buses near extended solar power generation are more desirable.

4.5   Conclusions

In the paper, we propose the first multi-stage stochastic formulation of the generation expansion planning problem, which accounts for the uncertainty of power demand and renewable generation as well as the AC nature of the power system. In order to solve the problem, we apply the strategy proposed in Kiszka and Wozabal (2024) and present a detailed and extensive explanation of the particular steps of the procedure.

In the numerical example of optimal renewable expansion and storage integration for the IEEE RTS-GMLC network, we demonstrate the computational tractability of the applied solution strategy for the generation expansion problems. Furthermore, the presented case study illustrates the relevance of the formulated problem for governments and communities that are going to actively participate in the transition to a low-carbon energy future and phase out fossil fuels. The model can support decision-makers by indicating the optimal direction of changes in the power infrastructure to achieve the minimum daily renewable generation requirement.

Analysis of the results indicates a notable impact of the weather conditions, represented by seasons, on investment decisions. In future work, it would be interesting to build a model that accounts for different seasons without solving the optimization

problem for the horizon of the year, which would be computationally very costly or even intractable.

Furthermore, a comparison of investment decisions obtained from simplifications commonly used in the literature (e.g. assumption of DC power system or representation of the random process using scenario tree instead of scenario lattice) would allow us to assess the advantage of the proposed generation expansion planning model.

Additionally, it would be interesting to extend the proposed framework by including the transmission expansion, which is also relevant to the energy transition. It would give a more detailed overview of the network capabilities and could potentially result in the development of costly competitive investment strategies.

Chapter 5

Conclusions

This doctoral thesis proposes a framework to effectively solve energy planning problems under uncertainty that involve power flow constraints. It covers the whole modeling chain from the approximation of random processes through the modeling of power flow problems to the solution strategy for the optimization problem. The research thus incorporates three important components simultaneously: multistage formulation, finitely supported Markov structure of random processes, and the alternating current nature of power flows.

In Chapter 2, I introduce a lattice distance, which is a semi-metric defined for Markov processes involved in multi-stage linear stochastic optimization problems. The distance takes into account not only the structure of the processes but also the data of the optimization problem. It allows for the derivation of quantitative stability results for problems with randomness in both objective functions and constraints.

The lattice distance can be used to find a discrete approximation of the Markov process involved in the linear optimization problem. The metric then provides a bound for the difference between optimal values of the original and the approximated problem and thus enables the bounding of the error introduced by replacing the original process with its discrete approximation. Solving the optimization problem for the approximation process decreases the complexity and improves the com-

putational tractability of the problem, and simultaneously can offer a high-quality solution.

The evaluation of how two Markov processes impact the optimal value of the optimization problem can be examined with the lattice distance. The metric enables comparing two Markov processes, but it doesn't guarantee obtaining the optimal approximation. In order to find an optimal approximation of the Markov process within a specified margin of error, further steps are required.

While determining the optimal approximation of a given distribution generally poses a nonconvex and nondifferentiable problem, there are different algorithmic approaches for achieving optimal quantization. These include stochastic gradient descent, stochastic approximation methods, and stochastic branch-and-bound techniques (see Bally and Pagès 2003a,b, Hochreiter and Pflug 2007, Pflug and Pichler 2015). In further research, the newly proposed distance could be integrated into existing algorithms to enhance scenario generation methods for Markov processes involved in linear optimization problems.

Additionally, optimal approximations and convergence rates have been established for Wasserstein metrics Graf and Luschgy (2000), suggesting analogous outcomes can be demonstrated for the introduced lattice distance.

In regard to energy planning problems where the demand and renewable generation can be modeled as Markov processes in many applications, the lattice distance can be employed to obtain a finitely supported representation of those processes. As the metric is defined for linear optimization problems and energy planning models incorporating AC OPF are nonconvex, the linear relaxation of the model (e.g. DC relaxation) can be applied to establish a discrete approximation of the Markov processes.

In Chapter 3, I propose an effective solution strategy for multi-stage stochastic optimal power flow problems in AC power systems where the Markov processes are employed to represent the uncertainty. The solution approach uses recent advances

in convex relaxations of OPF problems and the stochastic dynamic dual programming algorithm for Markovian optimization problems.

To facilitate the practical implementation of the proposed algorithm, I offer an in-depth explanation of the power flow dynamics and key components inherent in the AC OPF problem, such as the admittance matrix and phase-shifting transformers. Furthermore, I thoroughly describe the steps of the convex relaxation of the OPF problem, including reformulation, relaxation, and dualization, to ensure the applicability of the model across various energy planning problems. In addition, I provide a methodology for recovering a physically feasible solution in the event that the relaxation of the OPF problem is not exact.

The convergence properties of the algorithm are demonstrated in the case study on the storage siting, sizing, and operation for the widely utilized IEEE RTS-GMLC power network. Following the presented steps enables the application of the algorithm to solve other energy planning problems.

In future research, extending the model to incorporate unit commitment decisions could be explored and followed by an investigation into the performance of the proposed algorithm within this framework. For example, Fattahi et al. (2017) propose a semi-definite programming relaxation of unit commitment, which could be applied to the extended model. In the literature, Lara et al. (2020) introduce a multi-stage stochastic mixed-integer programming model to optimize generation expansion planning and apply stochastic dual dynamic integer programming (SD-DiP) algorithm to solve the problem. However, they don't take into account the alternating current nature of power flow and eventually consider a scenario tree as a representation of the random process. Hence, there remains a gap in the existing research that requires further contributions.

Moreover, a comparison of the algorithm's performance under various relaxation techniques could yield valuable insights. Systematical evaluation of the algorithm's effectiveness across different relaxation methods could provide a deeper understand-

ing of its robustness, efficiency, and suitability for diverse optimization scenarios.

In Chapter 4, I formulate a generation expansion planning model in order to find an optimal renewable and storage capacity required to phase out fossil fuels. The model aims to support decision-makers in the transition of the power network towards cleaner energy sources by providing optimal investment decisions.

The proposed model considers the uncertainty of demand and renewable generation as well as the physics of alternating current power flow, contributing to the research field addressing generation expansion planning problems. Moreover, it incorporates minimum daily renewable generation requirement to ensure that the future policy targets are met through the optimal investment plan.

I use the advances from Chapter 3 to solve the formulated generation expansion planning problem for the modified version of IEEE RTS GMLC network. Thereby, the presented case study demonstrates the importance and applicability of the model proposed in Chapter 3 to a wide range of energy planning problems.

The examination of the findings suggests that there is potential for improvement, given the notable impact of the weather conditions on investment decisions. In future investigations, creating a model that accounts for various seasons without significantly extending the time horizon could provide meaningful insights.

Furthermore, expanding the model to incorporate transmission expansion would enable a more comprehensive analysis of the network's capabilities. By considering the expansion of transmission infrastructure, the model can assess the system's ability to effectively accommodate future growth and changes in demand. Additionally, it would facilitate a better understanding of how potential expansions or upgrades to transmission lines can improve the overall performance and reliability of the energy system.

In conclusion, this thesis explores Markovian stochastic optimization formulations within energy planning contexts. The subsequent chapters present methodologies designed to handle the complexities of the proposed model. Firstly, an approach

is introduced to derive a discrete approximation of the Markov process involved in the optimization problem. Subsequently, an effective solution strategy is outlined to ensure the attainment of a reliable solution. Finally, the performance of the proposed algorithm is demonstrated through its application to the generation expansion planning problem. By systematically addressing the challenges posed by multi-stage stochastic optimization in energy planning, this research contributes to advancing the field and provides valuable insights for both future academic studies and practical applications.

Bibliography

A. Afful-Dadzie, E. Afful-Dadzie, I. Awudu, and J. Banuro. Power generation capacity planning under budget constraint in developing countries. *Applied Energy*, 188:71–82, 2017.

M. Andersen, A. Hansson, and L. Vandenberghe. Reduced-complexity semidefinite relaxations of optimal power flow problems. *IEEE Transactions on Power Systems*, 29(4): 1855–1863, 2014.

A. Attarha, N. Amjady, and A. Conejo. Adaptive robust ac optimal power flow considering load and wind power uncertainties. *International Journal of Electrical Power & Energy Systems*, 96:132–142, 03 2018.

H. Attouch and R. J.-B. Wets. A convergence theory for saddle functions. *Transactions of the American Mathematical Society*, 280(1):1–41, 1983.

W. Bai, D. Lee, and K. Lee. Stochastic dynamic ac optimal power flow based on a multivariate short-term wind power scenario forecasting model. *Energies*, 10(12), 2017.

K. Baker, G. Hug, and X. Li. Energy storage sizing taking into account forecast uncertainties and receding horizon operation. *IEEE Transactions on Sustainable Energy*, 8(1):331–340, 2017.

V. Bally and P. Pagès. A quantization algorithm for solving discrete time multi-dimensional optimal stopping problems. *Bernoulli*, 9(6):1003–1049, 2003a.

V. Bally and P. Pagès. Error analysis of the quantization algorithm for obstacle problems. *Stochastic Processes & Their Applications*, 106(1):1–40, 2003b.

C. Barrows, A. Bloom, A. Ehlen, J. Ikäheimo, J. Jorgenson, D. Krishnamurthy, J. Lau,

B. McBennett, M. O'Connell, E. Preston, A. Staid, G. Stephen, and J. Watson. The IEEE reliability test system: A proposed 2019 update. *IEEE Transactions on Power Systems*, 35(1):119–127, 2020.

R. Bent, G. L. Toole, and A. Berscheid. Transmission network expansion planning with complex power flow models. *IEEE Transactions on Power Systems*, 27(2):904–912, 2011.

D. Bertsekas. *Abstract Dynamic Programming.* Athena Scientific, 2013.

D. Bertsekas and S. Shreve. *Stochastic Optimal Control: The Discrete Time Case.* Mathematics in science and engineering. Academic Press, 1978. ISBN 9780120932603.

D. Bienstock and G. Muñoz. On linear relaxations of opf problems. *arXiv preprint arXiv:1411.1120.*, 2014.

D. Bienstock and A. Verma. Strong np-hardness of ac flows feasibility. *Operations Research Letters*, 47(6):494–501, 2019.

D. Bienstock, M. Chertkov, and S. Harnett. Chance-constrained optimal power flow: risk-aware network control under uncertainty. *SIAM Review*, 56(3):461–495, 2014.

C. Bingane, M. Anjos, and S. Le Digabel. Conicopf: Conic relaxations for ac optimal power flow computations. In *Proceedings of the IEEE PES General Meeting 2021.* IEEE PES, 2021.

J. Birge and F. Louveaux. *Introduction to Stochastic Programming.* Springer Series in Operations Research and Financial Engineering. Springer New York, 2011.

R. R. Booth. Optimal generation planning considering uncertainty. *IEEE Transactions on Power Apparatus and Systems*, PAS-91(1):70–77, 1972.

N. Bourbaki, H. G. Eggleston, and S. Madan. *Topological Vector Spaces.* Éléments de mathématique. Springer-Verlag, 1987.

M. Broadie and P. Glasserman. A stochastic mesh method for pricing high-dimensional american options. *Journal of Computational Finance 7*, 7(4):35–72, 2004.

M. Bucciarelli, S. Paoletti, and A. Vicino. Optimal sizing of energy storage systems under uncertain demand and generation. *Applied Energy*, 225:611–621, 2018.

W. Bukhsh, A. Grothey, K. McKinnon, and P. Trodden. Local solutions of the optimal power flow problem. *IEEE Transactions on Power Systems*, 28(4):4780–4788, 2013b.

C. Bussar, M. Moos, R. Alvarez, P. Wolf, T. Thien, H. Chen, Z. Cai, M. Leuthold, D. Sauer, and A. Moser. Optimal allocation and capacity of energy storage systems in a future european power system with 100% renewable energy generation. *Energy Procedia*, 46:40–47, 2014.

G. Byon, P. Van Hentenryck, R. Bent, and H. Nagarajan. Communication-constrained expansion planning for resilient distribution systems. *INFORMS Journal on Computing*, 32(4):968–985, 2020.

M. Carpentier. Contribution a l erude du dispatching economique. *Bull. de la Soc. Fran. des Elec.*, 8:431–447, 1962.

M. S. Casey and S. Sen. The scenario generation algorithm for multistage stochastic linear programming. *Mathematics of Operations Research*, 30:615–631, 2005.

Y.-H. Chang and M.-S. Lee. Incorporating markov decision process on genetic algorithms to formulate trading strategies for stock markets. *Applied Soft Computing*, 52:1143–1153, 2017. ISSN 1568-4946.

C. Chen, A. Atamtürk, and S. Oren. Bound tightening for the alternating current optimal power flow problem. *IEEE Transactions on Power Systems*, 31(5):3729–3736, 2016.

C. S. Chow and J. N. Tsitsiklis. An optimal one-way multigrid algorithm for discrete-time stochastic control. *IEEE Transactions on Automatic Control*, 36(8):898–914, 1991.

C. Coffrin and P. Van Hentenryck. A linear-programming approximations of ac power flows. *INFORMS Journal on Computing*, 26(4):718–734, 2014.

C. Coffrin, H. Hijazi, and P. Van Hentenryck. The qc relaxation: A theoretical and computational study on optimal power flow. *IEEE Transactions on Power Systems*, 31(4):3008–3018, 2016.

C. Coffrin, H. Hijazi, and P. Van Hentenryck. Strengthening the sdp relaxation of ac power flows with convex envelopes, bound tightening, and valid inequalities. *IEEE Transactions on Power Systems*, 32(5):3549–3558, 2017.

W. Cole and A. Frazier. Cost Projections for Utility-Scale Battery Storage: 2020 Update. Technical report, National Renewable Energy Laboratory, 2020.

S. Dehghan, N. Amjady, and A. Conejo. Reliability-constrained robust power system expansion planning. *IEEE Transactions on Power Systems*, 31(3):2383–2392, 2016.

R. Diewvilai and K. Audomvongseree. Generation expansion planning with energy storage systems considering renewable energy generation profiles and full-year hourly power balance constraints. *Energies*, 14(18), 2021.

S. Dolecki, G. Salinetti, and R. J. B. Wets. Convergence of functions: Equi-semicontinuity. *Transactions of the American Mathematical Society*, 276(1):409–429, 1983.

F. Dufour and T. Prieto-Rumeau. Approximation of markov decision processes with general state space. *Journal of Mathematical Analysis and Applications*, 388(2):1254 – 1267, 2012.

F. Dufour and T. Prieto-Rumeau. Finite linear programming approximations of constrained discounted markov decision processes. *SIAM Journal on Control and Optimization*, 51(2):1298–1324, 2013.

F. Dufour and T. Prieto-Rumeau. Approximation of average cost markov decision processes using empirical distributions and concentration inequalities. *Stochastics*, 87 (2):273–307, 2015.

J. Dupacová, G. Consigli, and S. W. Wallace. Scenarios for multistage stochastic programs. *Annals of Operations Research*, 100:25–53, 2000.

J. Dupacová, N. Gröwe-Kuska, and W. Römisch. Scenario reduction in stochastic programming an approach using probability metrics. *Mathematical Programming, Series B*, 95(3):493–511, 2003.

N. C. P. Edirisinghe. Bound-based approximations in multistage stochastic programming: Nonanticipativity aggregation. *Annals of Operations Research*, 85:103–127, 1996.

S. Fattahi, M. Ashraphijuo, J. Lavaei, and A. Atamtürk. Conic relaxations of the unit commitment problem. *Energy*, 134:1079–1095, 2017.

H. Föllmer and A. Schied. *Stochastic Finance: An Introduction in Discrete Time*. De Gruyter studies in mathematics. Walter de Gruyter, 2004.

B. Fox. Finite-state approximations to denumerable-state dynamic programs. *Journal of Mathematical Analysis and Applications*, 34(3):665 – 670, 1971.

S. Frank and S. Rebennack. An introduction to optimal power flow: Theory, formulation, and examples. *IIE Transactions*, 48(12):1172–1197, 2016.

S. Frank, I. Steponavice, and S. Rebennack. Optimal power flow: a bibliographic survey i. *Energy systems*, 3(3):221–258, 2012a.

S. Frank, I. Steponavice, and S. Rebennack. Optimal power flow: a bibliographic survey ii. *Energy systems*, 3(3):259–289, 2012b.

K. Frauendorfer. Barycentric scenario trees in convex multistage stochastic programming. *Mathematical Programming*, 75:277–293, 1996.

C. Füllner and S. Rebennack. Stochastic dual dynamic programming and its variant - a review. *Optimization Online*, 2023. URL `https://optimization-online.org/?p=16920`.

W. Gil-González, O. D. Montoya, L. F. Grisales-Noreña, A.-J. Perea-Moreno, and Q. Hernandez-Escobedo. Optimal placement and sizing of wind generators in ac grids considering reactive power capability and wind speed curves. *Sustainability*, 12 (7), 2020.

P. Girardeau, V. Leclere, and A. B. Philpott. On the convergence of decomposition methods for multistage stochastic convex programs. *Mathematics of Operations Research*, 40(1):130–145, 2015.

J. Glover, M. Sarma, and T. Overbye. *Power system analysis and design*. Australia: Thomson, 2008.

S. Graf and H. Luschgy. *Foundations of quantization for probability distributions*. Springer, 2000.

O. J. Guerra, D. A. Tejada, and G. V. Reklaitis. An optimization framework for the integrated planning of generation and transmission expansion in interconnected power systems. *Applied energy*, 170:1–21, 2016.

N. Gupta, R. Shekhar, and P. Kalra. Computationally efficient composite transmission

expansion planning: A pareto optimal approach for techno-economic solution. *International Journal of Electrical Power & Energy Systems*, 63:917–926, 2014.

G. Hanasusanto, D. Kuhn, and W. Wiesemann. A comment on "computational complexity of stochastic programming problems". *Mathematical Programming*, 159(1):557–569, Sep 2016.

Y. He, L. Xing, Y. Chen, W. Pedrycz, L. Wang, and G. Wu. A generic markov decision process model and reinforcement learning method for scheduling agile earth observation satellites. *IEEE Transactions on Systems, Man, and Cybernetics: Systems*, 52 (3):1463–1474, 2022.

H. Heitsch and W. Römisch. Scenario reduction algorithms in stochastic programming. *Computational Optimization and Applications*, 24(2-3):187–206, 2003.

H. Heitsch and W. Römisch. Scenario tree modeling for multistage stochastic programs. *Mathematical Programming*, 118:371–406, 2009.

H. Heitsch and W. Römisch. Stability and scenario trees for multistage stochastic programs. *International series in Operations Research & Management Science*, 150: 139–164, 2011.

H. Heitsch, W. Römisch, and C. Strugarek. Stability of multistage stochastic programs. *SIAM Journal on Optimization*, 17:511–525, 2006.

N. Helistö, J. Kiviluoma, J. Ikäheimo, T. Rasku, E. Rinne, C. O'Dwyer, R. Li, and D. Flynn. Backbone—an adaptable energy systems modelling framework. *Energies*, 12(17):3388, 2019.

R. Hemmati, H. Saboori, and M. Jirdehi. Multistage generation expansion planning incorporating large scale energy storage systems and environmental pollution. *Renewable Energy*, 97:636–645, 2016.

R. Hemmati, H. Saboori, and P. Siano. Coordinated short-term scheduling and long-term expansion planning in microgrids incorporating renewable energy resources and energy storage systems. *Energy*, 134:699–708, 2017.

C. Heuberger, E. Rubin, I. Staffell, N. Shah, and N. Mac Dowell. Power capacity expansion

planning considering endogenous technology cost learning. *Applied Energy*, 204:831–845, 2017.

K. Hinderer. Lipschitz continuity of value functions in markovian decision processes. *Mathematical Methods of Operations Research*, 62(1):3–22, Sep 2005.

V. Hinojosa and J. Velasquez. Improving the mathematical formulation of security-constrained generation capacity expansion planning using power transmission distribution factors and line outage distribution factors. *Electric Power Systems Research*, 140:391–400, 06 2016.

L. Hirth. The optimal share of variable renewables: how the variability of wind and solar power affects their welfare-optimal deployment. *The Energy Journal*, 0(1), 2015.

R. Hochreiter and G. Pflug. Financial scenario generation for stochastic multi-stage decision processes as facility location problems. *Annals of Operations Research*, 152: 257–272, 03 2007.

A. Hoffman. On approximate solutions of systems of linear inequalities. *Journal of Research of the National Bureau of Standards, Section B, Mathematical Sciences*, 49(4): 263–265, 1952.

R. A. Horward. *Dynamic Programming and Markov Processes*. MIT Press, 1960.

K. Høyland and S. W. Wallace. Generating Scenario Decision Trees for Multistage Problems. *Management Science*, 47(2):295–307, 2001.

K. Høyland, M. Kaut, and S. W. Wallace. A heuristic for moment-matching scenario generation. *Computational Optimization and Applications*, 24(2):169–185, 2003.

M. Huang, X. Lin, Z. Feng, D. Wu, and Z. Shi. A multi-agent decision approach for optimal energy allocation in microgrid system. *Electric Power Systems Research*, 221, 2023.

Intergovernmental Panel on Climate Change. Global warming of 1.5°c, 2018. `https://www.ipcc.ch/sr15/`.

International Energy Agency. *Status of Power System Transformation 2018*. 2018. URL `https://www.oecd-ilibrary.org/content/publication/9789264302006-en`.

International Renewable Energy Agency. Planning for the renewable fu-

ture,   January   2017a.   `https://www.irena.org/publications/2017/Jan/`
`Planning-for-the-renewable-future-Long-term-modelling-and-tools-to-expand-variable-r`

International Renewable Energy Agency. Renewable energy: A key climate solution,
November 2017b.

International Renewable Energy Agency. Power system flexibility for the energy transition,
November 2018.

International Renewable Energy Agency.   Renewable power generation costs
in   2020,   June   2021a.   `https://www.irena.org/Publications/2021/Jun/`
`Renewable-Power-Costs-in-2020`.

International Renewable Energy Agency.   World energy transitions outlook: 1.5°c
pathway, March 2021b.   `https://www.irena.org/publications/2021/March/`
`World-Energy-Transitions-Outlook`.

R. Jabr. Radial distribution load flow using conic programming. *IEEE Transactions on
Power Systems*, 21(3):1458–1459, 2006.

C. Josz, J. Maeght, P. Panciatici, and J. Gilbert. Application of the moment-sos approach
to global optimization of the opf problem. *IEEE Transactions on Power Systems*, 30
(1):463–470, 2015.

L. Kantorovich. On the translocation of masses. *C.R. Acad. Sci. URSS*, 1(37):199–201,
1942.

M. Kaut. Scenario generation by selection from historical data. *Computational Manage-
ment Science*, 18:411–429, 2021.

M. Kaut and S. W. Wallace. Evaluation of scenario generation methods for stochastic
programming. *Pacific Journal of Optimization*, 3(2):257–271, 2007.

A. Khodaei and M. Shahidehpour. Microgrid-based co-optimization of generation and
transmission planning in power systems. *IEEE Transactions on Power Systems*, 28
(2):1582–1590, 2012.

A. Kiszka and D. Wozabal. A stability result for linear Markovian stochastic optimization
problems. *Mathematical Programming*, 2022.

A. Kiszka and D. Wozabal. Stochastic Dual Dynamic Programming for Optimal Power Flow Problems with Uncertainty. 2024.

A. Kleywegt, A. SHapiro, and T. Homem-de Mello. The sample average approximation method for stohastic discrete optimization. *SIAM Journal of Optimization*, 12:479–502, 2001.

B. Kocuk, S. Dey, and X. Sun. Strong socp relaxations for the optimal power flow problem. *Operations Research*, 64(6):1177–1196, 2016b.

B. Kocuk, S. Dey, and X. Sun. Matrix minor reformulation and socp-based spatial branch-and-cut method for the ac optimal power flow problem. *Mathematical Programming*, pages 557–593, 2018.

N. Koltsaklis and M. Georgiadis. A multi-period, multi-regional generation expansion planning model incorporating unit commitment constraints. *Applied Energy*, 158:310–331, 2015.

N. Koltsaklis, A. Dagoumas, G. Kopanos, and E. Pistikopoulos. A spatial multi-period long-term energy planning model: A case study of the greek power system. *Applied Energy*, 115:456–482, 2014.

D. Kuhn. *Generalized Bounds for Convex Multistage Stochastic Programs*. Springer-Verlag Berlin Heidelberg, 2005.

G. Lan. Complexity of stochastic dual dynamic programming. *Mathematical Programming*, pages 1–38, 2020.

H.-J. Langen. Convergence of dynamic programming models. *Mathematics of Operations Research*, 6(4):493–512, 1981.

C. Lara, D. Mallapragada, D. Papageorgiou, A. Venkatesh, and I. Grossmann. Deterministic electric power infrastructure planning: Mixed-integer programming model and nested decomposition algorithm. *European Journal of Operational Research*, 271(3):1037–1054, 2018.

C. Lara, J. Siirola, and I. Grossmann. Electric power infrastructure planning under uncertainty: stochastic dual dynamic integer programming (sddip) and parallelization scheme. *Optimization and Engingeering*, (21):1243–1281, 2020.

D. Larrahondo, R. Moreno, H. R. Chamorro, and F. Gonzalez-Longatt. Comparative performance of multi-period acopf and multi-period dcopf under high integration of wind power. *Energies*, 14(15), 2021.

J. Lavaei and S. H. Low. Zero duality gap in optimal power flow problem. *IEEE Transactions on Power Systems*, 27(1):92–107, 2012.

J. Löfberg. Yalmip : A toolbox for modeling and optimization in matlab. In *In Proceedings of the CACSD Conference*, Taipei, Taiwan, 2004.

N. Löhndorf and D. Wozabal. Gas storage valuation in incomplete markets. *European Journal of Operational Research*, 280(1):318 – 330, 2021a.

N. Löhndorf and D. Wozabal. A Second-Order Gradient Descent Algorithm for the Discretization of Markov Processes in Stochastic Optimization. Submitted, 2021b.

N. Löhndorf, D. Wozabal, and S. Minner. Optimizing trading decisions for hydro storage systems using approximate dual dynamic programming. *Operations Research*, 61(4): 810–823, 2013.

F. López-Ramos, S. Nasini, and M. Sayed. An integrated planning model in centralized power system. *European Journal of Operational Research*, 287(1):361–377, 2020.

S. Low. Convex relaxation of optimal power flow part i: Formulations and equivalence. *IEEE Transactions on Control of Network Systems*, 1(1):15–27, 2014a.

S. Low. Convex relaxation of optimal power flow part ii: Exactness. *IEEE Transactions on Control of Network Systems*, 1(2):177–189, 2014b.

R. Madani, S. Sojoudi, and J. Lavaei. Convex relaxation for optimal power flow problem: mesh networks. *IEEE Transactions on Power Systems*, 30(1):199–211, 2015b.

J. Marley, D. Molzahn, and I. Hiskens. Solving multiperiod opf problems using an ac-qp algorithm initialized with an socp relaxation. *IEEE Transactions on Power Systems*, 32(5):3538–3548, 2017.

P. Massé and R. Gibrat. Application of linear programming to investments in the electric power industry. *Management Science*, 3:149–166, 1957.

O. Mégel, G. Andersson, and J. L. Mathieu. Reducing the computational effort of stochas-

tic multi-period dc optimal power flow with storage. *2016 Power Systems Computation Conference (PSCC)*, pages 1–7, 2016.

R. Meise, D. Vogt, and M. S. Ramanujan. *Introduction to Functional Analysis*. Clarendon Press, 1997.

M. Miletić, H. Pandžić, and D. Yang. Operating and investment models for energy storage systems. *Energies*, 13(18), 2020.

S. Misra, D. Molzahn, and K. Dvijotham. Optimal adaptive linearizations of the ac power flow equations. In *2018 Power Systems Computation Conference (PSCC)*, pages 1–7. IEEE, 2018.

D. Molzahn and I. Hiskens. Sparsity-exploiting moment-based relaxations of the optimal power flow problem. *IEEE Transactions on Power Systems*, 30(6):3168–3180, 2015c.

D. Molzahn and I. Hiskens. A survey of relaxations and approximations of the power flow equations. *Foundations and Trends in Electric Energy Systems*, 4(1-2):1–221, 2019.

D. Molzahn, J. Holzer, B. Lesieutre, and C. DeMarco. Implementation of a large-scale optimal power flow solver based on semidefinite programming. *IEEE Transactions on Power Systems*, 28(4):3987–3998, 2013.

A. Moreira, D. Pozo, A. Street, E. Sauma, and G. Strbac. Climate-aware generation and transmission expansion planning: A three-stage robust optimization approach. *European Journal of Operational Research*, 2021.

A. Müller. How does the value function of a markov decision process depend on the transition probabilities? *Mathematics of Operations Research*, 22(4):872–885, 1997.

K. Natarajan, D. Shi, and K.-C. Toh. A penalized quadratic convex reformulation method for random quadratic unconstrained binary optimization. *Optimization Online*, pages 1–26, 2013.

N. Neshat and M. Amin-Naseri. Cleaner power generation through market-driven generation expansion planning: an agent-based hybrid framework of game theory and particle swarm optimization. *Journal of Cleaner Production*, 105:206–217, 2015.

C. Opathella, A. Elkasrawy, A. Adel Mohamed, and B. Venkatesh. Milp formulation for generation and storage asset sizing and sitting for reliability constrained system

planning. *International Journal of Electrical Power & Energy Systems*, 116:105529, 2020.

V. Oree, S. Sayed Hassen, and P. Fleming. Generation expansion planning optimisation with renewable energy integration: A review. *Renewable and Sustainable Energy Reviews*, 69:790–803, 2017.

H. Pandzic, Y. Wang, T. Qiu, Y. Dvorkin, and D. Kirschen. Near-optimal method for siting and sizing of distributed storage in a transmission network. *IEEE Transactions on Power Systems*, 30(5):2288–2300, 2015.

A. Papavasiliou, Y. Mou, L. Cambier, and D. Scieur. Application of stochastic dual dynamic programming to the real-time dispatch of storage under renewable supply uncertainty. *IEEE Transactions on Sustainable Energy*, 9(2):547–558, 2018.

T. Pennanen. Epi-convergent discretizations of multistage stochastic programs. *Mathematics of Operations Research*, 30(1):245–256, 2005.

T. Pennanen. Epi-convergent discretizations of multistage stochastic programs via integration quadratures. *Mathematical Programming*, 116(1-2):461–479, 2009.

M. Pereira and L. Pinto. Multi-stage stochastic optimization applied to energy planning. *Mathematical Programming*, 52(2):359–375, 1991.

J. Peter and J. Wagner. Optimal allocation of variable renewable energy considering contributions to security of supply. *The Energy Journal*, 42, 2021.

G. Pflug and A. Pichler. From empirical observations to tree models for stochastic optimization: Convergence properties. *SIAM Journal on Optimization*, 26(3):1715–1740, 2016.

G. C. Pflug. Scenario tree generation for multiperiod financial optimization by optimal discretization. *Mathematical Programming, Series B*, 89(2):251–271, 2001.

G. C. Pflug and A. Pichler. A distance for multistage stochastic optimization models. *SIAM Journal on Optimization*, 22(1):1–23, 2012.

G. C. Pflug and A. Pichler. *Multistage Stochastic Optimization*. Springer Series in Operations Research and Financial Engineering, 2014.

G. C. Pflug and A. Pichler. Dynamic generation of scenario trees. *Computional Optimization and Applications*, 62(3):641–668, 2015.

G. C. Pflug and W. Römisch. *Modeling, Measuring and Managing Risk*. World Scientific, August 2007.

D. Phan. Lagrange duality and branch-and-bound algorithm for optimal power flow. *Operations Research*, 60(2):275–285, 2012.

A. Philpott and V. de Matos. Dynamic sampling algorithms for multi-stage stochastic programs with risk aversion. *European Journal of Operational Research*, 218(2):470 – 483, 2012.

A. Philpott and Z. Guan. On the convergence of stochastic dual dynamic programming and related methods. *Operations Research Letters*, 36(4):450–455, 2008.

S. Pineda, J. M. Morales, and T. K. Boomsma. Impact of forecast errors on expansion planning of power systems with a renewables target. *European Journal of Operational Research*, 248(3):1113–1122, 2016.

D. Pollard. *A User's Guide to Measure Theoretic Probability*. Cambridge Series in Statistical and Probabilistic Mathematics, 2002.

W. Powell. A unified framework for stochastic optimization. *European Journal of Operational Research*, 275(3):795–821, 2019.

M. L. Puterman. *Markov Decision Processes: Discrete Stochastic Dynamic Programming*. John Wiley & Sons, 1994.

T. Qiu, B. Xu, Y. Wang, Y. Dvorkin, and D. Kirschen. Stochastic multistage coplanning of transmission expansion and energy storage. *IEEE Transactions on Power Systems*, 32(1):643–651, 2017.

D. Quiroga, E. Sauma, and D. Pozo. Power system expansion planning under global and local emission mitigation policies. *Applied Energy*, 239(C):1250–1264, 2019.

Z. Ren and B. Krogh. State aggregation in markov decision processes. In *Proceedings of the 41st IEEE Conference on Decision and Control, 2002.*, volume 4, pages 3819–3824, Dec 2002.

A. Reyes, L. E. Sucar, P. H. Ibargüengoytia, and E. F. Morales. Planning under uncertainty

applications in power plants using factored markov decision processes. *Energies*, 13 (9), 2020.

L. Roald and G. Andersson. Chance-constrained ac optimal power flow: Reformulations and efficient algorithms. *IEEE Transactions on Power Systems*, 33(3):2906–2918, 2018.

S. M. Robinson. Stability theory for systems of inequalities. *SIAM Journal on Numerical Analysis*, 12:754–769, 1975.

W. Römisch and R. Schultz. Stability analysis for stochastic programs. *Annals of Operations Research*, 30:241–266, 1991.

A. W. Rosemberg, A. Street, J. D. Garcia, D. M. Valladão, T. Silva, and O. Dowson. Assessing the cost of network simplifications in long-term hydrothermal dispatch planning models. *IEEE Transactions on Sustainable Energy*, 13(1):196–206, 2021.

N. Saldi, S. Yüksel, and T. Linder. On the asymptotic optimality of finite approximations to markov decision processes with borel spaces. *Mathematics of Operations Research*, 42(4):945–978, 2017.

D. Schetinin. Efficient bound tightening techniques for convex relaxations of ac optimal power flow. *IEEE Transactions on Power Systems*, 34(5):3848–3857, 2019.

G. Schildbach and M. Morari. Scenario-based model predictive control for multi-echelon supply chain management. *European Journal of Operational Research*, 252(2):540–549, 2016.

S. Sethi and G. Sorger. A theory of rolling horizon decision making. *Annals of Operations Research*, 29(1):387–415, 1991.

A. Shapiro. On complexity of multistage stochastic programs. *Operations Research Letters*, 34(1):1–8, 2006.

A. Shapiro. Computational complexity of stochastic programming: Monte carlo sampling approach. *Proceedings of the International Congress of Mathematicians*, pages 2979–2995, 2010.

A. Shapiro. Analysis of stochastic dual dynamic programming method. *Eur J Oper Res*, 209(1):63–72, 2011.

A. Shapiro and A. Nemirovski. *On Complexity of Stochastic Programming Problems*, pages 111–146. Springer US, 2005.

A. Shapiro, D. Dentcheva, and A. Ruszczyński. *Lectures on Stochastic Programming: Modeling and Theory.* MOS-SIAM series on optimization. Society for Industrial and Applied Mathematics, 2009.

J. Shin and J. H. Lee. Mdp formulation and solution algorithms for inventory management with multiple suppliers and supply and demand uncertainty. In K. V. Gernaey, J. K. Huusom, and R. Gani, editors, *12th International Symposium on Process Systems Engineering and 25th European Symposium on Computer Aided Process Engineering*, volume 37 of *Computer Aided Chemical Engineering*, pages 1907–1912. Elsevier, 2015.

J. Skolfield and A. Escobedo. Operations research in optimal power flow: A guide to recent and emerging methodologies and applications. *European Journal of Operational Research*, 2021.

B. Stott, J. Jardim, and O. Alsac. DC Power Flow Revisited. *IEEE Trans. Power Syst.*, 24(3):1290–1300, 2009.

G. Terça and D. Wozabal. Envelope Theorems for Multi-Stage Linear Stochastic Optimization. *Operations Research*, 2020.

United Nations Framework Convention on Climate Change. Paris agreement, Dezember 2015. `https://unfccc.int/sites/default/files/resource/parisagreement_publication.pdf`.

C. Villani. Topics in optimal transportation. *American Mathematical Society*, vol. 58 of Graduate Studies in Mathematics, 2003.

C. Villani. Optimal transport, old and new. *Springer*, vol. 338 of Grundlehren der Mathematischen Wissenschaften, 2009.

D. Walkup and R. J. B. Wets. A lipschitzian characterization of convex polyhedra. *Proceedings of the American Mathematical Society*, 23:167–173, 1969.

W. Wei, J. Wang, N. Li, and S. Mei. Optimal power flow of radial networks and its variations: A sequential convex optimization approach. *IEEE Transactions on Smart Grid*, 8(6):2974–2987, 2017.

D. White. Finite state approximations for denumerable state infinite horizon discounted markov decision processes. *Journal of Mathematical Analysis and Applications*, 74: 292 – 295, 1980.

D. White. Finite state approximations for denumerable state infinite horizon discounted markov decision processes with unbounded rewards. *Journal of Mathematical Analysis and Applications*, 86(1):292 – 306, 1982.

B. K. Williams. Markov decision processes in natural resources management: Observability and uncertainty. *Ecological Modelling*, 220(6):830–840, 2009.

S. Wogrin and D. Gayme. Optimizing storage siting, sizing, and technology portfolios in transmission-constrained networks. *IEEE Transactions on Power Systems*, 30(6): 3304–3313, 2015.

D. Wu, D. Molzahn, B. Lesieutre, and K. Dvijotham. A deterministic method to identify multiple local extrema for the ac optimal power flow problem. *IEEE Transactions on Power Systems*, 33(1):654–668, 2018a.

P. Xiong and C. Singh. Optimal planning of storage in power systems integrated with wind power generation. *IEEE Transactions on Sustainable Energy*, 7(1):232–240, 2016.

H. Yang and H. Nagarajan. Optimal power flow in distribution networks under n-1 disruptions: A multistage stochastic programming approach. *INFORMS Journal on Computing*, 2021.

Y. Zhang, S. Shen, and J. Mathieu. A integrated source-grid-load planning model at the macro level: Case study for china's power sector. *Energy*, 126:231–246, 2017.

F. Zohrizadeh, C. Josz, M. Jin, R. Madani, J. Lavaei, and S. Sojoudi. A survey on conic relaxations of optimal flow problem. *European Journal of Operational Research*, 287 (2):391–409, 2020.

Appendix A

Proofs

A.1 Proof of Lemma 3.1

We start by noting that for any vector $x \in \mathbb{R}^n$ and matrix $A \in \mathbb{R}^{n \times n}$ the following holds

$$x^\top A x = x^\top \left(\frac{2A}{2} \right) x = \frac{x^\top A x + x^\top A x}{2} = \frac{x^\top A x + x^\top A^\top x}{2} = x^\top \left(\frac{A + A^\top}{2} \right) x.$$

(A.1)

We also note that for a matrix $A \in \mathbb{C}^{n \times n}$ and a vector $y \in \mathbb{C}^n$, we have

$$Ay = (\mathfrak{Re}(A) + i\mathfrak{Im}(A))(\mathfrak{Re}(y) + i\mathfrak{Im}(y))$$

$$= (\mathfrak{Re}(A)\mathfrak{Re}(y) - \mathfrak{Im}(A)\mathfrak{Im}(y)) + i(\mathfrak{Re}(A)\mathfrak{Im}(y) + \mathfrak{Im}(A)\mathfrak{Re}(y))$$

By (A.1), this implies that

$$\widetilde{Ay} = \begin{pmatrix} \mathfrak{Re}(A) & -\mathfrak{Im}(A) \\ \mathfrak{Im}(A) & \mathfrak{Re}(A) \end{pmatrix} \tilde{y} \quad \text{and} \quad \mathfrak{Re}(y^H A y) = \tilde{y}^\top \begin{pmatrix} \mathfrak{Re}(A) & -\mathfrak{Im}(A) \\ \mathfrak{Im}(A) & \mathfrak{Re}(A) \end{pmatrix} \tilde{y} = \tilde{y}^\top \mathbb{A} \tilde{y},$$

(A.2)

which is what we used to prove in the formula for real power in Section 3.2.4.

Turning to injected imaginary power, we obtain for similar reasons

$$\mathfrak{Im}(y^H A y) = \tilde{y}^\top \begin{pmatrix} \mathfrak{Im}(A) & \mathfrak{Re}(A) \\ -\mathfrak{Re}(A) & \mathfrak{Im}(A) \end{pmatrix} \tilde{y} = -\tilde{y}^\top \tilde{\mathbb{A}} \tilde{y} \qquad (A.3)$$

Starting from the equality for injected reactive power, we obtain

$$Q_{tk} = \mathfrak{Im}(V_{tk} I_{tk}^*) = -\mathfrak{Im}(V_{tk}^* I_{tk}) = -\mathfrak{Im}(V_t^H e_k e_k^\top I_t) = -\mathfrak{Im}(V_t^H Y_k V_t)$$

$$= \tilde{V}_t^\top \hat{\mathbb{Y}}_k \tilde{V}_t = \operatorname{tr}(\tilde{V}_t^\top \hat{\mathbb{Y}}_k \tilde{V}_t) = \operatorname{tr}(\hat{\mathbb{Y}}_k \tilde{V}_t \tilde{V}_t^\top) = \operatorname{tr}(\hat{\mathbb{Y}}_k W_t) = \hat{\mathbb{Y}}_k \bullet W_t,$$

where the second equality follows from $\mathfrak{Im}(V_{tk} I_{tk}^*) = -\mathfrak{Im}(V_{tk}^* I_{tk})$, the fourth from $I_t = Y V_t$ and the definition of $Y_k = e_k e_k^\top Y$ and the rest from (A.3) and the properties of the trace.

For the squared voltage, we get

$$|V_{tk}|^2 = V_{tk}^* V_{tk} = V_t^H e_k e_k^\top V_t = \tilde{V}_t^\top M_k \tilde{V}_t = \operatorname{tr}(M_k \tilde{V}_t \tilde{V}_t^\top) = M_k \bullet W_t.$$

To prove relations for lines, we recall the definitions in (3.4) via Y_{lm}

$$|I_{tlm}|^2 = (e_l^\top Y_{lm} V_t)^H (e_l^\top Y_{lm} V_t) = (Y_{lm} V_t)^H (Y_{lm} V_t) = (\mathbb{Y}_{lm} \tilde{V}_t)^\top (\mathbb{Y}_{lm} \tilde{V}_t) = \tilde{V}_t^\top \mathbb{Y}_{lm}^\top \mathbb{Y}_{lm} \tilde{V}_t$$

$$= \operatorname{tr}(\mathbb{Y}_{lm}^\top \mathbb{Y}_{lm} \tilde{V}_t \tilde{V}_t^\top) = \mathbb{Y}_{lm}^\top \mathbb{Y}_{lm} \bullet W_t$$

$$|S_{tlm}|^2 = \mathfrak{Re}(V_t^H Y_{lm} V_t)^2 + \mathfrak{Im}(V_t^H Y_{lm} V_t)^2 = (\mathbb{Y}_{lm} \bullet W_t)^2 + (\hat{\mathbb{Y}}_{lm} \bullet W_t)^2$$

and the result of the active power on the line immediately follows. Finally, the relation for voltage difference can be proven in the same way as for the squared voltage

$$|V_{tl} - V_{tm}|^2 = (V_{tl} - V_{tm})^* (V_{tl} - V_{tm}) = V_t^H (e_l - e_m)(e_l - e_m)^T V_t = \tilde{V}_t^T M_{lm} \tilde{V}_t$$

$$= \operatorname{tr}(M_{lm} \tilde{V}_t \tilde{V}_t^T) = M_{lm} \bullet W_t.$$

A.2   Proof of Proposition 3.1

If $C_t(\xi_t, X_{t-1})$ has an optimal solution (X_t, W_t) with $\mathrm{rank}(W_t) = 1$, then there is a voltage vector $V_t \in \mathbb{C}^n$ such that $W_t = \tilde{V}_t \tilde{V}_t^\top$. The vectors V_t are thus physically feasible for the original AC-OPF problems in state (ξ_t, X_{t-1}). If all (ξ_t, X_{t-1}) have that property, the approximations of the non-convex AC-OPF problem on the nodes are tight, and (X_t, V_t) are the solutions of the dynamic programming equations for the original problem $(\mathcal{P}^{nc})$ and thus optimal.

A.3   Proof of Proposition 3.2

The first three points follow from Proposition 3.1 and Girardeau et al. (2015). To see the last point, we define C_t^{nc} as the cost function of the non-convex problem and note that due to our assumption $C_T(X_{T-1}, \xi_{Tj}) = C_T^{nc}(X_{T-1}, \xi_{Tj})$ for all optimal decisions X_{T-1} and all lattice nodes ξ_{Tj}, which establishes that $\mathcal{C}_T = \mathcal{C}_T^{nc}$ at all lattice nodes and all points chosen by the optimal policy.

In the second last stage, we note that due to 2, we have

$$F_{T-1} \bullet X_{T-1,L} + \bar{\mathcal{C}}_{TL}(X_{T-1,L}, \xi_{T-1,j}) \xrightarrow{L \to \infty} F_{T-1} \bullet X_{T-1} + \mathcal{C}_T(X_{T-1}, \xi_{T-1,j})$$

where $X_{T-1,L}$ and X_{T-1} are the optimal decisions for the problem with value functions $\bar{\mathcal{C}}_{TL}$ and $\mathcal{C}_T$ respectively. At the same time, due to the above and our assumption that

$$F_{T-1} \bullet X_{T-1,L}^{nc} + \bar{\mathcal{C}}_{TL}(X_{T-1,L}^{nc}, \xi_{T-1,j}) = F_{T-1} \bullet X_{T-1,L} + \bar{\mathcal{C}}_{TL}(X_{T-1,L}, \xi_{T-1,j})$$

where $X_{T-1,L}^{nc}$ is the optimal decision for the non-convex problem at lattice node $\xi_{T-1,j}$ and some resource state X_{T-2}, we have $\mathcal{C}_{T-1} = \mathcal{C}_{T-1}^{nc}$. Continuing in this manner until the first stage establishes 4.

A.4   Proof of Proposition 3.3

Denote by $\mathcal{K}_l$ the normed eigenvectors of W_t with positive eigenvalues. Since

$$\text{tr}(G(\alpha)W_t)$$

is part of the Lagrangian, it has to hold that for every $\mathcal{K}_l$

$$G(\alpha)\mathcal{K}_l = 0,$$

i.e., that $\mathcal{K}_l$ is in the null space of $G(\alpha)$. If this is not the case, then one could choose a W_t' such that the eigenvalue of $\mathcal{K}_l$ is zero, thereby reducing the objective of the inner optimization problem in the Lagrangian, leading to a contradiction to the optimality of W_t.

Therefore if the dimension of the kernel of $G(\alpha)$ is at most two, there are at most 2 linearly independent eigenvectors of W_t with positive eigenvalues. If there is only one, then $W_t = \tilde{V}_t \tilde{V}^\top$ for some vector $\tilde{V}_t$ whose components can be directly interpreted as voltages. In case there are two, we note that by the structure of $\mathbb{Y}_k$ and $\hat{\mathbb{Y}}_k$, the matrix $G(\alpha^*)$ has the form

$$G(\alpha)) = \begin{pmatrix} T(\alpha) & \bar{T}(\alpha) \\ -\bar{T}(\alpha) & T(\alpha) \end{pmatrix},$$

for some matrices T dependent on α.

Therefore, if $\mathcal{K} = (\mathcal{K}_1^\top, \mathcal{K}_2^\top)^\top$ is one of the two eigenvectors, then the orthogonal vector $\mathcal{K}_\perp = (-\mathcal{K}_2^\top, \mathcal{K}_1^\top)^\top$ also has a non-zero eigenvalue, since $G(\alpha)\mathcal{K}_\perp$ yields a the same vector as $G(\alpha)\mathcal{K}$ with flipped components. We can, therefore, conclude that

$$W_t = \rho_1 \mathcal{K}\mathcal{K}^\top + \rho_2 \mathcal{K}_\perp \mathcal{K}_\perp^\top.$$

Since for any matrix A of the general form of G it holds that $\text{tr}(A\mathcal{K}\mathcal{K}^\top) = \text{tr}(A\mathcal{K}_\perp \mathcal{K}_\perp^\top)$, for a given choice of the other primal and dual variables the rank 1

matrix

$$W_t^\star = (\rho_1 + \rho_2)\mathcal{K}\mathcal{K}^\top$$

yields the same results as W_t in the constraints of $\bar{C}_{tl}(\xi_{tn}, X_{t-1})$ and therefore is a feasible solution with the same objective as W_t. This proves the first point of the proposition.

To prove the second point, we have to find the vector $\tilde{V}_t = (\tilde{V}_{t1}, \tilde{V}_{t2})^\top$ in the null space of $G(\alpha)$ whose components can be interpreted as the real and imaginary component of the voltage vector such that $\tilde{V}_t \tilde{V}_t^\top$ is the physically correct rank one solution of the problem.

To find such a vector, we find parameters g_1, $g_2 \in \mathbb{R}$ such that

$$\tilde{V}_t = g_1 \begin{pmatrix} \mathcal{K}_1 \\ \mathcal{K}_2 \end{pmatrix} + g_2 \begin{pmatrix} -\mathcal{K}_2 \\ \mathcal{K}_1 \end{pmatrix}$$

and the reconstructed voltages

$$V_t^\star = (g_1\mathcal{K}_1 - g_2\mathcal{K}_2) + i(g_1\mathcal{K}_2 + g_2\mathcal{K}_1)$$

fit the known voltages at nodes m_1 and m_2, i.e.,

$$\mathfrak{Re}(V_{t,m_1}) = g_1\mathcal{K}_{1,m_1} - g_2\mathcal{K}_{2,m_1}, \quad \mathfrak{Im}(V_{t,m_2}) = g_2\mathcal{K}_{1,m_2} + g_1\mathcal{K}_{2,m_2},$$

which finishes the proof. $\square$

A.5 Proof of Proposition 3.4

We have to show that the primal problem has a finite optimal value and that the dual problem has a feasible solution in the interior of the feasible set. Clearly, since the demand and the production are finite on every lattice node, the finiteness of the optimal objective of the primal holds.

To show that the feasible set of the dual problem has an interior point, set

$$\lambda_{hk} = 0, \quad \zeta_{hgi} = \frac{1}{r_g - 1}, \quad \overline{\lambda}_{hg} = \left| \frac{1}{r_g - 1} \sum_{i \in [r_g - 1]} m_{gi} \right| + 1,$$

$$\gamma_{hk} = 0, \quad \overline{\gamma}_{hg} = \underline{\gamma}_{hg} = 1,$$

$$\overline{\mu}_{hk} = 2, \quad \underline{\mu}_{hk} = 1$$

$$\sigma_{hk} = 25 - h, \quad \overline{\kappa}_{hk} = 1, \quad \delta_k = 1$$

$$\overline{\beta}_{hk}^+ = (25 - h)\eta + 1, \quad \overline{\beta}_{hk}^- = 1, \quad \nu_i = \frac{1}{l - 1}$$

$$r_{hlm}^1 = r_{hlm}^4 = r_{hlm}^5 = 1, \quad r_{hlm}^2 = r_{hlm}^3 = 0$$

for $k \in \mathcal{N}, h \in \mathcal{H}, g \in \mathcal{G}, i \in [r_g - 1]$ and $(l, m) \in \mathcal{L}$. Observe that all variables except λ_{hk} and γ_{hk}, which are not sign-constrained, are thus strictly positive.

It is easy to verify that all dual constraints hold and in particular

$$r_{hlm} = \mathbb{I} \succ 0$$

$$G_h(\alpha) = \sum_{k \in \mathcal{N}} M_k = \mathbb{I} \succ 0,$$

establishing that there is a strictly feasible point for the dual problem.

Appendix B

Additional Material on AC Power Flow

B.1   Phase-Shifting Transformers with Off-Nominal Turns Ratios

As outlined in Section 3.2.1, current that flows through a conductor induces a magnetic field, which increases in strength with the amount of current and if the conductor is wound up in a coil. In an AC network, the magnetic field, therefore, pulsates and changes polarity along with the current.

This electromagnetic effect works *in both directions*, i.e., if magnetic field lines are moved over a conductor, a current is induced. Hence, if a second coil is placed in close proximity to a coil for which a fluctuating magnetic field is induced by AC current passing through the coil, the field induces an AC current in the second coil because the change in intensity and direction of the magnetic field constantly disturbs the free electrons in the second coil and forces them to move.

This is the basic principle of a transformer, which converts an AC voltage in the primary coil *in front* of the transformer to a different AC voltage in the secondary

coil *behind* of the transformer. Note that if the coils would just be placed next to another, a significant part of the magnetic field from the primary side would not be *in range* of the secondary coil. Therefore, in real transformers, a core of ferromagnetic material is placed in a loop between primary and secondary coils to prevent the wastage of energy.

The change of voltage between the primal and secondary coil depends on the *turns ratio* of the two coils, and for an ideal transformer (without any losses), it can be expressed as

$$\frac{V_1}{V_2} = \frac{N_1}{N_2} = \frac{I_2}{I_1}$$

where N_1 and N_2 are the numbers of turns of the respective coils and V_1, I_1 and V_2, I_2 are the primary and secondary voltages and currents, respectively.

It follows that the induced voltage in the secondary coil $V_2 = V_1 \frac{N_2}{N_1}$ increases in the primary voltage and in the proportion of turns in the secondary coil to the primary one. Hence, V_2 can be *stepped up* by using more windings in the secondary coil and *stepped down* by using less windings. While higher voltages V_2 imply lower currents I_2 (by the conservation of power) and, therefore, lower transmission losses (which are proportional to current), lower voltages are safer to handle and, therefore, more suitable for end-consumers. The ability to easily switch between voltage levels using transformers is one of the main advantages of AC current over DC current and the reason why AC technology is used in contemporary electric grids.

We distinguish transformers with nominal and off-nominal turns ratio. When the ratio of selected voltage bases for the per-unit system on either side of the transformer is equal to the turns ratio, the transformer is called a transformer with *nominal turns ratio*. In such a situation, the transformer can effectively be eliminated from power flow calculations as voltages, currents, external impedances, and admittances expressed in the per-unit system do not change when they are referred from one side of a transformer to the other. Taking voltages as an example, we see
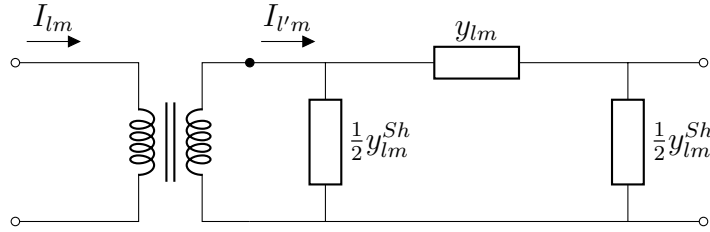
Figure B.1: Graph presents two buses connected with the line including transformer and respective admittances.

that

$$\frac{V_{1,p.u.}}{V_{2,p.u.}} = \frac{\frac{V_1}{V_{1,base}}}{\frac{V_2}{V_{2,base}}} = \frac{V_1}{V_2}\frac{V_{2,base}}{V_{1,base}} = \frac{N_1}{N_2}\frac{N_2}{N_1} = 1$$

for a transformer with a nominal turns ratio.

However, in some cases, it is impossible to select voltage bases in this manner – see Glover et al. (2008) for an example of two parallel transformers where this is the case. Such transformers have *off-nominal turns ratios* and require correction to the admittance matrix to account for the additional voltage magnitude T relative to the nominal case, i.e.,

$$\frac{N_1}{N_2} = \frac{V_{1,base}}{V_{2,base}}T.$$

This implies that when we are operating in a per-unit system, the *effective turns ratio*, i.e., the factor of proportionality between the two per unit voltages, equals T, since

$$\frac{V_{1,p.u.}}{V_{2,p.u.}} = \frac{V_1}{V_2}\frac{V_{2,base}}{V_{1,base}} = \frac{N_1}{N_2}\frac{V_{2,base}}{V_{1,base}} = \frac{V_{1,base}}{V_{2,base}}T\frac{V_{2,base}}{V_{1,base}} = T.$$

Apart from transformers having an off-nominal turns ratio, another complication relative to the simple situation described in Section 3.2 is that transformers can be used to control the phase angle. Such transformers are called *phase-shifting transformers* and are modeled by a (hypothetical) complex turns ratio $e^{i\phi}$, which allows to represent a phase shift ϕ for transformers in power flow calculations.

To sum up, consider a phase-shifting transformer with an off-nominal turns ratio represented by a magnitude T_{lm} and a phase shift ϕ_{lm} and assume that the transformer is placed on the line (l, m) and assigned to bus l. Then the effective turns ratio of the transformer is

$$\frac{V_l}{V_{l'}} = T_{lm} e^{i\phi_{lm}}.$$

where l and l' refer to the left and right side of the transformer, respectively, as presented in Figure B.1 and V_l and $V_{l'}$ represent voltage values in the per-unit system just before and just after the current passes through the transformer. Note that l' acts as a new node in the network, and we will see below how to get rid of it again for the price of an asymmetric admittance matrix.

Since the power loss is negligible in the ideal transformer, we have

$$V_l I_{lm}^* = V_{l'} I_{l'm}^*$$

where I_{lm} is the current flowing through line (l, m) from bus l to m, which implies

$$\frac{I_{lm}}{I_{l'm}} = \left(\frac{V_{l'}}{V_l}\right)^* = \left(\frac{1}{T_{lm} e^{i\phi_{lm}}}\right)^* = \frac{1}{T_{lm} e^{-i\phi_{lm}}}. \tag{B.1}$$

B.2   The Admittance Matrix

In Section 3.2, we discuss a simple form of the admittance matrix, which does neither take into account shunt admittances of lines nor phase-shifting transformers or transformers with off-nominal turns ratios. While this simpler view is sufficient for modeling many power systems, we discuss the general case here since it is required for our application example in Section 3.4.

We start by noting that besides buses, branches may also have a shunt admittance y_{lm}^{Sh} (also called total charging susceptance) representing leakage of current from within the branch (l, m) to the reference node. As is common, we apply this admittance equally to the buses at the end of the branch to incorporate leakage

along the branch.

Furthermore, we assume that there is a transformer represented by magnitude T_{lm} and phase shift ϕ_{lm} placed at the branch (l, m) and assigned to bus l (see Figure B.1).

To model this situation, we start by applying Kirchhoff's current law to node l' behind the transformer. Since there are no losses associated with the transformer, the current flowing into l' is just $I_{l'm}$. To transform this current into the per-unit system *in front* the transformer and thereby eliminate l', we use (B.1) to write $I_{l'm} = I_{lm}T_{lm}e^{-i\phi_{lm}}$. The current flowing out of node l' is on the one hand the current lost due to half of the shunt admittance, which due to Ohm's law, can be written as $V_{l'}\frac{1}{2}y_{lm}^{Sh}$ and the current that flows from l' to m, which is $(V_{l'} - V_m)y_{lm}$. In summary, we can write

$$0 = I_{lm}T_{lm}e^{-i\phi_{lm}} - V_{l'}\frac{1}{2}y_{lm}^{Sh} - (V_{l'} - V_m)y_{lm}$$

which can be re-written as

$$
\begin{aligned}
I_{lm} &= (T_{lm}e^{-i\phi_{lm}})^{-1}\left(V_{l'}\frac{1}{2}y_{lm}^{Sh} + (V_{l'} - V_m)y_{lm}\right)\\
&= (T_{lm}e^{-i\phi_{lm}})^{-1}\left(\left(y_{lm} + \frac{1}{2}y_{lm}^{Sh}\right)V_{l'} - y_{lm}V_m\right)\\
&= (T_{lm}e^{-i\phi_{lm}})^{-1}\left(\left(y_{lm} + \frac{1}{2}y_{lm}^{Sh}\right)\frac{1}{T_{lm}e^{i\phi_{lm}}}V_l - y_{lm}V_m\right)\\
&= \frac{1}{T_{lm}^2}\left(y_{lm} + \frac{1}{2}y_{lm}^{Sh}\right)V_l - \frac{1}{T_{lm}e^{-i\phi_{lm}}}y_{lm}V_m,
\end{aligned}
\tag{B.2}
$$

where in the third line we used the definition of $V_{l'}$ in terms of V_l in order to eliminate the node l' from the equation and y_{lm} is series admittance of the line (l, m).

Similarly, we can use Kirchhoff's current law for (m, l), which, expressed in the per-unit system of bus m, yields

$$0 = I_{ml} - V_m\frac{1}{2}y_{lm}^{Sh} - (V_m - V_{l'})y_{lm}$$

which we can re-arrange to

$$I_{ml} = \left(y_{lm} + \frac{1}{2}y_{lm}^{Sh}\right)V_m - \frac{1}{T_{lm}e^{i\phi_{lm}}}y_{lm}V_l. \tag{B.3}$$

Inspecting (B.2) and (B.3), it becomes clear that allowing for transformers with off-nominal turns ratios and non-zero phase shifts introduces an asymmetry in the admittance matrix when using the per-unit system. In order to deal with this in the definition of the admittance matrix, we define $\tilde{\mathcal{L}} = \mathcal{L} \cup \{(m,l) : (l,m) \in \mathcal{L}\}$ and set $y_{ml} = y_{lm}, y_{ml}^{Sh} = y_{lm}^{Sh}, T_{ml} = 1, \phi_{ml} = -\phi_{lm}$ for every $(l,m) \in \mathcal{L}$ with the transformer assigned to the bus l.

In order to define the partial admittance matrix Y_{lm} in the presence of phase-shifting transformers with off-nominal turns ratios and shunt admittances, we write

$$Y_{lm} = \frac{1}{T_{lm}^2}\left(y_{lm} + \frac{1}{2}y_{lm}^{Sh}\right)e_l e_l^\top - \frac{1}{T_{lm}T_{ml}e^{-i\phi_{lm}}}y_{lm}e_l e_m^\top, \quad \forall(l,m) \in \tilde{\mathcal{L}}.$$

Note that for the above definition $I_{lm} = e_l^T Y_{lm}V$ and $I_{ml} = e_m^T Y_{ml}V$ are satisfied.

Finally, to derive the relationships between voltage and current on the buses in the setting of this section, based on Ohm's law and Kirchoff's current law, we write

$$I_k = I_{k0} + \sum_{j:(k,j)\in\tilde{\mathcal{L}}} I_{kj} = y_k V_k + \sum_{j:(k,j)\in\tilde{\mathcal{L}}} \left(\frac{1}{T_{kj}^2}\left(y_{kj} + \frac{1}{2}y_{kj}^{Sh}\right)V_k - \frac{1}{T_{kj}T_{jk}e^{-i\phi_{kj}}}y_{kj}V_j\right)$$

$$= \left(y_k + \sum_{j:(k,j)\in\tilde{\mathcal{L}}} \frac{1}{T_{kj}^2}\left(y_{kj} + \frac{1}{2}y_{kj}^{Sh}\right)\right)V_k + \sum_{j:(k,j)\in\tilde{\mathcal{L}}} \left(-\frac{1}{T_{kj}T_{jk}e^{-i\phi_{kj}}}y_{kj}\right)V_j$$

for every $k \in \mathcal{N}$. In order to represent this in the compact form $I = YV$ as in Section 3.2.1, we define the elements of the admittance matrix Y as

$$(Y)_{kk} = y_k + \sum_{j:(k,j)\in\tilde{\mathcal{L}}} \frac{1}{T_{kj}^2}\left(y_{kj} + \frac{1}{2}y_{kj}^{Sh}\right),$$

$$(Y)_{kj} = -\sum_{(k,j)\in\tilde{\mathcal{L}}} \frac{1}{T_{kj}T_{jk}e^{-i\phi_{kj}}}y_{kj}, \quad j \neq k.$$

Appendix C

Modeling of Randomness

We model conventional demand, wind power production, and photovoltaic production as random. For each of these variables, we use hourly data on day-ahead forecasts to estimate a 24-dimensional aggregate stochastic process in daily resolution for the whole network. Since there is only one bus in area 1 that has installed wind power capacities, we directly model wind power production at this bus. To disaggregate load and PV power production to single buses, we apply fixed scaling factors. More specifically, for load, we apply the scaling factors given in the case description to arrive at bus-level active and reactive power demands, while for PV production, we model cumulative production at all buses and then disaggregate it to individual buses proportional to yearly production volumes.

This implies that we model a $3 \times 24 = 72$ dimensional stochastic process that evolves in daily time increments. In order to model the process, we first capture the variation that can be attributed to seasonal effects and then reduce the dimensionality of the process using principal component analysis (PCA).

To this end, for each of the three random processes, we set up a linear regression model with a constant term, 23 dummies for the hours of the day, a weekend dummy, and yearly seasonality modeled by the two regressors $\cos\left(2\pi d/366\right)$, $\sin\left(2\pi d/366\right)$, which together represent a yearly sinusoidal pattern with a variable amplitude and phase

shift dependent on the day $d \in [366]$ of the year. We then use all quadratic interactions of these regressors and end up with 299 regressors in each of the models. To avoid overfitting, we estimate the model with LASSO regression, where the degree of regularization is chosen by 10-fold cross-validation.

While the fit of the model for PV production and load is rather good with a R^2 of 93% and 96.3% respectively, the fit for wind power production is, as expected, considerably worse with an R^2 of 23.4%, since wind speeds do not follow a clear seasonal pattern.

We base our stochastic model on the residuals u_{dhj} on the day d, in hour h for variable $j = 1, 2, 3$ of the regression models. To deal with the pronounced heteroskedasticity of the residuals, we employ quantile transformations, i.e., we transform $\kappa_{djh} = F_{jh}^{-1}(u_{dhj})$, where F_{jh}^{-1} is the inverse empirical distribution of all the residuals of variable j in hour h. In this way, the residuals are uniformly distributed on $[0, 1]$ for every hour h and variable j.

Finally, for every day d, we end up with a vector of residuals $\kappa_d \in \mathbb{R}^{72}$, which collects the transformed errors for all three technologies for the 24 hours of the day. To reduce the dimensionality of this process, we perform a PCA on the 366 vectors κ_d associated with the one year of data provided with the case and model the first 6 principle components $\Lambda_1, \ldots, \Lambda_6$, which together account for more than 95% of the variance as basic stochastic factors in our model. To capture the day-by-day autocorrelation structure of the components, we use LASSO regression with 10-fold cross-validation to estimate a six-dimensional vector autoregressive model

$$\Lambda_d = \mathfrak{L}\Lambda_d + \tau_d, \tag{C.1}$$

where $\mathfrak{L}$ is the lag operator.

To simulate our stochastic process, we resample the residuals $\tau_d \in \mathbb{R}^6$ of the regression model (C.1) to generate scenarios $\hat{\Lambda}_d$. These scenarios are, in turn, transformed to residuals $\hat{\kappa}_d \in \mathbb{R}^{72}$ by multiplying with the first 6 rows of the coefficient

matrix of the PCA, which is further transformed to $\hat{u}_d$ with linearly interpolated versions of F_{jh}.

Finally, the seasonal linear models are used to predict seasonal means for wind and solar production as well as load to which the corresponding simulated residuals $\hat{u}_d$ are added to arrive at scenarios for the three variables of interest.